STRUCTURAL OPTIMISATION OF GATA4-TARGETING COMPOUNDS TO REDUCE STEM CELL TOXICITY

Samuli Auno
University of Helsinki
Faculty of Pharmacy
Division of Pharmaceutical
Chemistry and Technology

April 2019

Faculty Faculty of Pharmacy	Department Department of Pharmaceutical Chemistry and Technology

Author
Samuli Auno

Title
Structural optimisation of GATA4-targeting compounds to reduce stem cell toxicity

Subject
Pharmaceutical chemistry

Level Master's thesis	Month and year April 2019	Number of pages 77

Abstract

Heart failure is a disease of major social and economic impact. The disease is most commonly onset by extensive cardiomyocyte death following a myocardial infarction. Five-year mortality of heart failure is higher than some cancers. Loss of cardiac muscle tissue leads to pathological thickening and fibrosis of the left ventricular wall, which eventually further diminish cardiac function. Cardiomyocytes hardly proliferate, which also exacerbates the problem. Several cell signalling pathways are indicated in pathological reprogramming of the heart and the exact significance of these pathways remains to be demonstrated. Treatment strategies based on renewing cardiac muscle, such as direct injection of stem cells into the myocardium, have failed to reach clinically significant effects on heart failure patients. Direct inhibition of pathological cardiac reprogramming by using small molecule modulators remains as an auspicious strategy to treat heart failure.

GATA4, or GATA binding protein 4, is a transcription factor expressed mainly in heart, lung, intestine, gonad and liver tissues, which regulates tissue renewal and cell proliferation by controlling protein transcription. GATA4 binds to GATA sequences in DNA with two zinc finger moieties and enables transcription of target genes. Interactions of GATA4 and several other transcription factors are in central role of guiding heart development, hypertrophy and fibrosis. One of these transcription factors is NKX2-5, which synergistically interacts with GATA4. Inhibition of this interaction in rat myocardial infarction model has been shown to protect against development of heart failure. A screening campaign against the transcriptional synergy of GATA4 and NKX2-5 found potent small molecule inhibitors of this interaction, but these compounds are characterised with stem cell toxicity.

The aim of the study was to design and synthesise novel derivatives of GATA4-NKX2-5 synergy inhibitor hit molecule with reduced stem cell toxicity. Modifications on the phenyl ring of the hit molecule were designed, which either increase electron density of the ring or possibly alter the torsional angle between the phenyl and isoxazole ring moieties. Activity of the compounds was studied on a luciferase reporter gene system in COS-1 cells and toxicity was analysed on IMR90 human induced pluripotent stem cell line. 3-(4,5-dimethylthiazol-2-yl)-2,5-diphenyltetrazolium (MTT) bromide and lactate dehydrogenase (LDH) assays were selected to measure toxicity on stem cells. Stem cell toxicity of several previously synthesised compounds was assayed in parallel with the novel derivatives.

Ten novel derivatives were designed, synthesised and assayed. Four of the new compounds, a mono-ortho-methyl, a di-ortho-methyl, a di-meta-methoxy and cyclohexyl derivatives were found to be equipotent inhibitors of reporter gene activity compared to the hit compound. Additionally, the mono-ortho-methyl, di-ortho-methyl and di-meta-methoxy derivatives were less toxic to stem cells than the hit molecule in the MTT assay. Several other derivatives were found to be less toxic, but also non-active in the luciferase assay. None of the studied compounds exhibited notable necrotic toxicity on stem cells, as examined by the LDH assay.

According to this study it may be concluded that substituents of the hit molecule phenyl ring may be altered to decrease stem cell toxicity of the compound. Some of the alterations, most notably substituents in the para-position of the phenyl ring and substitution of the phenyl ring with smaller saturated hydrocarbon rings, diminish the activity of the hit compound. Remarkable toleration of ortho-substitution reinforces the hypothesis of phenyl-isoxazole torsional angle significance for toxicity. On the other hand, addition of two methoxy groups to both meta positions most likely lacks any substantial effect on the torsional angle, which implies another mechanism of toxicity avoidance. Activity and improved safety of the novel inhibitors should be confirmed in animal models before any decisive conclusions on the effects of structural modifications on the hit molecule can be made. In addition, other mechanisms of toxicity should be studied with relevant cell-based assays.

Keywords
GATA4, NKX2-5, stem cells, toxicity, protein-protein interaction

Where deposited
Department of Pharmaceutical Chemistry and Technology

Additional information
Instructors: Mikael Jumppanen, Tuuli Karhu, Virpi Talman

Tiedekunta/Fakultet Farmasian tiedekunta	Osasto/Sektion Farmaseuttisen kemian ja teknologian osasto

Tekijä/Författare
Samuli Auno

Työn nimi / Arbetets titel
Structural optimisation of GATA4-targeting compounds to reduce stem cell toxicity
GATA4:än kohdennettujen yhdisteiden rakenteen optimointi kantasolutoksisuuden vähentämiseksi

Oppiaine /Läroämne
Farmaseuttinen kemia

Työn laji/Arbetets art	Aika/Datum	Sivumäärä/ Sidoantal
Maisterin tutkielma	Huhtikuu 2019	77

Tiivistelmä/Referat

Sydämen vajaatoiminta on merkittävä sairaus, joka syntyy useimmin sydäninfarktin aiheuttaman sydänsolujen kuoleman seurauksena. Sairaus on vakava; sen viisivuotiskuolleisuus on suurempi kuin monilla syövillä. Sydänlihassolukon kuolema johtaa patologiseen vasemman kammion seinämän paksuuntumiseen ja fibroosiin, jotka edelleen heikentävät sydänlihaksen toimintaa. Sydänlihassolut eivät juurikaan uusiudu, mikä pahentaa ongelmaa. Useat soluviestintäreitit ohjaavat sydämen patologista uudelleenohjelmointia, eikä reittien merkitystä sydämen vajaatoiminnan syntyyn tunneta täysin. Erilaiset sydänlihassolujen uusiutumiseen perustuvat strategiat, kuten kantasolujen suora injektointi infarktiarven alueelle, ovat menestyneet kliinisissä tutkimuksissa heikosti. Sen sijaan sydänlihaksen patologisen uudelleenohjelmoimisen estäminen pienmolekyyleillä on yhä mahdollinen keino sydämen vajaatoiminnan synnyn ehkäisemiseksi.

GATA4, eli GATAan sitoutuva proteiini 4, on sydämessä, keuhkoissa, suolistossa, sukuelimissä ja maksassa ilmentyvä transkriptiotekijä, joka aktivoi useita keskeisiä kudosten uusiutumiseen ja solunjakautumiseen vaikuttavia viestireittejä säätelemällä proteiinisynteesiä. Se sitoutuu DNA:ssa sijaitseviin GATA-jaksoihin kahden sinkkisormilenkin avulla ja käynnistää kohdegeenien luennan. GATA4:n merkittävin vaikutus on sydämessä, jossa sen vuorovaikutukset useiden muiden transkriptiotekijöiden kanssa ohjaavat sydämen kehitystä sekä sydänlihaksen paksuuntumista ja fibroosia. NKX2-5 on eräs GATA4:n kanssa synergisesti vuorovaikuttavista transkriptiotekijöistä ja tämän vuorovaikutuksen estämisen on havaittu rotan sydäninfarktimallissa ehkäisevän sydämen vajaatoiminnan syntyä. GATA4:n ja NKX2-5:n välistä proteiini-proteiini-interaktiota kohtaan on yhdisteseulontatutkimuksessa löydetty inhibiittoreita, mutta nämä yhdisteet ovat toksisia kantasoluille.

Tutkimuksen tarkoituksena oli vähentää GATA4-NKX2-5 -vuorovaikutusta estävien molekyylien kantasolutoksisuutta syntetisoimalla hit-yhdisteen johdannaisia. Hit-yhdisteen fenyyliseen renkaaseen suunniteltiin muutoksia, jotka lisäävät fenyylirenkaan elektronitiheyttä tai mahdollisesti vaikuttavat fenyyli- ja isoksatsolirenkaan välisen kiertokulman suuruuteen. Yhdisteiden aktiivisuus testattiin COS-1 -soluihin transfektoidun lusiferaasireportterijärjestelmän ja toksisuus ihmisen indusoitujen pluripotenttien kantasolujen (IMR90) avulla. Toksisuuskokeiksi valittiin 3-(4,5-dimetyylitiatsol-2-yyli)-2,5-difenyylitetratsoliumbromidi- (MTT) ja laktaattidehydrogenaasikokeet (LDH). Uusien johdannaisten lisäksi tutkittiin viiden aiemmin syntetisoidun johdannaisen kantasolutoksisuutta samoissa kokeissa.

Kymmenen uutta johdannaista syntetisoitiin ja testattiin solumalleissa. Yhdisteistä neljä, mono- ja di-orto-metyyli-, di-meta-metoksi- sekä sykloheksyylijohdannainen, estivät reportterigeenin aktiivisuutta hit-yhdistettä vastaavalla voimakkuudella. Lisäksi mono- ja di-orto-metyylijohdannaiset sekä di-meta-metoksijohdannainen olivat hit-yhdistettä vähemmän toksisia kantasoluille MTT-kokeessa. Myös muiden yhdisteiden joukossa oli heikosti toksisia johdannaisia, mutta niiden vaikutus GATA4-NKX2-5-synergiaan oli vähäinen. LDH-kokeiden mukaan yksikään yhdisteistä ei aiheuttanut kantasoluissa merkittävää nekroottista toksisuutta.

Tutkimuksen perusteella voidaan todeta, että hit-yhdisteen fenyylirenkaan substituentteihin vaikuttamalla voidaan vähentää yhdisteen kantasolutoksisuutta. Osa muutoksista, erityisesti para-asemaan tehdyt muutokset ja fenyylirenkaan korvaaminen pienemmällä tyydyttyneellä hiilivetyrenkaalla, johti yhdisteaktiivisuuden vähenemiseen. Orto-asemaan tehtyjen muutosten vähäinen toksisuus vahvistaa hypoteesia, jonka mukaan fenyylirenkaan kiertokulma isoksatsolirenkaaseen nähden on merkittävä toksisuuden kannalta. Toisaalta, metoksiryhmän liittämisen fenyylirenkaan molempiin meta-asemoihin ei luultavasti vaikuta oleellisesti renkaan kiertokulmaan, mikä tarkoittaisi paremman siedettävyyden johtuvan muusta vaikutuksesta yhdisteen sitoutumiseen. Yhdisteiden aktiivisuus ja parantunut turvallisuusprofiili on vahvistettava eläinkokeilla, ennen kuin merkittäviä johtopäätöksiä yhdisteen rakennemuutosten vaikutuksista voidaan tehdä. Lisäksi muita toksisuuden mekanismeja tulisi tutkia solumalleilla.

Avainsanat – Nyckelord
GATA4, NKX2-5, kantasolut, toksisuus, proteiini-proteiini-interaktio

Säilytyspaikka – Förvaringställe
Farmaseuttisen kemian ja teknologian osasto

Muita tietoja – Övriga uppgifter
Ohjaajat: Mikael Jumppanen, Tuuli Karhu, Virpi Talman

LIST OF ABBREVIATIONS

ACE	Angiotensin-converting enzyme
ACEI	Angiotensin-converting enzyme inhibitor
ACF	Adult cardiac fibroblast
ACTC1	Actin alpha cardiac muscle 1
ADMET	Absorption, distribution, metabolism, elimination and toxicity
AML	Acute myeloid leukaemia
ANOVA	Analysis of variance
ANP	A-type natriuretic peptide
AT1aR	Angiotensin II type 1a receptor
AT2	Angiotensin II
ATP	Adenosine triphosphate
β-AR	β-adrenergic receptor
BAK	BCL2 homologous antagonist/killer 1
BAX	BCL2 associated X, apoptosis regulator
BCL2	B-cell lymphoma 2
BCL-XL	BCL-2-like 1
BET	Bromo- and extra-terminal domain
BMSC	Bone marrow-derived stem cell
BNP	B-type natriuretic peptide
CaM	Calmodulin
CaMKII	Ca^{2+}/calmodulin-dependent kinase II
CaN	Calcineurin
CLL	Chronic lymphocytic leukaemia
CM	Cardiomyocyte
CO_2	Carbon dioxide
CPC	Cardiac progenitor cell
DCM	Dichloromethane
df	Degree of freedom
DIABLO	Diablo IAP-binding mitochondrial protein
DIB	(Diacetoxyiodo)benzene

DIPEA	*N,N*-diisopropylethylamine
DM2	Diabetes mellitus type 2
DMEM	Dulbecco's modified Eagle's medium
DMF	*N,N*-dimethylformamide
DMSO	Dimethyl sulfoxide
DNA	Deoxyribonucleic acid
EMA	European Medicines Agency
Eq	Equivalent
ERK	Extracellular signal-regulated kinases
ESC	Embryonic stem cell
ET-1	Endothelin-1
ET_AR	Endothelin type A receptor
EtOAc	Ethyl acetate
FBS	Fetal bovine serum
FDA	Food and Drug Administration
GATA4	GATA binding protein 4
GHMT	GATA4, HAND2, MEF2C and TBX5
GMT	GATA4, MEF2C and TBX5
GPCR	Guanine nucleotide-binding protein (G-protein) coupled receptors
GSK3β	Glycogen synthase kinase 3 beta
HAND2	Heart- and neural crest derivatives-expressed protein 2
HAT	Histone acetyltransferase
HBTU	*N,N,N′,N′*-Tetramethyl-O-(1H-benzotriazol-1-yl)uronium hexafluorophosphate
HDL	High-density lipoprotein
HF	Heart failure
HFF	Human foreskin fibroblast
HFmrEF	Heart failure with mid-range ejection fraction
HFpEF	Heart failure with preserved ejection fraction
HFrEF	Heart failure with reduced ejection fraction
hiPSC	Human induced pluripotent stem cell
HOPX	Homeodomain-only protein

HPLC	High-performance liquid chromatography
HRMS	High resolution mass spectrometry
HSD	Honestly significant difference
HTS	High-throughput screening
ICAM-1	Intracellular adhesion molecule 1
IGF1	Insulin-like growth factor 1
iPSC	Induced pluripotent stem cell
LC-MS	Liquid chromatography-mass spectrometry
LDH	Lactate dehydrogenase
LFA-1	Lymphocyte function-associated antigen 1
LVEF	Left ventricular ejection fraction
MAPK	Mitogen-activated protein kinase
MAPKKK	Mitogen-activated protein kinase kinase kinase
MDM2	Mouse double minute 2 homolog
Me	Methyl
MEK	Mitogen-activated protein kinase kinase
MEF2C	Myocyte-specific enhancer factor 2C
MI	Myocardial infraction
miRNA	Micro-RNA
MS	Mass spectrometry
MTT	3-(4,5-dimethylthiazol-2-yl)-2,5-diphenyltetrazolium bromide
NE	Noradrenaline
NFAT	Nuclear factor of activated T-cells
NFATc4	Nuclear factor of activated T-cells, cytoplasmic 4
NKX2-5	NK2 homeobox 5
NMR	Nuclear magnetic resonance
NSTE-ACS	Non-ST elevation acute coronary syndrome
PI3K	Phosphoinositide 3-kinase
PIAS1	Protein inhibitor of activated STAT1
PKB	Protein kinase B
PKC	Protein kinase C
PPI	Protein-protein interaction

ppm	Parts per million
PRC2	Polycomb-repressive complex 2
RAAS	Renin-angiotensin-aldosterone system
RHOA	Ras homolog family, member A
ROCK	Rho-associated protein kinase
RTK	Receptor tyrosine kinase
SERCA	Sarcoplasmic reticulum $Ca2^{+}$-ATPases
SPSS	Statistical Package for the Social Sciences
SUMO-1	Small ubiquitin-like modifier 1
TBX5	T-box transcription factor TBX5
TF	Transcription factor
TGF-β	Transforming growth factor-β
THF	Tetrahydrofuran
TLC	Thin-layer chromatography
TMS	Tetramethylsilane
UGT	Uridine 5'-diphospho-glucuronosyltransferase
UPLC	Ultra-high performance liquid chromatography

TABLE OF CONTENTS

1 INTRODUCTION

Heart failure (HF) is a major economic and social burden, which leads to significant loss of money and lives throughout the world (Ponikowski et al. 2014). Heart failure is most commonly caused by the loss of cardiac cells following a myocardial infarction (MI). The loss of cardiac tissue is compensated by the formation of scar tissue and other mechanisms of pathological remodelling (Talman & Ruskoaho 2016). Despite advances in therapeutic strategies since the introduction of selective β-blockers and angiotensin converting enzyme inhibitors (ACEI), the 5-year mortality of HF exceeds that of many cancers. Consequently, new therapy strategies are desperately needed to address this growing, fatal issue of human health.

In the past decade, an attractive treatment strategy for HF has emerged in the form of renewing the cardiac tissue lost during a myocardial infarction (Garbern & Lee 2013). Extensive research and even clinical trials were conducted in the early 21st century, where stem cells of embryonic origin were injected into the hearts of the patients with the hopes of regaining some lost cardiac function. These studies were deemed failures, with only minor benefit found for the treatments. Since then, it has been found that the pluripotent nature of fully differentiated cells may be regained with the induction of selected transcription factors (Takahashi & Yamanaka 2006). Shortly after, it was found that other cell types, including cardiomyocytes (CM), could be produced from these novel induced pluripotent stem cells (Gai et al. 2009). Direct conversion of both mouse and human fibroblasts into CMs was also found to be possible, which sparked renewed interest into the field of cardiac regeneration (Efe et al. 2011; Song et al. 2012; Wada et al. 2013).

While reprogramming cardiac scar tissue into beating heart muscle is an alluring strategy, safety of the treatment, proper transcription factor delivery and dosing remain as issues. Induction of these transcription factors by small molecules solves some of these issues, but other strategies are still sought after (Cao et al. 2016). Inhibition of the synergistic activation of NK2 homeobox 5 (NKX2-5) by GATA binding protein 4 (GATA4) has emerged as a means of controlling the pathological

remodelling of cardiac tissue following a myocardial infarction (Pikkarainen et al. 2004; Talman & Ruskoaho 2016; Välimäki et al. 2017; Kinnunen et al. 2018). The small molecular inhibitor found by Välimäki et al. is characterised with toxicity on stem cells, managing of which requires further studies (Karhu et al. 2018).

2 REVIEW OF LITERATURE

2.1 Heart failure

Heart failure is a major global health issue, affecting more than 23 million people globally, which accounts for 1-2 % of adult population in developed countries (Bui et al. 2011; Ponikowski et al. 2016). Five-year mortality of HF is higher than some cancers, being up to 75% for the non-age-adjusted population (Levy et al. 2002; Shah et al. 2017; Bonsu et al. 2017). No significant improvements in HF prognosis have occurred since the beginning of 21st century. The condition is characterised by an insufficient cardiac function, which leads to dyspnea, edema of lower limbs and decreased physical performance (Ponikowski et al. 2016). Heart failure is divided into 2 main conditions called heart failure with preserved ejection fraction (HFpEF) and heart failure with reduced ejection fraction (HFrEF). Diagnostic criteria include left ventricular ejection fraction (LVEF), characteristic symptoms and specific biomarkers, such as B-type natriuretic peptide (BNP) (de Lemos et al. 2003; Ponikowski et al. 2016). A third class, which has characteristics of both previously mentioned disorders, called heart failure with mid-range ejection fraction (HFmrEF) has recently been suggested by the European Society of Cardiology to account for “gray-area” cases of HF.

Modern HF treatment focuses on reducing cardiac output, moderating cardiac remodelling and alleviating HF symptoms (Ponikowski et al. 2016). Strategies include renin-angiotensin-aldosterone system (RAAS) modulation, reduction of natriuretic peptide metabolism and control of adrenergic system. In addition, potential arrhythmias are treated accordingly. Heart selective β-blockers, ACEIs and

mineralocorticoid receptor antagonists are the most effective and recommended groups of medicine to use in HF treatment, with sacubitril/valsartan, a combination of neprilysin inhibitor and angiotensin II type 1 receptor antagonist, showing promising results (Heart failure: Current Care Guideline 2019; Jhund et al. 2015; Ponikowski et al. 2016). Current treatment methods, while effective, only aid in delaying the progress of HF and do not provide a cure for the condition (Ponikowski et al. 2016).

2.1.1 Pathophysiological changes in heart failure

The most common leading cause of HF is acute coronary artery disease, with chronic hypertension, high blood cholesterol, diabetes mellitus type 2 (DM2) and smoking being strong predisposing factors (Bui et al. 2011; Chen et al. 2011). The disease is most often onset by a MI, but a more chronic development in patients with cardiomyopathies, valvular heart diseases or hypertension-induced cardiac hypertrophy is also possible. This thesis focuses on HF caused by cardiac remodelling following MI.

In MI, the obstruction of coronary artery and the subsequent hypoxia of myocardial tissue results in, depending on the size and site of the obstruction, necrotic cell death of up to a billion cardiac cells (Laflamme & Murry 2005). Rapid revascularisation of infarcted area begins immediately after the infarction, as shown in a zebrafish infarction model (Marin-Juez et al. 2016). The infracted area is subsequently colonized by immune cells, which clear the infracted area of cellular debris and initiate wound healing processes (Laflamme & Murry 2005). Formation of granulation tissue rich in fibroblasts and endothelial cells begins simultaneously with removal of necrotic tissue. After two months of repair, the necrotic tissue is completely replaced by scar tissue, which is mostly composed of collagen.

As the newly-formed scar tissue is unable to fully contract with the surrounding ventricular tissue, the remaining healthy myocardium is left to maintain sufficient cardiac output. The heart responds with left ventricular hypertrophy and fibrosis,

or thickening and stiffening, to compensate for the increased demand of contractive force (Sutton & Sharpe 2000; Tham et al. 2015; Talman & Ruskoaho 2016). Interestingly, fibrotic events are not restricted to the initial necrotic scar, but instead spread to the surrounding healthy myocardium. While scar formation is initially intended to protect the ventricular wall from ruptures, this reactive fibrosis causes further detrimental effects on cardiac output.

2.1.2 Molecular mechanisms of cardiac hypertrophy

Intracellular signalling pathways related to cardiac hypertrophy are highly complex and integrated (Heineke & Molkentin 2006; Bernardo et al. 2010; van Berlo et al. 2013). A simplified representation of key pathways is presented in Figure 1. Calcium is at the centre of cardiomyocyte function (Dewenter et al. 2017). Defects in calcium-mediated signalling pathways are key elements in both physiological and pathological hypertrophy. In fact, pathways involving calcineurin (CaN) and Ca2+/calmodulin-dependent kinase II (CaMKII) have been recognized as potential targets for drug discovery. Downstream targets of β-adrenergic and angiotensin II guanine nucleotide-binding protein (G-protein) coupled receptors (GPCR) include protein kinase C (PKC), CaMKII and sarcoplasmic reticulum $Ca2^{+}$-ATPases (SERCA). These proteins are associated with cardiac hypertrophy and their suppression could explain the cardioprotective effects of drugs targeting β-adrenergic and angiotensin II receptors (Bernardo et al. 2010; van Berlo et al. 2013; Ponikowski et al. 2016).

Mechanical stress activates mitogen-activated protein kinase kinase kinase (MAPKKK) cascade, which induces pro-hypertrophic transcription factors (TF) through the activity of p38 (Heineke & Molkentin 2006). The RAS-RAF-MEK-ERK-pathway is a major factor in regulating physiological hypertrophy (Bueno & Molkentin 2002; Lorenz et al. 2009). Insulin-like growth factor 1 (IGF1) has a specific receptor tyrosine kinase target on the cell membrane, which phosphorylates phosphoinositide 3-kinase (PI3K) and subsequently Akt (Kim et al. 2008; McMullen 2008). Akt, or protein kinase B (PKB), is a general anti-apoptotic and pro-growth kinase with a large variety of intracellular up- and downstream targets and

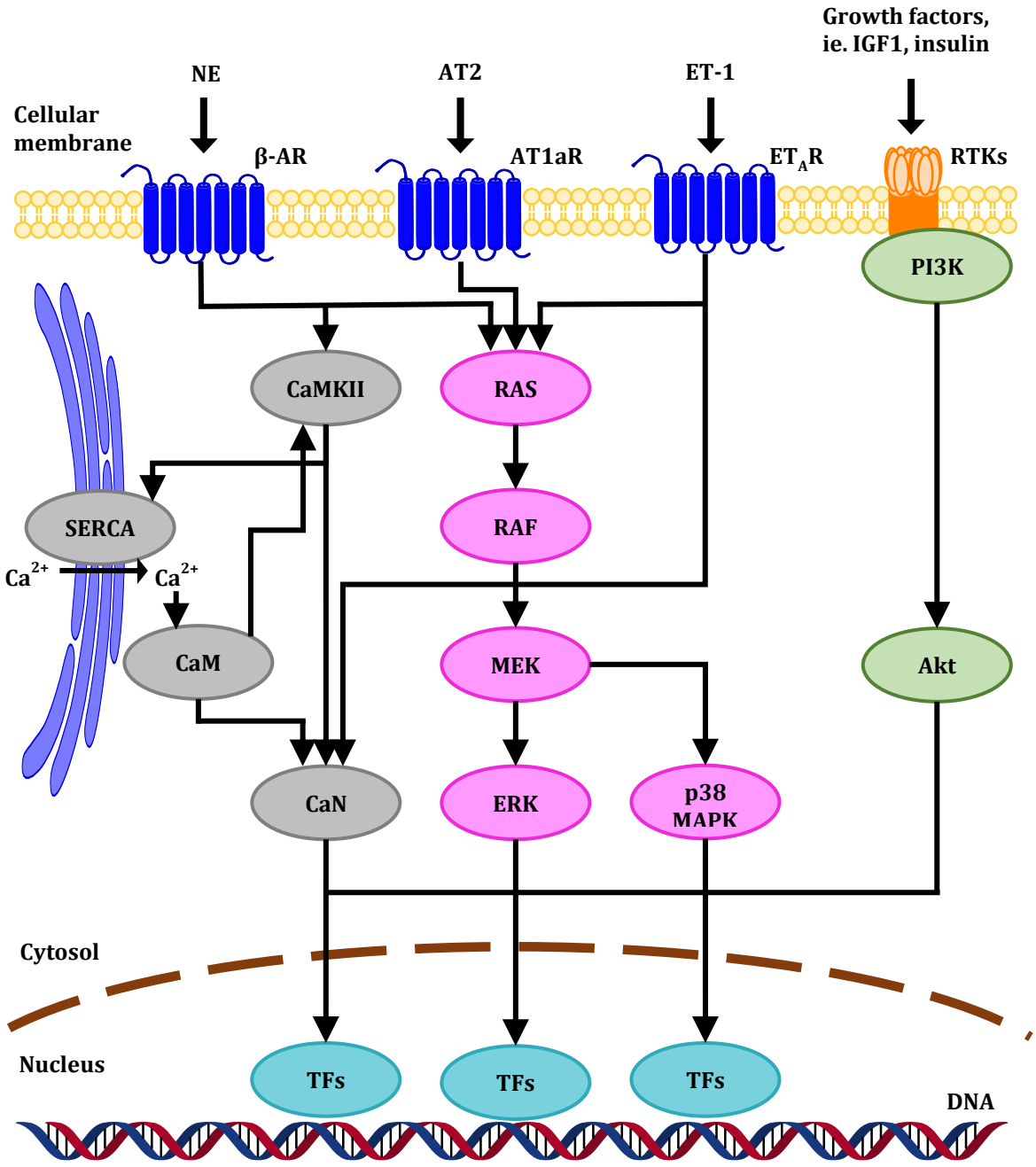

Figure 1. Simplified diagram of pathways mediating hypertrophic signals. AT1aR, angiotensin II type 1a receptor; AT2, angiotensin II; β-AR, β-adrenergic receptor; CaM, calmodulin; CaMKII, Ca^{2+}/calmodulin-dependent kinase II; CaN, calcineurin; DNA, deoxyribonucleic acid; ERK, extracellular signal–regulated kinases; ET-1, endothelin-1; ET_AR, endothelin type A receptor; IGF1, insulin-like growth factor 1; MAPK, mitogen-activated protein kinase; MEK, mitogen-activated protein kinase kinase; NE, noradrenaline; PI3K, phosphoinositide 3-kinase; RTK, receptor tyrosine kinase; SERCA, sarcoplasmic reticulum Ca^{2+}-ATPases; TF, transcription factor.

high relevance in settings of cardiac disease (Sussman et al. 2011; Manning & Toker 2017). While IGF1 is found to be a general regulator of organ size, several downstream effectors of IGF1 have been linked to cardiac hypertrophy as well (McMullen 2008). Additionally, IGF1 stimulation has improved cardiac function in several *in vivo* disease models.

2.2 Regeneration of the heart

Occurrence and mechanism of cardiac regeneration have puzzled scientists for decades (Laflamme & Murry 2011). Zebrafish and newts are capable of regenerating lost heart tissue after a myocardial injury (Oberpriller & Oberpriller 1974; Poss et al. 2002). Following these discoveries, zebrafish have been extensively studied to characterise molecular pathways responsible for this regenerative potential (Sahara et al. 2015). Studies published in the past decade show that human cardiac cells are in fact able to proliferate as well, albeit with very limited capacity (Bergmann et al. 2009; Mollova et al. 2013; Senyo et al. 2013; Sahara et al. 2015). Evidence on regenerative capability of mammalian heart was provided by Porrello et al. (2011), who found that neonatal mice can recover from a cardiac injury through the proliferation of pre-existing cardiomyocytes. However, this ability is lost by day 7 from birth. More detailed knowledge of mechanisms regulating CM proliferation could provide us with means to treat HF (Talman & Ruskoaho 2016; Leach & Martin 2018; Talman & Kivelä 2018). Current knowledge on cardiac proliferation and use of stem cells in the treatment of HF is presented briefly in the following chapters. Potential strategies of cardiac regeneration include transplantation of stem cells or differentiated cardiac cells, induction of CM proliferation and transdifferentiation of other cell types, mainly cardiac fibroblasts, into CMs.

2.2.1 Stem cells and heart disease

Pluripotent stem cells are cells capable of differentiating into all cell types of the body. Embryonic stem cells (ESC), which may be isolated from fertilized blastocysts, are a physiological example of a pluripotent stem cell type (Evans & Kaufman 1981;

Thomson et al. 1998). These cells differentiate into multipotent tissue progenitor cells, which are responsible for normal tissue regeneration, and finally into fully differentiated cells. However, no distinct proof exists of stem cell presence in adult human hearts (Sultana et al. 2015). This lack of rapid endogenous regenerative potential of cardiomyocytes by stem cell division and differentiation exacerbates the detrimental effects of MI. Recent article by Lesizza et al. (2017) highlights the potential of micro-RNAs (miRNA) in inducing CM proliferation.

Treating MI and subsequent HF by restoring lost CMs is an alluring, yet complicated therapy option (Laflamme & Murry 2011; Garbern & Lee 2013; Srivastava & Yu 2015; Leach & Martin 2018). Delivering cells capable of differentiating into CMs into the regions of lost heart tissue has been hypothesised to restore cardiac function after MI. Initial strategies involved delivering cardiac progenitor cells (CPCs), bone-marrow-derived stem cells (BMSC) or skeletal myoblasts via intravenous, intracoronary or intramyocardial injection, infusion or direct transplantation with a suitable biodegradable patch (Garbern & Lee 2013; Talman & Kivelä 2018). Benefits of autologous stem cell transplantation seem to originate mainly from paracrine effects instead of differentiation into functioning CMs (Nguyen et al. 2016).

A Cochrane review recently concluded that inadequate evidence exists of the benefits of BMSC transplantation over standard care; study populations have been very limited (Fisher et al. 2015). However, a large European study of 3000 patients called BAMI (NCT01569178) is ongoing to evaluate the effects of intracoronary infusion of BMSCs (US National Institute of Health 2019). This study will give statistically powerful insight to the benefits of autologous stem cell transplantation in HF. The role of cardiac tissue as a secretory organ has been under extensive evaluation in recent years, with *in vivo* experiments showing some promise on therapies affecting infarction scar neovascularization (Talman & Kivelä 2018). Furthermore, transplantation of endothelial cells and fibroblasts in addition to CMs seems to be more effective than sole transplantation of CMs.

Recently, it has been found that the pluripotent nature of fully differentiated cells may be renewed by exposing them to certain well-established mixtures of TFs (Takahashi & Yamanaka 2006; Yu et al. 2007; Takahashi et al. 2007; Kim et al. 2009). These cells, termed induced pluripotent stem cells (iPSC), retain the genetic information of the person they were harvested from, but may be differentiated into other cell types. Additionally, iPSC cells may be cultured seemingly indefinitely without falling into senescence. Human iPSCs (hiPSC) have successfully been differentiated into CMs via several different methods (Gai et al. 2009; Lian et al. 2012; Witty et al. 2014). Transplantation of hiPSC-derived CMs into the myocardium has shown some promise *in vivo* (Talman & Kivelä 2018). Safety concerns regarding observed ventricular arrhythmias have currently prevented hiPSC-derived CMs from progressing to clinical trials.

2.2.2 Reprogramming cardiac cells

Following the discovery of iPSC cells by Takahashi and Yamanaka, it was quickly found that direct transdifferentiation from another cell type to CM-like cells was also possible. Conversion of mouse fibroblasts into CM-like cells was first observed by the Srivastava group via viral transfection of GATA4, myocyte-specific enhancer factor 2C (MEF2C) and T-box transcription factor TBX5 (TBX5) TFs, which are abbreviated as GMT factors, into mouse cardiac and dermal fibroblasts (Ieda et al. 2010). GMT factors improve cardiac function *in vivo* following induced cardiac injury as well (Qian et al. 2012; Inagawa et al. 2012). Song et al. (2012) replicated and fine-tuned the GMT method and managed to produce beating CMs by transfecting heart- and neural crest derivatives-expressed protein 2 (HAND2) into tail-tip and cardiac fibroblasts in addition to GMT TFs. This combination, abbreviated GHMT, improved cardiac performance *in vivo* as well. In addition to TF methods, a miRNA approach was successful both *in vitro* and *in vivo* (Jayawardena et al. 2012).

First reports of human fibroblasts being used to create CM-like cells was by Nam et al. (2013). The study used a combination of GATA4, HAND2, TBX5, myocardin,

miRNA-1 and miRNA-133 to reprogram human foreskin fibroblasts (HFF), adult cardiac fibroblasts (ACF) and dermal fibroblasts into expressing cardiac markers and developing sarcomere-like structures. The group concluded that HAND2 was required for efficient CM reprogramming and MEF2C was replaceable by heart-specific miRNAs. Based on their previous study on mice, Srivastava group found a combination of 9 small molecules which could reprogram HFF into cells expressing cardiac genes and displaying Ca^{2+} transients (Wang et al. 2014; Cao et al. 2016). A combinational approach of GMT TFs, myocardin and two small molecules (a transforming growth factor-β (TGF-β) inhibitor and a Wnt inhibitor) was reported by Srivastava group to achieve rapid and efficient method of human ACF to CMs (Mohamed et al. 2017). While reprogramming non-cardiomyocytes into beating cardiac tissue is an intriguing strategy to treat HF, therapies relying on cardiac reprogramming have yet to reach human trials. Presently several approaches for both mouse and human CM reprogramming have been developed and interested readers are directed towards some thorough reviews (Sahara et al. 2015; Srivastava & Yu 2015; Tani et al. 2018).

2.3 Toxicity of small molecules

Significant amount of drug discovery regimes fail to produce an approved drug to the market (Kola & Landis 2004; Waring et al. 2015). The further the research progresses in the so-called phases of drug development, the more significant costs are involved in the process. Thus, early identification and termination of soon-to-fail projects is crucial to save resources and allow for adequate focus on promising drug candidates (Roberts et al. 2014). In addition, early optimization of toxicity may extend the therapeutic window of lead molecules and help to avoid dose-limiting toxicity. Utilization of a broad range of *in vitro* and *in vivo* studies are required for appropriate detection of toxicity (Roberts et al. 2014; Karhu et al. 2018). Potential of hiPSC cells in preclinical drug development is considerable, for they may be differentiated into all tissue types, while preserving the genotype, including mutations, of the person from whom they were originally isolated (Scott et al. 2013a).

2.3.1 Pharmacodynamics of small molecule toxicity

Toxicity and adverse effects caused by small molecule drugs and other xenobiotics may stem from several mechanisms (Liebler & Guengerich 2005). The molecule may simply exhibit an overexaggerated pharmacological response, which is most evident in the event of an overdose. A good example would be constipation and insufficient breathing caused by an opioid overdose (Pathan & Williams 2012). A drug molecule with low specificity to a receptor may bind to non-desired targets and inhibit non-intended systems. This attribute is called promiscuity in medicinal chemistry research (Leeson & Springthorpe 2007). Off-target binding is evident in drug molecules blocking enzyme cofactor binding sites, such as adenosine triphosphate (ATP) binding sites in protein kinases (Wu et al. 2016). While broad target specificity may be beneficial, other strategies of inhibition, such as allosteric modulation, are commonly warranted in this group of medicine for safety reasons.

Genotoxicity may be considered as a subgroup of off-target binding, in which the drug binds to deoxyribonucleic acid (DNA) strands (Liebler & Guengerich 2005). Planar molecules with rigid ring structures and hydrogen bond acceptors are at risk of binding to DNA. Many chemotherapeutic agents, such as groove binders and intercalators, take advantage of this mode of action to achieve therapeutic benefit (Palchaudhuri & Hergenrother 2007). Carcinogenicity, or tumour formation, may arise via several pathways, such as epigenetic modulation, genotoxicity and undesired inhibition of anti-tumour signalling pathways.

2.3.2 Pharmacokinetics of small molecule toxicity

Pharmacokinetics of a molecule may give rise to toxicity (Lin & Lu 1997). High lipophilicity, lack of adequate metabolism route and other factors, such as high volume of distribution, may cause a drug to accumulate in the body, potentially causing drug overdose. The drug may also be metabolized into harmful derivatives, which cause problems by mechanisms discussed in chapter 2.3.1. Examples of metabolically activated toxic molecules include benzo[a]pyrene, which acts as an

intercalator after oxidation, and paracetamol, a potent alkylating agent after metabolism by oxidizing cytochrome P450 (CYP) liver enzymes (Hall & Kier 1986; Bessems & Vermeulen 2001).

Interpersonal changes in drug activity, transportation and metabolism are studied by the field of pharmacogenetics (Lin & Lu 1997; Meyer 2000). Polymorphism of metabolic enzymes may cause multiple-fold variation in drug exposure. Classic examples of clinically relevant problems caused by polymorphism include excessive activation of codeine by CYP2D6 and changes in warfarin efficacy (Meyer 2000; Gasche et al. 2004). Conjugation enzymes, such as uridine 5'-diphospho-glucuronosyltransferases (UGT), may be subject to polymorphism as well. Focus of pharmacogenetic studies has recently shifted towards transporter proteins (DeGorter et al. 2012). Some drug molecules are substrates to only a single type of transporter proteins. If drugs are transported through membranes almost exclusively by transporters, even slight changes in transporter efficacy through polymorphism may have a major impact on the half-life of these drugs.

2.4 Protein-protein interactions as drug targets

Protein-protein interactions (PPI) are, as their name suggests, direct associations of protein monomers through electrostatic or chemical interactions (Jones & Thornton 1996; Nooren & Thornton 2003). These interactions may occur between any protein classes, including transcription factors, enzymes, receptors, antibodies and signalling molecules. Even quaternary structures of proteins may, in a liberal sense, be classified as PPIs. In this thesis, PPIs are classified as allosteric associations of two or more polypeptides in the absence of cofactors. Intracellular signalling pathways mediated via PPIs are linked to cell proliferation, metabolic activity, lifecycle management and diseases, especially cancers (Cox et al. 2010; Ivanov et al. 2013; Huttlin et al. 2017). Although the name suggests that PPIs occur only between proteins, protein-peptide and peptide-peptide interactions take place as well (Jones & Thornton 1996; Scott et al. 2016). In addition to structural distinction, PPIs may also be classified through the length of the interaction (transient or stable),

constitution of monomers (homomeric or heteromeric) and nature of the interaction (obligate or non-obligate) (Nooren & Thornton 2003). For proteins participating in obligate PPIs, the interaction is required for correct folding of monomer proteins, while proteins existing as stable monomers may form non-obligate PPIs.

Since the characterisation of PPI mechanisms, drug discovery campaigns against PPIs have been executed in the hopes of finding means to alter signalling pathways which have been considered undruggable by conventional receptor antagonists. However, these efforts are thwarted by weakly-defined and small binding pockets, very broad interaction regions and problems with identifying significant amino acid (aa) residues to reach PPI antagonism (Scott et al. 2016). Peptidomimetic approaches, including stapled peptides, pseudopeptides and truncated peptides, have yielded potent PPI antagonists against several targets (Walensky & Bird 2014; Nevola & Giralt 2015; Scott et al. 2016). These molecules often have challenges with drug-likeness that prevent further clinical development; regardless, they remain as vital tools in chemical biology research. In addition to peptide-based approaches, fragment-based drug discovery has been established as an effective strategy to find active small molecules against these broadly scattered small binding sites (Hajduk & Greer 2007; Scott et al. 2013b).

Despite hardships associated with PPI inhibition, several small molecule inhibitors have been discovered, most notably against inhibitor of apoptosis protein (IAP)/Diablo IAP-binding mitochondrial protein (DIABLO) and B-cell lymphoma 2 (BCL2)/ BCL-2-like 1 (BCL-XL) interactions with BCL2 associated X, apoptosis regulator (BAX) and BCL2 homologous antagonist/killer 1 (BAK) proteins (Vogler et al. 2009; Rathore et al. 2017). These inhibitors are characterised with large, complex structures and high lipophilicity. Preclinical success has translated rather poorly into clinical success: few PPI inhibitors end up being marketed to patients (Scott et al. 2016). The following paragraph presents drug molecules approved for human use by the Food and Drug Administration (FDA) or European Medicines

Agency (EMA), which act by inhibiting PPIs (US National Institute of Health 2019; Scott et al. 2016).

Tirofiban and eptifibatide are inhibitors of the protein-protein interaction between fibrinogen and the platelet integrin receptor glycoprotein IIb/IIIa (Phillips & Scarborough 1997; McClellan & Goa 1998; King et al. 2016). Both are approved by FDA and EMA for prevention of MI in suspected non-ST elevation acute coronary syndrome (NSTE-ACS). Tirofiban is a small molecule, while eptifibatide is a cyclic peptide (Figure 2). Lymphocyte function-associated antigen 1 (LFA-1)/intercellular adhesion molecule 1 (ICAM-1) inhibitor lifitegrast has been approved by FDA for the treatment of dry eye syndrome, while the drug has yet to gain approval from EMA (Holland et al. 2017; Keating 2017). Venetoclax, a BCL-2 inhibitor developed by AbbVie/Genentech, is approved by FDA and European Medicines Agency (EMA) for treatment of chronic lymphocytic leukaemia (CLL) with 17p deletion as a monotherapy and to all CLL patients when combined with rituximab after at least one prior treatment (Stilgenbauer et al. 2016; Deeks 2016; Roberts et al. 2016; Seymour et al. 2018). Additionally, several compounds against PPIs are currently in late-stage clinical trials (Table 1, Figure 3).

2.5 Transcription factor GATA binding protein 4

GATA4 is a TF that belongs to a family of six similar proteins, named GATA1-GATA6 (Pikkarainen et al. 2004). Transcription factors are proteins which bind to specific DNA sequences at promoter regions of target genes and regulate gene transcription (Lambert et al. 2018). The GATA family is characterized by specific binding to 5'-(A/T)GATA(A/G)-3' DNA sequences (Pikkarainen et al. 2004). While these factors have a broad expression pattern around various tissues and cell types, GATA4 is found especially in the heart, lungs, intestines, gonads and liver tissues. This chapter explores the structure, function and regulation of GATA4 in the heart.

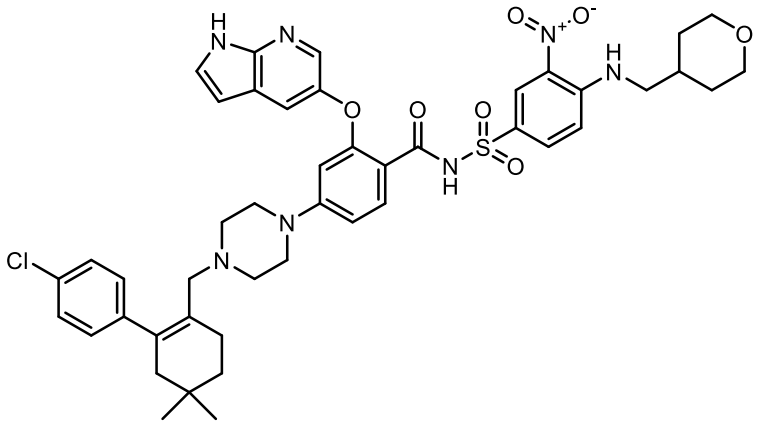

Venetoclax

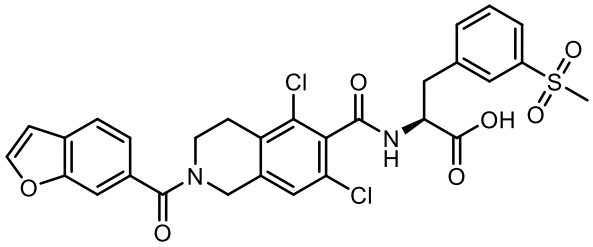

Lifitegrast

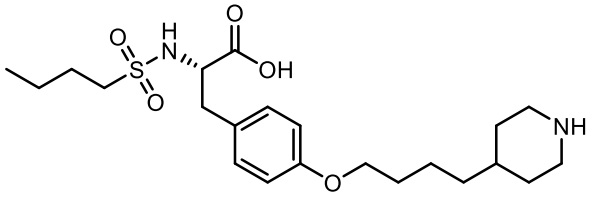

Tirofiban

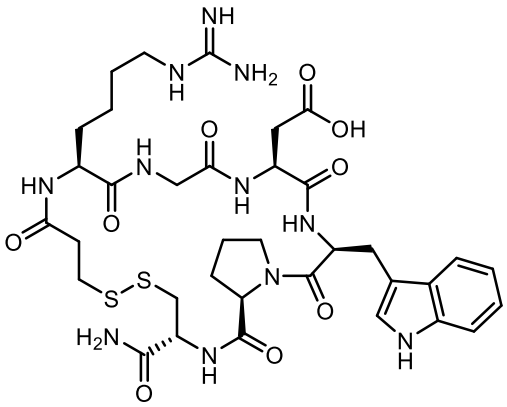

Eptifibatide

Figure 2. Structures of PPI-inhibitors approved for marketing.

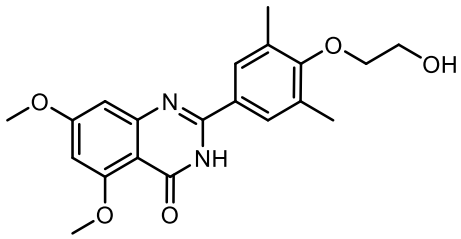

Apabetalone

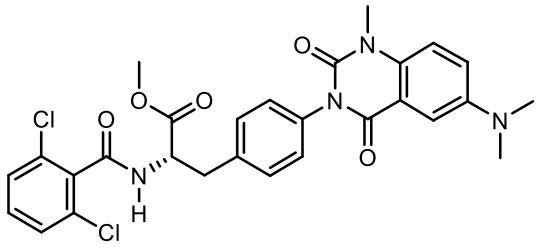

Carotegrast methyl

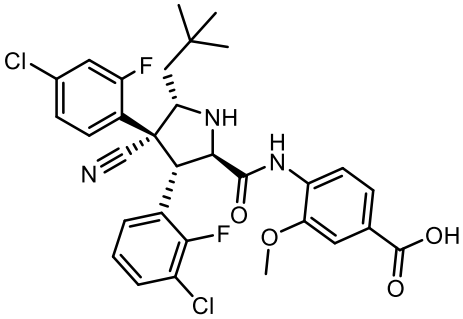

Idasanutlin

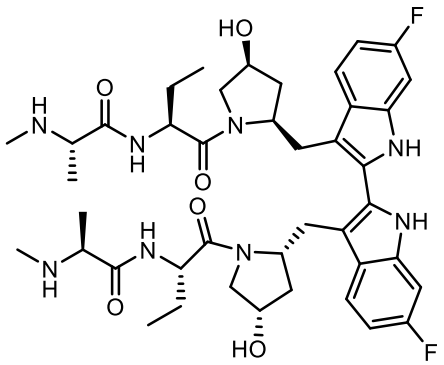

Birinapant

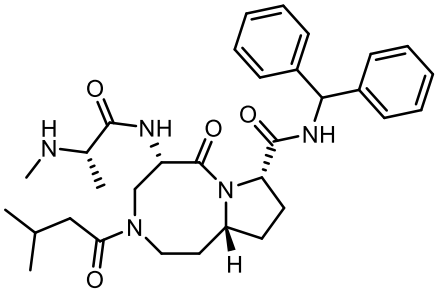

AT-406

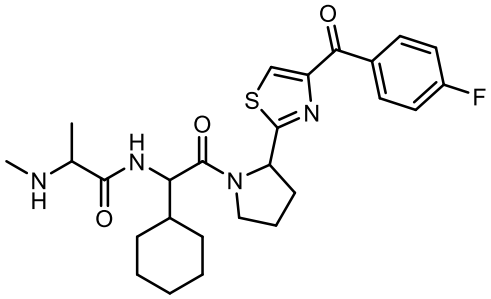

LCL-161

Figure 3. Structures of selected PPI-inhibitors in clinical trials.

2.5.1 Structure of GATA4

GATA4 is a 442 amino acid long and 44,5 kDa heavy soluble protein with two zinc-finger moieties, which are responsible for DNA binding (The UniProt Consortium 2019; Molkentin 2000). The zinc fingers, starting from amino acids 217 and 271 respectively in human GATA4, consist of four cysteine residues, which form coordination bonds with a Zn^{2+} ion, and 17 aa long loops of mostly hydrophilic

amino acids. The fingers are separated by 29 amino acids. Amino acid sequences of zinc finger regions are highly homologous across the members of GATA family and structurally very conserved across different species (Molkentin 2000; Pikkarainen et al. 2004). While a NMR structure of the C-terminal zinc finger region is available (PDB ID 2m9w), features responsible for interactions with other transcription factors are currently structurally unknown. Several target sites of posttranslational modifications are present in the protein, which will be discussed in chapter 2.5.3.

Table 1. Selected PPI inhibitors in clinical trials. Data was retrieved from ClinicalTrials.gov (US National Institute of Health 2019; Scott et al. 2016). MDM2, mouse double minute 2 homolog; AML, acute myeloid leukaemia; BET, bromo- and extra-terminal domain; DIABLO, second mitochondria-derived activator of caspases; HDL, high-density lipoprotein

Drug molecule	Developer	Mechanism	Indication	Phase	References
Apabetalone	Resverlogix	BET inhibition, reduces HDL levels	Cardiovascular diseases + others	III	(Picaud et al. 2013; Siebel et al. 2016)
Carotegrast methyl (AMJ300)	Ajinomoto	α4β1 integrin antagonist	Ulcerative colitis	III	(Yoshimura et al. 2015)
Idasanutlin	Roche	MDM2 inhibition	AML, Non-Hodgin lymphoma, follicular lymphoma	III/II	(Reis et al. 2016; Mascarenhas et al. 2017)
Birinapant	Tetralogic	DIABLO mimetic	Solid tumors	II	(Perimenis et al. 2016)
AT-406 (DEBIO-1143)	Ascenta Therapeutics	DIABLO mimetic	Solid tumors	II	(Thibault et al. 2018)
LCL-161	Novartis	DIABLO mimetic	Solid tumors	II	(Bardia et al. 2018)

2.5.2 Role of GATA4 in cardiac development and function

GATA4 has a substantial relevance in the development of the heart and differentiation of cardiac myocytes. Expression of GATA4 begins at 7 days postcoitum (dpc) and remains strong after the birth of the rat (Heikinheimo et al. 1994; Bisping et al. 2006). Development of rat heart requires GATA4 to progress and newly fertilized rat embryos with GATA4 deletion die due to insufficient heart tube

formation at 9 dpc (Molkentin et al. 1997; Kuo et al. 1997). Additionally, deletion of GATA4 at different stages of embryonic development and adulthood of rats and gene mutations in humans have been linked to several malignities, such as cardiomyopathies, congenital heart defects (CHD), deteriorated heart function and CM apoptosis (Garg et al. 2003; Oka et al. 2006; Tomita-Mitchell et al. 2007; Li et al. 2013). While GATA4 is indispensable in precardiac tissue development, GATA6 seems to function as an adequate substitute for GATA4 in cardiomyocyte differentiation (Kuo et al. 1997; Molkentin et al. 1997).

In adult mice, GATA4 acts as a mediator of pro-hypertrophic signals (Liang et al. 2001a; Suzuki 2011). Liang et al. (2001) performed extensive experiments and imaging *in vitro* and on GATA4 transgenic mouse models. The group established a direct link between forced cardiac-specific over-expression of GATA4 and hypertrophic events, such as cellular area and total protein amount increase of CMs, thickening of the left ventricular wall and overall weight gain of the heart. The effect hypertrophic effect was observed both after treatment with α_1-agonist phenylephrine (PE) and without additional treatment. GATA4-mediated pathways are involved in pressure overload and stretch-induced hypertrophy of CMs as well (Herzig et al. 1997; Hasegawa et al. 1997; Pikkarainen et al. 2003). Overexpression of GATA4 after MI has cardioprotective effects through revascularization of the affected tissue (Rysä et al. 2010). In addition, cardiac toxicity associated with anthracycline chemotherapeutics is alleviated by overexpression of GATA4, which further demonstrates the cardioprotective effects of GATA4 (Kim et al. 2003; Kobayashi et al. 2010).

2.5.3 GATA4 regulation by cellular signalling and epigenetics

Several posttranslational modifications affect GATA4, including phosphorylation, acetylation, sumoylation and ubiquitination (Suzuki 2011; Katanasaka et al. 2016). Several phosphorylation sites exist, with different factors targeting different residues. ERK and p38 MAPK activate GATA4 by increasing DNA binding activity via phosphorylation of serine-105 (Liang et al. 2001b; Tenhunen et al. 2004;

Pikkarainen et al. 2004). Serine-105 phosphorylation is directly linked to increased hypertrophy *in vivo* and seems to protect GATA4 from proteasomal degradation (van Berlo et al. 2011; Jun et al. 2013b). Additionally, PKC directly phosphorylates GATA4 at serine-419/420 and subsequently increases the DNA binding activity (Wang et al. 2005). Interestingly, phosphorylation at an unknown site by glycogen synthase kinase 3 beta (GSK3β) increases GATA4 efflux from the nucleus, which inhibits GATA4 activity (Morisco et al. 2001; Kerkelä et al. 2008).

Acetylation of proteins is commonly linked to histone modification and regulation of gene transcription (Grunstein 1997). However, other proteins with amine residues may be acetylated as well. Protein p300 is a nucleus-residing protein with histone acetyltransferase (HAT) activity, which acetylates GATA4 at several lysine residues (Yanazume et al. 2003; Takaya et al. 2008). Acetylation promotes GATA4 activity and seems to protect GATA4 from ubiquitin-mediated degradation (Yanazume et al. 2003; Suzuki et al. 2004). Phosphorylation at serine-261, which lies in the region between the zinc finger moieties, has been found to enhance p300-mediated acetylation of GATA4 (Jun et al. 2013a). Deacetylation of GATA4 occurs through the cooperation of homeodomain-only protein (HOPX) and histone deacetylase 2 and genetic homozygous knockout of both proteins leads to increased GATA4 activity *in vivo* (Trivedi et al. 2010).

He and co-workers (2012) studied the effect of methylating enzyme polycomb-repressive complex 2 (PRC2) on GATA4 *in vitro.* PRC2 was found to trimethylate GATA4 at lysine-299 to inhibit acetylation by p300. However, lysine-299 is non-required for p300 binding. Linking small ubiquitin-like modifier 1 (SUMO-1) to GATA4 by the SUMO E3 ligase protein inhibitor of activated STAT1 (PIAS1) increases GATA4 by increasing nuclear residence of the TF (Wang et al. 2004). The sumoylation occurs on lysine-366 of GATA4, as shown by point mutation experiments. Sumoylation has a role in the regulation of other cardiac TFs as well (Wang & Schwartz 2010).

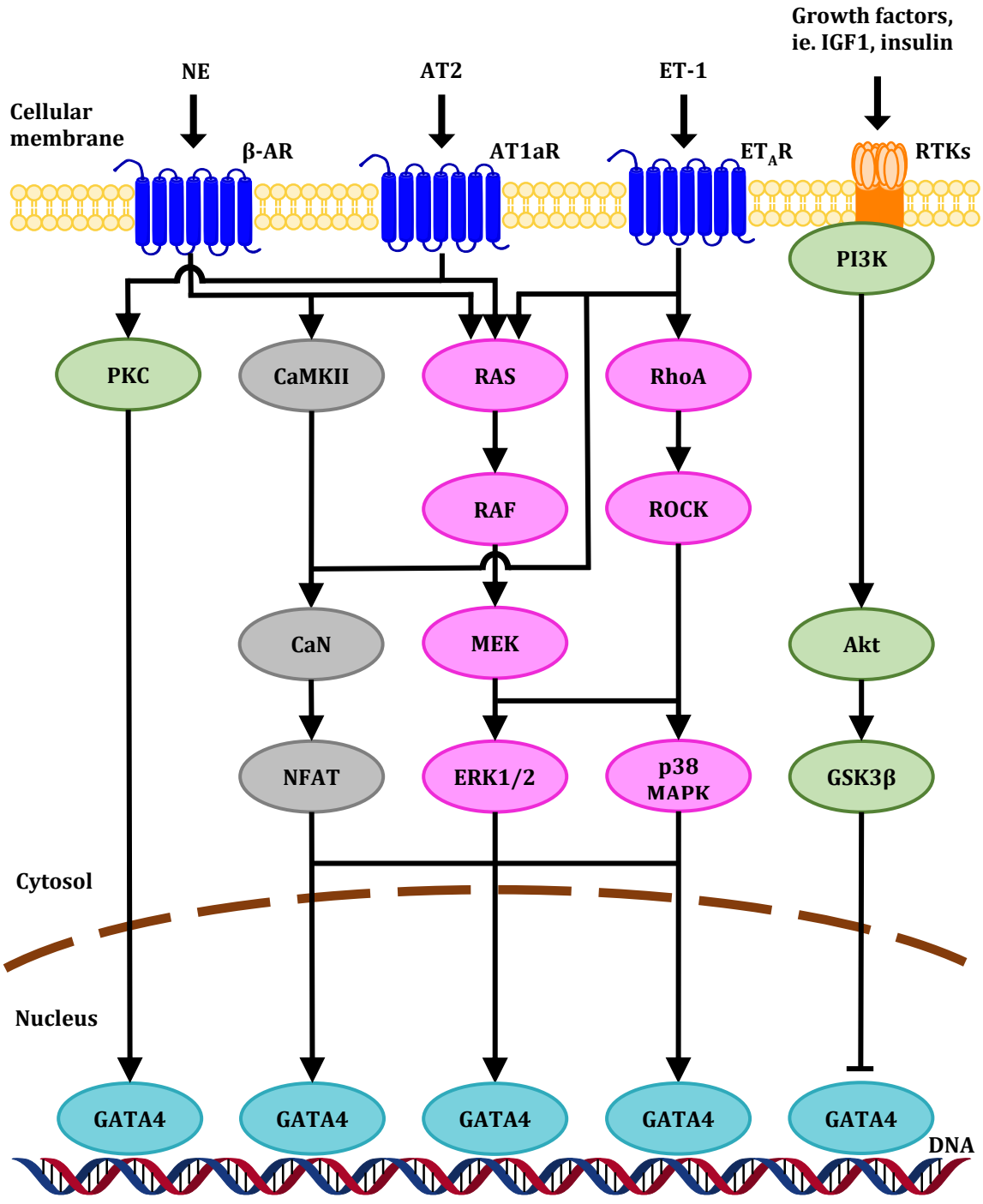

Figure 4. GATA4 activity is regulated by a complex network of extra-and intracellular signals. AT1aR, angiotensin II type 1a receptor; AT2, angiotensin II; β-AR, β-adrenergic receptor; CaMKII, Ca^{2+}/calmodulin-dependent kinase II; CaN, calcineurin; DNA, deoxyribonucleic acid; ERK, extracellular signal–regulated kinases; ET-1, endothelin-1; ET_AR, endothelin type A receptor; GATA4, GATA binding protein 4; GSK3β, glycogen synthase kinase 3 beta; IGF1, insulin-like growth factor 1; MAPK, mitogen-activated protein kinase; MEK, mitogen-activated protein kinase kinase; NE, noradrenaline; NFAT, nuclear factor of activated T-cells, cytoplasmic 4; PI3K, phosphoinositide 3-kinase; PKC, phosphokinase C; RhoA, Ras homolog family, member A; ROCK, Rho-associated protein kinase; RTK, receptor tyrosine kinase.

Expression and activity of GATA4 is highly regulated by several extra- and intracellular factors (Pikkarainen et al. 2004; Suzuki 2011; Tham et al. 2015). Extracellular messengers angiotensin II, endothelin-1 (ET-1) and noradrenaline (through β-adrenergic receptors [β-AR]) are major influencers of blood pressure, but also mediators of pro-hypertrophic signalling (Figure 4). Intracellular pathways, which are downstream of extracellular regulators, include PKC pathway and RAS-RAF-MEK-ERK-pathways. Additionally, intracellular calcium is a major factor in regulation of GATA4 activity.

Pathways downstream of angiotensin II type 1a receptor (AT1aR) involving GATA4 resemble those of β-AR, with PKC associated especially to angiotensin II -mediated GATA4 activation (Wang et al. 2005; Tham et al. 2015). GATA4 is directly phosphorylated by PKC, as shown by Wang et al. (2005), which increases GATA4 activity. PKC activation is sufficient to induce maladaptive hypertrophy by itself, but deletion of PKC activity lacks a cardioprotective effect (Bowman et al. 1997; Roman et al. 2001).

ET-1 is a 21 aa long highly potent vasoconstricting peptide which has been strongly linked to pro-hypertrophic signalling (Bupha-Intr et al. 2012; Davenport et al. 2016). ET-1 binds to at least four subtypes of GPCR endothelin receptors, of which ET_A receptor (ET_AR) is the most abundant in the heart. Activation of ET_AR leads to phosphorylation of GATA4 in a mitogen-activated protein kinase kinase (MEK) -dependent manner as shown by Kitta et al. (2001). GATA4 binding to BNP promoter region was enhanced by pressure overload *in vivo* and direct left ventricular wall stretch *ex vivo* (Hautala et al. 2001; Hautala et al. 2002). These effects were attenuated with a non-selective ET-receptor antagonist bosentan. Furthermore, ET-1 activates CaN, which in turn activates nuclear factor of activated T-cells, cytoplasmic 4 (NFATc4) to induce GATA4 activity (Kakita et al. 2001).

Stimulation of β-AR has been found to cause cardiac hypertrophy (Engelhardt et al. 1999). These receptors regulate GATA4 through several mechanisms. β-AR stimulation by a selective β-agonist isoproterenol increases expression of GATA4

(Saadane et al. 1999). The same study found an increase in GATA4 expression by PE, which Morimoto et al. (2000) linked to an increase in ET-1 expression (discussed below). An increase in GATA4 activity by β-AR stimulation is caused by phosphorylation of GATA4 by ERK and activation CaMKIIγ and CaMKIIδ subtypes (Lorenz et al. 2009; Tham et al. 2015; Dewenter et al. 2017). Thus, β-AR are major regulators of Ca^{2+} signalling as well.

Ras homolog family, member A (RHOA) is a RAS-protein belonging to a group of small GTPases (guanosine-5'-triphosphate). It functions downstream of GPCRs and activates other signal transducers in the cytosol. RHOA stimulation has been found to activate GATA4 via p38 MAPK-mediated phosphorylation (Aikawa et al. 1999; Charron et al. 2001). However, other reports have concluded that RHOA activates GATA4 by ERK-mediated phosphorylation (Yanazume et al. 2002).

2.5.4 Downstream targets of GATA4

GATA4 interacts with promoters of several genes associated with the heart, including atrial natriuretic peptide (*NPPA*), B-type natriuretic peptide (*NPPB*), α-myosin heavy chain (*MYH6*), β-myosin heavy chain (*MYH7*), cardiac troponin I (*TNNI3*), cardiac troponin C (*TNNC1*), AT1aR and actin alpha cardiac muscle 1 (*ACTC1*), to mention a few (Akazawa & Komuro 2003; Pikkarainen et al. 2004; Peterkin et al. 2005). In addition to being biomarkers for MI, natriuretic peptides lower blood pressure through increased sodium excretion via the kidneys, vasodilatation and RAAS inhibition (Ruskoaho 1992; Martinez-Rumayor et al. 2008; Sergeeva & Christoffels 2013). Additionally, release of natriuretic peptides, especially BNP, serves as a clinical biomarker of cardiac hypertrophy, MI and HF.

In hypertrophic stimulation, expression of structural proteins of cardiomyocytes is enhanced. Troponins I and C are structural components of tropomyosin complex, which functions as a regulator of Ca^{2+} ion concentration in muscle tissue (Ebashi et al. 1968; Katrukha 2013). Sarcoplasmic reticulum releases Ca^{2+} ions into the cytosol during cardiac action potential. Tropomyosin binds the excess calcium through

troponin, which progresses the contraction cascade of myofibrils, the basic components of sarcomeres. Actin alpha cardiac muscle 1 (ACTC1), α-myosin heavy chain (α-MHC) and β-myosin heavy chain (β-MHC) are long, linear proteins, which are major structural component of muscle cells and are incorporated in the structure of myofibrils (Walker & Spinale 1999). ACTC1 and tropomyosin along with troponin are constituents of thin filaments, while α-MHC and β-MHC monomers are part of the thick filaments in atrial and ventricular cardiac muscle, respectively. Joint overexpression of these structural proteins allows hypertrophy of cardiomyocytes, which leads to growth of the heart.

2.5.5 Interactions of GATA4 and other transcription factors

GATA4 interacts with numerous TFs inside the nucleus (Pikkarainen et al. 2004; Peterkin et al. 2005). GATA-binding protein 6 (GATA6) was identified early as a cooperative factor of GATA4 (Charron et al. 1999). Association of these GATA factors increases the expression of natriuretic peptide genes and thus leads to lowered blood pressure and cardioprotection. Friend of GATA-2 (FOG-2) belongs to a family of TFs which bind to and modulate the activity of GATA factors, as the name suggests (Tevosian et al. 1999). Interaction of FOG-2 with GATA4, which occurs through association by several zinc fingers, suppresses GATA-4-mediated transcription of natriuretic peptides and α-MHC (Fox et al. 1999; Svensson et al. 2000; Hirai et al. 2004). Suppressive effects of FOG-2 are linked to inhibition of p300-mediated acetylation of GATA4 (Hirai et al. 2004).

MEF2C interacts synergistically with GATA4 (and GATA6) to activate GATA binding sites (Morin et al. 2000; Dong et al. 2017). Of note, the activity of MEF2C is at least partially dependent of CaMKII-mediated release of suppression by histone deacetylase 4 (Lu et al. 2000). Transcription products of MEF2C-GATA4 interaction include A-type natriuretic peptide (ANP), BNP, ACTC1 and α-MHC (Morin et al. 2000). Thus, MEF2C and FOG-2 may be regarded as a counter-effectors. TBX5 is another cardiac TF which interacts with GATA4. Transfection of GATA4 and TBX5 into cervical cancer (HeLa) cells revealed cooperative GATA binding site-induced

ANP reporter gene transcription by these TFs and G296S mutation of GATA4 abolishes this interaction (Garg et al. 2003; Ang et al. 2016). Additionally, serious cardiac defects occur in mice following disruption of TBX5-GATA4 interaction (Maitra et al. 2009; Misra et al. 2014).

Calcium signalling effector NFATc4 is a TF with several activities in the cardiac setting (Molkentin et al. 1998; Bushdid et al. 2003). Transcription of BNP is synergistically upregulated through the association of NFATc4 and GATA4. NFATc4-mediated hypertrophy is abolished by ciclosporin, a CaN inhibitor (Sussman et al. 1998). NFATc4 activity is regulated through phosphorylation by GSK3β, which facilitates export from the nucleus and subsequent ubiquitin-mediated degradation (Beals et al. 1997; Fan et al. 2008).

Serum response factor (SRF) is a TF which interacts with GATA4 and other TFs in a synergistic manner to activate several cardiac genes, including *NPPA*, *NPPB* and *MYH6* (Belaguli et al. 2000; Morin et al. 2001). In addition, concomitant overexpression of GATA4, NKX2-5 and SRF revealed a tripartite synergistic interaction and increased transcription of cardiac genes (Nishida et al. 2002; Sepulveda et al. 2002). In a similar manner to MEF2C, suppression of SRF by histone deacetylase 4 is lifted by CaMK-mediated phosphorylation (Davis et al. 2003). Signal transducers and activators of transcription (STATs) are a family of proteins which are effectors downstream of janus kinases (JAKs) and significance in a cardiac setting (Booz et al. 2002). More specifically, STAT1α has been found to synergistically activate GATA4-mediated ANP transcription (Wang et al. 2005). STAT3 on the other hand has been described as a direct modulator of TBX5, GATA4 and NKX2-5 transcription, with implications in CM differentiation (Snyder et al. 2010).

Synergy of GATA4 and NKX2-5 was first observed by Durocher et al. (1997), who observed a synergistic induction of ANP and BNP transcription upon co-transfection of the two TFs into HeLa cells. Interestingly, both NKE, a designated binding site for NKX2-5, and GATA binding sites are required for the synergy to occur and deletion

of either binding site from the promoter region of *NPPA* abolishes transcriptional synergy. Similar synergy was observed for ACTC1 transcription as well (Sepulveda et al. 1998). Upon synergistic activation, a physical contact of C-terminal zinc finger of GATA4 and homeodomain of NKX2-5 occurs, with the deletion of homeobox domain abolishing synergy (Lee et al. 1998; Sepulveda et al. 1998). As briefly discussed above in this chapter, NKX2-5 additionally interacts with several other TFs, such as TBX5, SRF and GATA6 (Molkentin et al. 2000; Nishida et al. 2002; Sepulveda et al. 2002; Luna-Zurita et al. 2016). Chromatin immunoprecipitation studies have affirmed the importance of NKX2-5, among other TFs, in early cardiac development (He et al. 2011). A recent paper discusses the importance of JAK kinase signalling, p38 MAPK and temporal control of TFs, including GATA4 and NKX2-5, in CM differentiation (Li et al. 2019).

2.5.6 Modulating the synergy of GATA4 and NKX2-5 by small molecules

The interaction between GATA4 and NKX2-5 has been studied in detail by Kinnunen et al. (2015). The group built a homology model of GATA4 zinc finger region and homeodomain of NKX2-5 based on previously crystallized, highly identical proteins GATA1/GATA3 and thyroid receptor factor 1. Key amino acid interactions between the proteins were predicted by using the model and previous studies as a starting point. Following the identification of the C-terminal extension of NKX2-5 and the C-terminal zinc finger of GATA4 as key regions of successful PPI, point mutations to the GATA4 protein were designed and produced *in vitro*. The study revealed several activating and inactivating point mutations in the PPI region. An *in silico* model for GATA4-NKX2-5 interaction was constructed with the acquired data, which revealed a nuclear receptor-like binding mode for these TFs.

Following the identification of the interaction region of GATA4 and NKX2-5, *in vitro* and *in silico* screening campaigns were launched to discover inhibitors of the interaction (Välimäki et al. 2017). Screening campaign of 800 compounds on immunoprecipitation and luciferase reporter gene assays *in vitro* revealed several micromolar inhibitors of the GATA4-NKX2-5 transcriptional synergy. The most

potent hit was *N*-[4-(diethylamino)phenyl]-5-methyl-3-phenylisoxazole-4-carboxamide (compound **1**; Figure 5), which inhibited the interaction with a half maximal inhibitory concentration (IC_{50}) of 3 μM. Several other hits with IC_{50} in the low micromolar region were found as well. Further tests showed no significant inhibition of GATA4 or NKX2-5 binding to DNA. Thus, the reduction of luciferase activity by **1** may be attributed to decrease in transcriptional synergy instead of direct inhibition of DNA binding. Compound **1** was shown to decrease ET-1-induced *NPPB* transcription statistically significantly and *NPPA* transcription non-statistically significantly. In addition, molecular modelling experiments concluded that dislocation of NKX2-5 C-terminal loop extension and subsequent blockade of GATA binding sites is required to inhibit GATA4-NKX2-5 interaction.

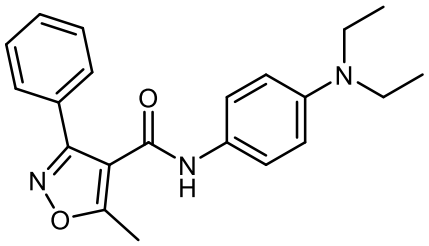

1

Figure 5. Structure of *N*-[4-(diethylamino)phenyl]-5-methyl-3-phenylisoxazole-4-carboxamide (compound **1**).

The activity of **1** was further evaluated *in vitro* and *in vivo* (Kinnunen et al. 2018). The suppressive effect on *NPPA* and *NPPB* transcription was re-confirmed in cultured neonatal rat CMs both with and without PE stimulation. PE-enhanced phosphorylation of GATA4 was likewise significantly reduced by co-cultured compound **1**. A significantly attenuated decrease of left ventricular ejection fraction and fractional shortening following MI was found in mice treated with **1** compared to non-treated mice. Similar trend without significance was found on rats. In an angiotensin II-induced pressure overload rat model a significant improvement of ejection fraction and fractional shortening was observed for mice treated with compound **1** compared to vehicle-treated controls.

While the initial report by Välimäki et al. (2017) found no significant cytotoxicity for **1**, as measured by adenylate kinase release, further studies on the toxicity of **1** and selected derivatives were conducted (Karhu et al. 2018). In this study, the toxicity of the GATA4-acting compounds was studied with the lactate dehydrogenase (LDH) and 3-(4,5-dimethylthiazol-2-yl)-2,5-diphenyltetrazolium (MTT) bromide assays in eight different cell lines. LDH assay measures necrotic cell death by investigating LDH leakage through cell membrane perforations, while MTT assay assesses oxidoreductase enzyme activity in mitochondria and other intracellular compartments. The study found significant differences in mitochondrial toxicity depending on the cell type and molecular structure of the compounds. Of note, compound **1** was found to be significantly toxic to hiPSC cells at 3 μM and mouse ESCs at 30 μM, while no significant reduction in viability of other cell types was found in the studied concentration range of 1–30 μM. Several other compounds in the study set were found to be toxic to hiPSC cells, while lacking toxicity on hiPSC-derived CMs. Structure-toxicity relationship studies identified a correlation between the dihedral angle of the two southern part rings, which in the case of compound **1** are the isoxazole ring and non-substituted phenyl ring, and stem cell toxicity. Thus, structural modifications on the non-substituted phenyl ring are warranted to allow for further pre-clinical advancement of compound **1**.

3 AIMS OF THE STUDY

The aim of this work was to design and synthesise derivatives of hit compound **1** with electron-donating substituents and to study the effects of these modifications on stem cell toxicity of **1**. In a previous study by Karhu et al. (2018) the torsional angle between the southern isoxazole ring and phenyl ring was hypothesised to be a major contributor to toxicity of **1**. Increasing the biplanar angle between the two southern rings by introducing substituents to the phenyl ring could alleviate this toxicity. In addition, modulating the electron density of the phenyl ring could modify interactions between **1** and the receptors responsible for toxicity.

The newly synthesised compounds would be tested on the luciferase, MTT and LDH assays as previously described (Välimäki et al. 2017; Karhu et al. 2018). MTT and LDH assays were chosen to account for different mechanisms of toxicity, while the luciferase reporter system was chosen to allow for robust comparison with previously acquired data on other derivatives of **1**. In addition, stem cell toxicity of five previously synthesised compounds was to be evaluated in conjunction with the new compounds and **1** would partake the biological assays as a control. Previously synthesised and assayed derivatives of **1** lacked moieties which donate electrons or drastically change the biplanar torsion angle. Thus, these newly designed compounds could help in refining the *in silico* model of GATA4-NKX2-5 interaction and improve the knowledge of structure-toxicity-relationships of **1**.

4 MATERIALS AND METHODS

4.1 Synthetic procedures

Chemicals used in organic synthesis are presented in table 2 and were obtained from Sigma-Aldrich (Steinheim, Germany), TCI Europe (Zwijndrecht, Belgium), Combi-Blocks (San Diego, CA, USA), Enamine (Kyiv, Ukraine), Altia (Rajamäki, Finland), Apollo Scientific (Stockport, UK) and VWR Chemicals (Radnor, PA, USA). While the synthesis of compound **1** has been reported previously (Välimäki et al. 2017; Karhu et al. 2018), the compound in this study was obtained from Pharmatory (Oulu, Finland). Other test compounds were synthesised in-house. Water-sensitive reactions were conducted under inert argon atmosphere in oven-dried glassware. The progress of reactions was monitored by thin-layer chromatography (TLC) on 0.2-mm silica gel plates (silica gel 60, F254, Merck KGaA, Darmstadt, Germany). Visualisation of compounds was achieved by UV light or 2,4-dinitrophenylhydrazine stain (Brady's test), where suitable. The molecular weights of products in TLC analysis were measured with Advion® expression^{S} CMS compact mass spectrometer (Ithaca, NY, USA) equipped with an Advion® Plate express TLC plate extraction device. Chemical ionisation mode was used in the mass spectrometer.

Table 2. Chemicals used in synthetic work were obtained from several manufacturers and suppliers.

Name	CAS number	Supplier
Starting materials		
p-tolualdehyde	104-87-0	Sigma-Aldrich
m-tolualdehyde	620-23-5	Sigma-Aldrich
o-tolualdehyde	529-20-4	Sigma-Aldrich
2,6-dimethylbenzaldehyde	1123-56-4	Sigma-Aldrich
p-anisaldehyde	123-11-5	Sigma-Aldrich
m-anisaldehyde	591-31-1	Combi-Blocks
3,5-dimethoxybenzaldehyde	7311-34-4	TCI
3-cyclopropyl-5-methyl-1,2-oxazole-4-carboxylic acid	1082420-70-9	Enamine
3-cyclopentyl-5-methyl-1,2-oxazole-4-carboxylic acid	1082369-20-3	Enamine
3-cyclohexyl-5-methyl-1,2-oxazole-4-carboxylic acid	55278-64-3	Enamine
Reagents		
Hydroxylammonium chloride	5470-11-1	Sigma-Aldrich
Pyridine (anhydrous)	110-86-1	Sigma-Aldrich
(Diacetoxyiodo)benzene (DIB)	3240-34-4	Sigma-Aldrich
Ethyl-2-butynoate	4341-76-8	Apollo Scientific
Lithium hydroxide	1310-65-2	Sigma-Aldrich
N,N,N′,N′-Tetramethyl-O-(1H-benzotriazol-1-yl)uronium hexafluorophosphate (HBTU)	94790-37-1	Sigma-Aldrich
N,N-diisopropylethylamine (DIPEA)	7087-68-5	Sigma-Aldrich
N,N-diethyl-1,4-phenylenediamine	93-05-0	Sigma-Aldrich
Solvents		
Dry ethanol (99,5 % m/m)	64-17-5	Altia
Acetonitrile	75-05-8	Sigma-Aldrich
Tetrahydrofuran (THF)	109-99-9	Sigma-Aldrich
Methanol	67-56-1	Sigma-Aldrich
N,N-dimethylformamide (DMF; anhydrous)	68-12-2	Sigma-Aldrich
Ethyl acetate (EtOAc)	141-78-6	VWR Chemicals
n-heptane	142-82-5	VWR Chemicals
n-hexane	110-54-3	VWR Chemicals

Compounds were purified on a Biotage® Isolera™ Spectra One flash chromatography system (cat. # ISO-1SW, Biotage AB, Uppsala, Sweden) on Biotage® SNAP KP-SIL (10g, 25g or 50g; cat. # FSKO-1107-0010, FSKO-1107-0025 and FSKO-1107-0050, respectively) or SNAP Ultra (10g or 25g, cat. # FSUL-0442-0010 and FSUL-0442-0010, respectively) cartridges. Nuclear magnetic resonance (NMR) spectra (^{1}H and ^{13}C) were recorded on a Bruker Ascend™ 400 – Avance III HD NMR spectrometer (Bruker Corporation, Billerica, MA, USA). NMR spectra were analysed on MestReNova software (MestReLab, Santiago de Compostela, Spain).

Chemical shifts (δ) are reported in parts per million (ppm) relative to tetramethylsilane (TMS) signal. Exact mass and purity (>95%) of all tested compounds was evaluated by liquid chromatography-mass spectrometry (LC-MS) analyses with a Waters Acquity® ultra-high performance liquid chromatography (UPLC) system (Waters, Milford, MA, USA) equipped with an Acquity UPLC® BEH C18 column (1.7 µm, 50 × 2.1 mm, Waters, Ireland), an Acquity PDA detector and a Waters Synapt G2 HDMS mass spectrometer via an electrospray ion source in positive mode. High resolution mass data (HRMS) was reported for the molecular ions $[M+H]^+$.

4.2 Luciferase assay

Immortalised monkey kidney fibroblast (COS-1) cells were cultured in Dulbecco's Modified Eagle's Medium (DMEM; Media Kitchen, Institute of Biotechnology, University of Helsinki) supplemented with 10 % fetal bovine serum (FBS; cat. # 10500-064, Gibco, ThermoFisher Scientific, MA, USA) and 100 U/mL penicillin and 100 µg/mL streptomycin (cat. # 15140-122, Gibco) at 37 °C in a humidified atmosphere of 5 % carbon dioxide (CO_2). Cells were dissociated using Trypsin/EDTA solution (Media Kitchen) and seeded on Isoplate™-96 TC 96-well plates (cat. # 6005070, PerkinElmer, Turku, Finland) at 10 000 cells/well. On the following day, the cells were transfected with pGL3-3xHA luciferase reporter plasmid (100 ng/well), pMT2-Gata4 and pMT2-Nkx2-5 (total of 50 ng/well) using Fugene®6 transfection reagent (Fugene:DNA ratio 3:1; cat. # E2691, Pro-mega, WI, USA). All plasmid dilutions were performed to non-supplemented DMEM. pGL3-3xHA reporter gene plasmid contains three NKE-binding sites for NKX2-5 and a firefly luciferase gene (Kinnunen et al. 2015). Separate wells with empty pMT2 plasmid and either pMT2-Gata4 or pMT2-Nkx2-5 (total 50 ng/well) and reporter plasmid were used to confirm the presence of synergistic activation in each separate experiment.

Transfection cocktails were incubated on cells for 6 hours at 37 °C in a humidified atmosphere of 5 % CO_2 and the transfection solutions were replaced with study

compounds in supplemented DMEM. Control wells were treated with 0,25 % dimethyl sulfoxide (DMSO). After a 24-hour incubation the luciferase activity was measured with neolite® Reporter Gene Assay System (cat. # 6016711, PerkinElmer) according to manufacturer's instructions. Luminescence was measured by using a Victor^2 plate reader (PerkinElmer). Each compound was tested as 3 technical replicates in 3 or 4 experiments. Luminescent background values obtained from wells devoid of cells were subtracted from study values and luciferase scores were normalized to the combined mean of DMSO-treated GATA4-NKX2-5 synergy controls.

4.3 Toxicity assays

Cells from iPS(IMR90)-4 line (WiCell, Madison, WI, USA) were cultured in Essential 8™ medium (cat. # A1517001, Gibco) at 37 °C in a humidified atmosphere of 5 % CO_2. Cells were seeded on Costar® 3596 96-well plates (Corning Inc., NY, USA), which were treated with Matrigel® Matrix basement membrane (cat. # 354320, Corning Inc.), at 10 000 cells/well. During passaging, cells were dissociated using 1x Versene (cat. # 15040-066, Gibco) and resuspended in Essential 8™ medium containing 10 µM ROCK inhibitor (Y-27632) prior seeding. Cells were allowed to attach to well bottoms overnight and study compounds diluted with Essential 8™ medium were added to cells, followed by a 24-hour incubation. Control and maximal LDH release well were treated with 0,3 % DMSO to reflect maximal DMSO concentration in study compound dilutions. To determine the maximal release of LDH, cell membranes were dissociated with 0.9% Triton® X-100 (Sigma-Aldrich) 45-60 minutes prior to analysis protocol.

Toxicity assays were initiated by transferring 50 µl of cell culture medium from each well onto a fresh Nunc™ MicroWell™ non-sterile 96-well microplate (cat. # 260836, ThermoFisher). For LDH assays, substrate solution (1,3 mM β-nicotineamideadeninedinucleotide, 660 µM iodonitrotetrazolium, 54 mM L-(+)-lactic acid and 280 µM phenazine methosulphate in 0,2 M Tris-HCl buffer, pH 8,2) was prepared before the experiments. The chemicals were acquired from Sigma-

Aldrich, while the Tris-HCl buffer was received from Media Kitchen. Substrate solution (50 µL) was added to the medium-containing wells and the well plates were shaken at 400 rotations per minute for 10 minutes protected from light, followed by 20 minutes of incubation at room temperature. Colorimetric reaction was stopped by the addition of 50 µl 1 M acetic acid to each well and the plates were subsequently analysed with Victor^2 plate reader (1s measurement, 490 nm wavelength). Background absorbance was measured from wells without cells and was removed prior to calculation of cytotoxicity. Cytotoxicity percentage was calculated with the following formula: cytotoxicity (%) = [(sample − spontaneous LDH release)/(maximal LDH release − spontaneous LDH release)] * 100. Spontaneous LDH release is reflected by analysing DMSO-treated, non-lysed cells.

Mitochondrial toxicity measurement was initiated by the addition of 3-(4,5-dimethylthiazol-2-yl)-2,5-diphenyltetrazolium bromide solution to the cell-containing wells (final concentration 0,5 mg/mL). After incubating the plates for 100-120 minutes at 37 °C in a humidified atmosphere of 5 % CO_2, medium was aspirated and formazan crystals were dissolved in DMSO. The specific absorbance of formazan was measured with a Bio-Rad 680 microplate reader (Bio-Rad Laboratories Inc., CA, USA) at 550 nm, with absorbance at 650 nm subtracted as reference. MTT readouts were analysed as described in chapter 4.4 without further processing.

4.4 Statistical methods

The results were analysed by randomized block analysis of variance (ANOVA) method with treatments as fixed factors and different repeats as random factors in the model (Lew 2007). This way day-to-day variation of control values was accounted for. Tukey's HSD (honestly significant difference) post-hoc test was used to analyse the effects of individual treatments. For the analyses, non-normalized data was used to avoid omitting the variance of control values and violating the rules of ANOVA. Additionally, Grubbs's test for outliers was used to remove outliers from the raw data (Grubbs 1950). IBM Statistical Package for the Social Sciences (SPSS)

software package version 25 was used to conduct statistical analyses. Statistical significance is expressed in relation to DMSO-treated control values ($p < 0,05$).

5 RESULTS

5.1 Synthesis of study compounds

Modifications to the structure of **1** were designed and subsequently synthesised (Figure 6). In addition to the four *para* and *meta* derivatives presented in chapter 3 (compounds **2**-**5**), *ortho*-methyl **6** and *ortho*-dimethyl **7** derivatives of **1** were synthesised. Three derivatives with the phenyl ring substituted by a saturated hydrocarbon ring were prepared as well: cyclopropyl **8**, cyclohexyl **9** and cyclopentyl **10** derivatives. Based on initial luciferase results of compounds **2**-**5**, a *meta*-dimethoxy-substituted derivative **11** was designed and synthesised. Structures of previously synthesised compounds **12-16**, which were selected for toxicity assays on hiPSC cells, are presented in Figure 7.

The general synthesis route for **1** is reported previously by Karhu et al. (2018). A slightly modified version of this route was used for compounds **2**-**11,** which is described in more detail in chapter 8 (Scheme 1). The first step involves the conversion of aryl aldehydes **18a-g** to the corresponding aldoximes **19a-g** in reaction **a**. This reaction is an S_n2 reaction between the aldehyde carbonyl and hydroxylamine, which in basic conditions is proposed to proceed through a nucleophilic attack of hydroxylamine nitrogen to the carbonyl carbon to form a tetrahedral intermediate. The carbonyl oxygen is subsequently protonated by the two *N*-hydrogens, releasing the oxygen as a water molecule and forming a double bond between the carbon and nitrogen atoms. Yields 13–100%.

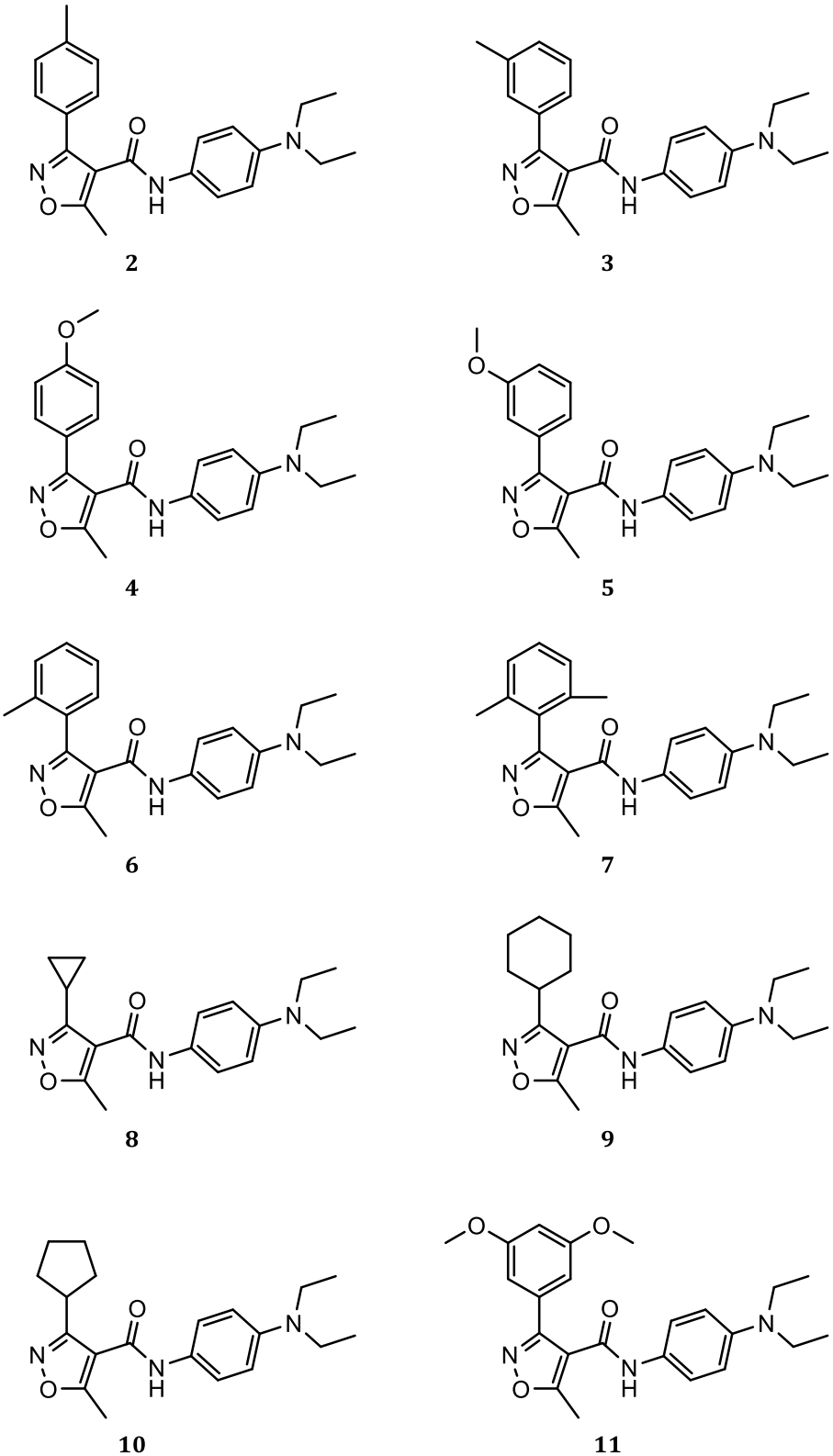

Figure 6. Structures of successfully synthesised, purified and analysed novel inhibitors of GATA4-NKX2-5 synergy.

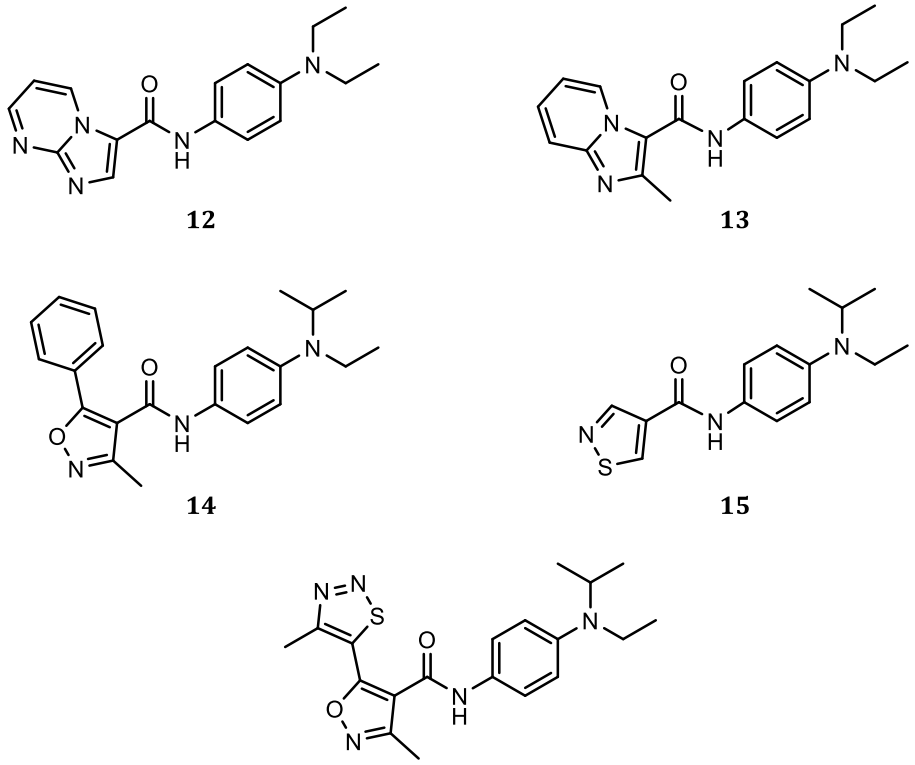

Figure 7. Structures of previously synthesised compounds, which partook the toxicity assays.

Reaction **b** is a 1,3-dipolar cycloaddition of an alkyne-containing carboxylic acid ester and an oxime, which involves a nitrile oxide intermediate (Huisgen 1963). First, the hypervalent iodine reagent (diacetoxy)iodobenzene (DIB) deprotonates the oxime, which forms a nitrile oxide intermediate (Singhal et al. 2016). This 1,3-dipole then reacts with the triple bond in ethyl-2-butynoate to form a five-membered intermediate, which formed isoxazoles **20a-g** after the rearrangement of electrons. Yields 13–73%. The ethyl group of carboxylic acid esters was removed by base-catalysed hydrolysis (reaction **c**) to yield carboxylic acids **21a-g**. A 1:1:1 mixture of tetrahydrofuran (THF), methanol (MeOH) and H_2O as solvent. Yields 67–93%.

Lastly, the final products **2**-**11** were obtained by amide coupling (reaction **d**) of *N,N*-diethyl-1,4-phenylenediamine to acids **21a-g** obtained in reaction **c** and commercially available acids **21h-j**. The coupling reagent of choice was *N,N,N′,N′*-tetramethyl-O-(1H-benzotriazol-1-yl)uronium hexafluorophosphate (HBTU),

which belongs to the commonly used class of uronium salt coupling agents (Valeur & Bradley 2009). The acid is deprotonated by a base, which was *N,N*-diisopropylethylamine (DIPEA) in this study, after which the carboxylate ion attacks HBTU through the proposed mechanism shown in Scheme 2. A sterically hindered base was chosen to avoid non-desired amide coupling with the base. The benzotriazole moiety is displaced by the amine in an Sn2 reaction, forming the end products **2-11**. Yields 50–97%. All products were of >95% purity, as analysed by LC-MS.

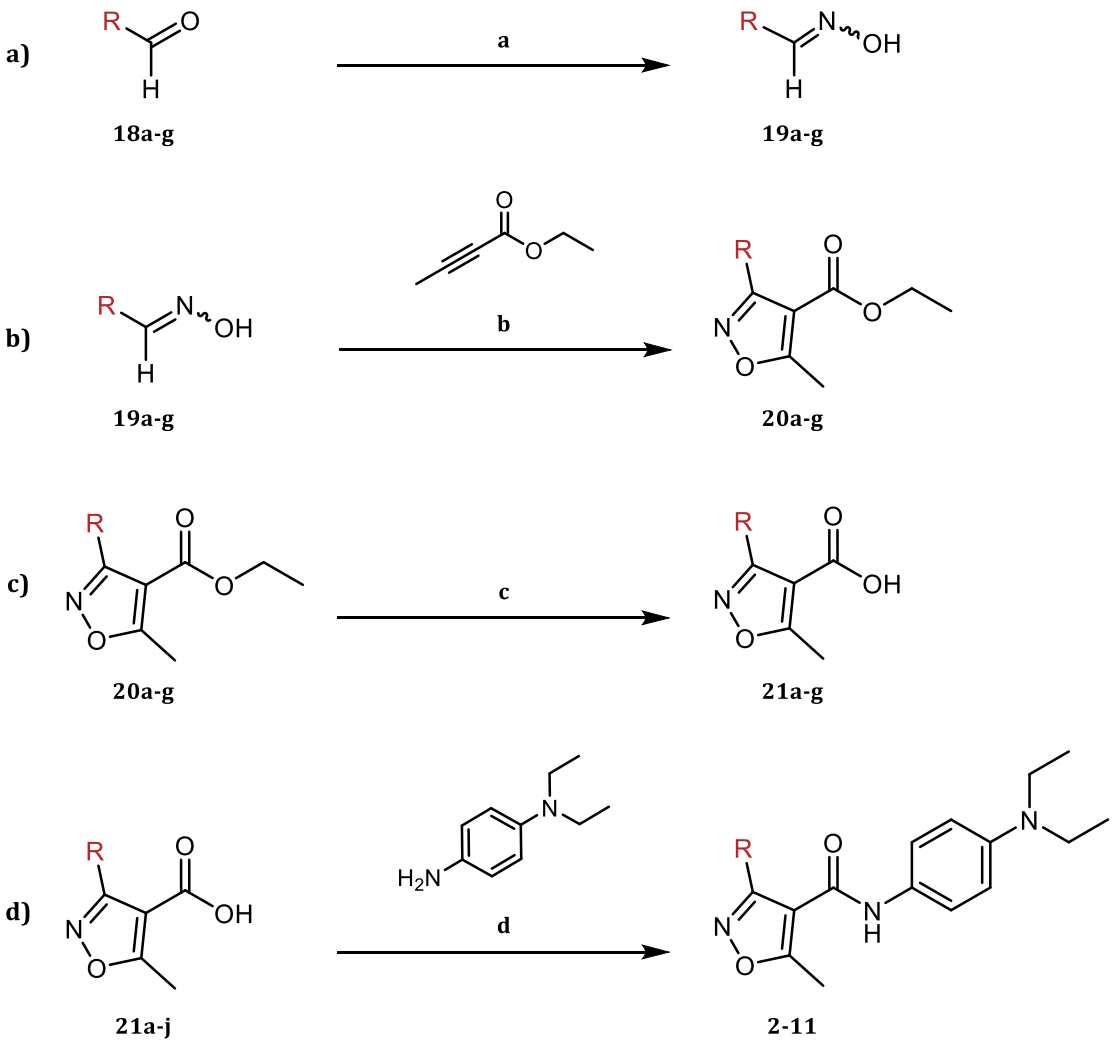

Scheme 1. General synthesis route of compounds **2-11**. Reagents and conditions: (a) NH_2OH-HCl, pyridine, EtOH, 13–100% (b) Dropwise DIB in MeCN/H_2O, 2:1 MeCN/H_2O, 0 °C, 13–73% (c) LiOH, 1:1:1 THF/MeOH/H_2O 67–93% (d) HBTU, DIPEA, DMF, argon 50–97% .

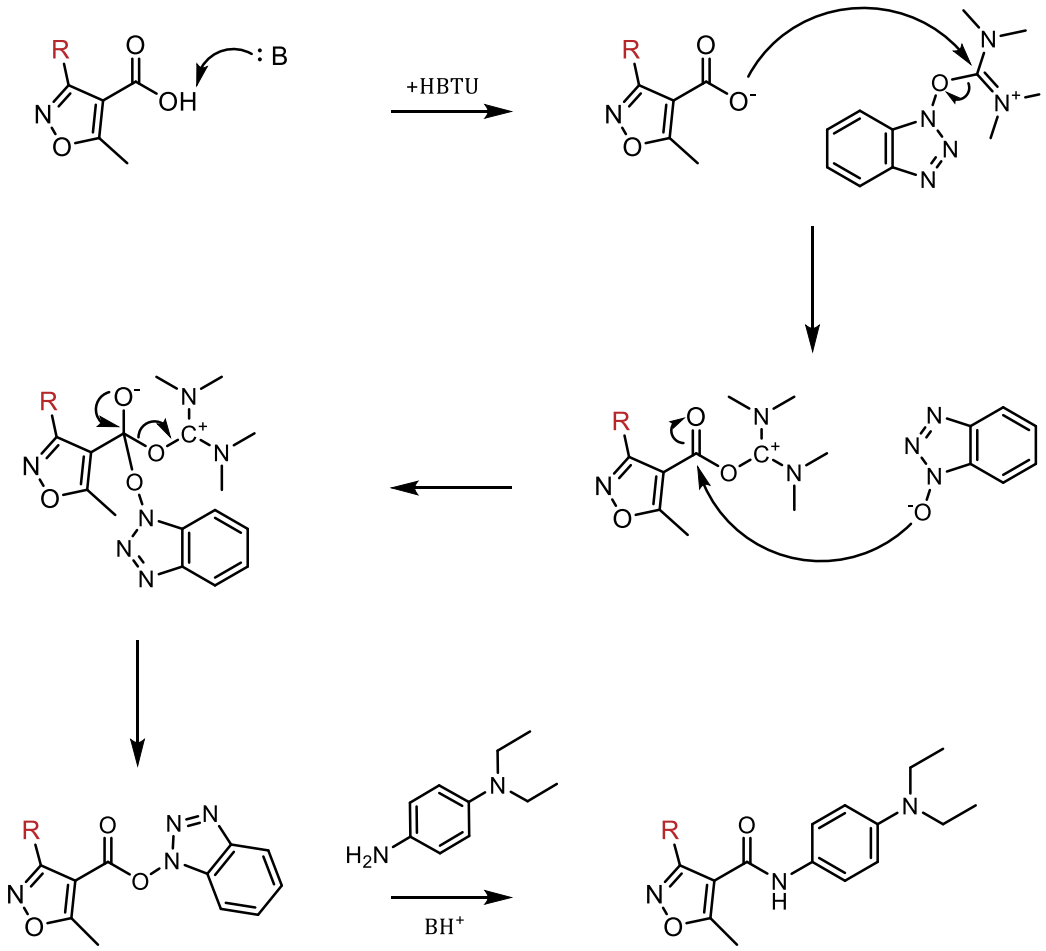

Scheme 2. Proposed mechanism for HBTU-mediated amide coupling (Valeur & Bradley 2009). HBTU, *N,N,N′,N′*-Tetramethyl-O-(1H-benzotriazol-1-yl)uronium hexafluorophosphate.

5.2 Effects of study compounds on GATA4-NKX2-5 transcriptional synergy

Results of the luciferase assays are presented in Figure 8. None of the compounds in the first test set achieved statistically significant reduction of luciferase activity compared to DMSO-treated GATA4-NKX2-5 synergy controls. Compound **5** exhibited a non-significant trend of increasing transcriptional activity mediated by the NKE promoter site. On the other hand, the second set of compounds included several compounds with statistically significant effects on luciferase activity. Compounds **6** ($F(2,6)=8{,}583$, $p=0{,}026$), **7** ($F(2,6)=14{,}200$, $p=0{,}004$), **9** ($F(2,6)=6{,}932$, $p=0{,}023$) and **11** ($F(2,6)=6{,}547$, $p=0{,}033$) inhibited the luciferase activity statistically significantly at 10 µM concentration compared to control. Additionally,

in this test set the reference compound **1** statistically significantly inhibited the luciferase activity at 10 µM concentration ($F(2,6)=12{,}390$, $p=0{,}006$).

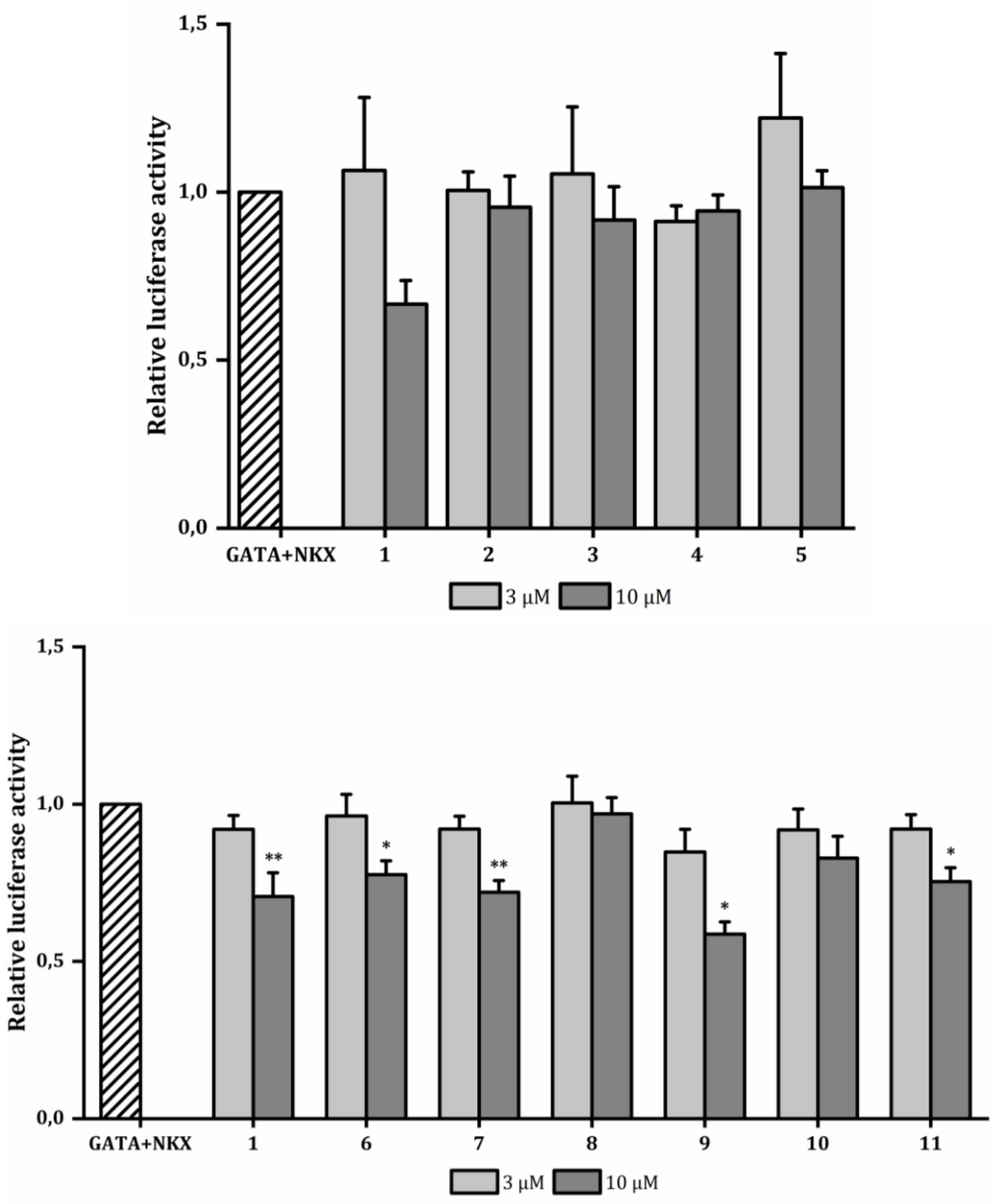

Figure 8. Results of the luciferase assays. Luciferase activity is normalized to DMSO-treated control (GATA+NKX). $^{**}p < 0.01$ vs. DMSO; $^{*}p < 0.05$ vs. DMSO (randomized block ANOVA followed by Tukey's HSD).

5.3 Effects of study compounds on stem cell viability

Structurally modified analogues of **1** showed significant changes in mitochondrial toxicity as assayed by the MTT assay (Figure 9). Compounds **2**, **4**, **8** and **12** lacked statistically significant toxicity, while other compounds showed variable levels of toxicity at concentrations 0,3–30 μM (Table 3). More specifically, compounds **9**, **13** and **14** share the level of toxicity with **1**, compounds **2**-**8**, **10**-**12** and **15** are less toxic and compound **16** is more toxic than **1**. None of the compounds induced significant necrotic cell death, as shown by the results of the LDH assay (Figure 10).

Table 3. List of statistically significant mitochondrial toxicity for inhibitors of GATA4-NKX2-5 synergy. df, degree of freedom.

Compound	Concentration	*F*	df_1	df_2	*p*
1	3	16,242	5	10	0,022
	10	16,242	5	10	0,003
	30	16,242	5	10	0,003
3	10	27,448	5	10	0,007
	30	27,448	5	10	<0,001
4	30	9,455	5	10	0,043
6	30	39,713	5	10	<0,001
7	10	48,411	5	10	0,002
	30	48,411	5	10	<0,001
9	10	8,901	5	10	0,044
	30	8,901	5	10	0,031
10	30	10,242	5	10	0,014
11	30	8,550	5	10	0,026
13	10	12,604	5	10	0,008
	30	12,604	5	10	0,006
14	3	14,535	5	10	0,040
	10	14,535	5	10	0,006
	30	14,535	5	10	0,005
16	1	18,051	5	10	0,003
	3	18,051	5	10	0,001
	10	18,051	5	10	0,002
	30	18,051	5	10	0,002

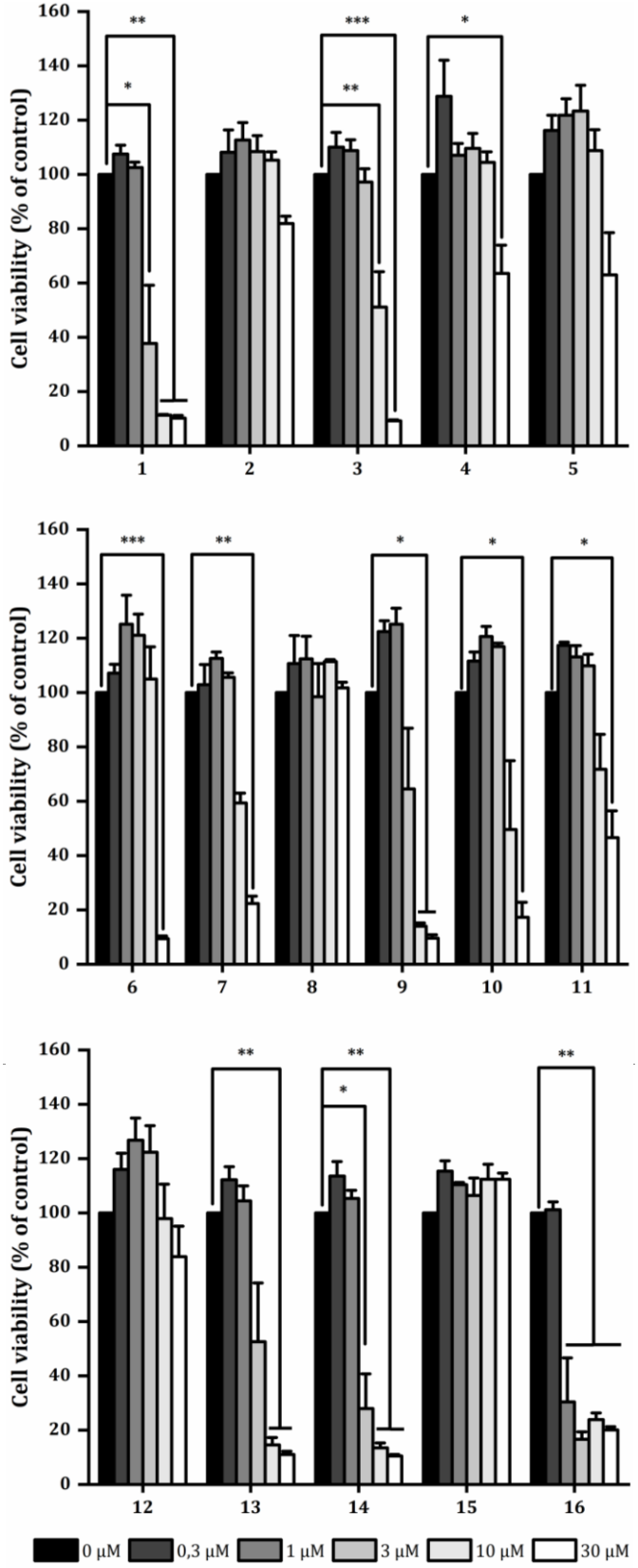

Figure 9. Results of the MTT assays. Viability is normalized to DMSO-treated control (0 µM). ***$p < 0.001$ vs. DMSO; **$p < 0.01$ vs. DMSO; *$p < 0.05$ vs. DMSO (randomized block ANOVA followed by Tukey's HSD)

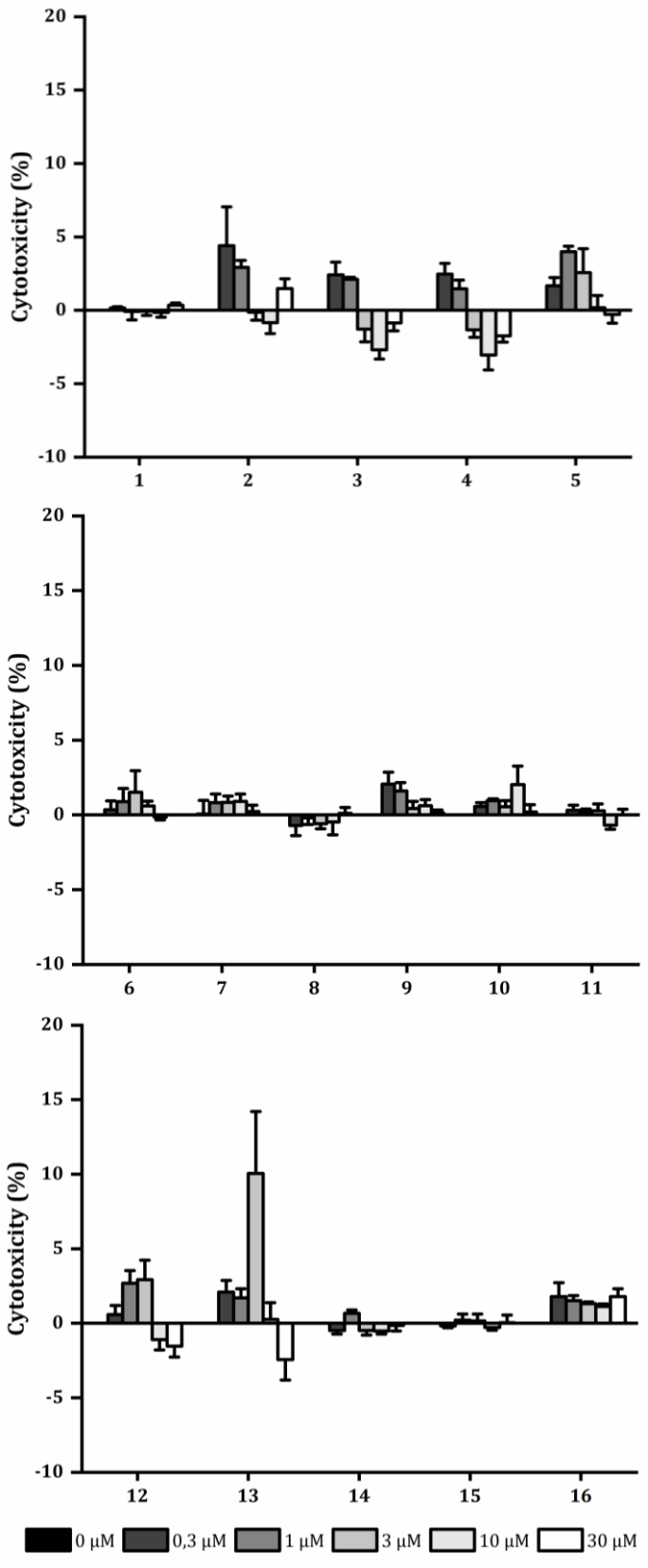

Figure 10. Results of the LDH assays. Viability is normalized to DMSO-treated control (0 µM). No statistical signifigance (randomized block ANOVA followed by Tukey's HSD)

6 DISCUSSION

GATA4 is a TF which has a major impact on cardiac development, cardiac function and transcriptional regulation (Pikkarainen et al. 2004; Schlesinger et al. 2011). Thus, targeting GATA4 may be a viable method of treating various cardiac diseases, including HF. While several key interactions of GATA4 and other TFs have been identified, transcriptional synergy of GATA4 and NKX2-5 is appreciated as a potential strategy to treat MI-induced HF. Välimäki et al. (2017) identified compound **1** as a potent inhibitor of GATA4-NKX2-5 synergy, but studies by Karhu et al. (2018) found dose-limiting toxicity for **1** and its derivatives. Previously synthesised derivatives lacked modifications which donate electron density to the southern phenyl ring of **1**. In addition, the torsional angle between the isoxazole and phenyl rings was found to correlate with stem cell toxicity of derivatives of compound **1**. Novel structural modifications were sought after to account for this void in chemical space surrounding **1** and its use in inhibiting GATA4-NKX2-5 transcriptional synergy.

We managed to synthesize and characterize 10 novel inhibitors of GATA4-NKX2-5 transcriptional synergy. Four of these compounds (**6**, **7**, **9** and **11**) were found to have similar activity as the reference compound **1** in the luciferase reporter assay. In addition, compounds **6**, **7** and **11** were also found to be less toxic than the reference compound in the MTT assay. It should be noted that compound **1** did not reach the previously-reported activity of almost total loss of synergy (Kinnunen et al. 2018). In previous studies, **1** reduced the luciferase activity to the level of NKX2-5 treated cells, which was not the case in this study (results not shown). Despite these considerations, the study may be considered successful and the goals of the study appropriately met, with compounds **6**, **7** and **11** being of similar activity and less toxic than to compound **1**.

The torsional angle between the southern isoxazole and phenyl rings of **6** and **7** is hypothesised to differ from the corresponding angle in compound **1**, which could explain the alleviated toxicity. The factual torsion angle would need to be calculated

or experimentally evaluated to confirm this hypothesis. Electronic effect of electron-donating substituents seems to have played a more ambiguous role in activity and toxicity of study compounds. While each methyl- and methoxy-substituted derivative was less toxic than **1**, some were not active in the luciferase assay. Surprisingly, compound **9** with saturated hexagonal ring in place of the phenyl ring had similar activity and toxicity characteristics as **1** in this study. A less polar ring with more hydrogens, larger three-dimensional size and inability to participate in π-π bonds was initially predicted to have modified binding characteristics compared to **1**.

The inactive compounds are also of interest. *Para*-substitution of the phenyl ring seems to prevent appropriate binding according to the luciferase assay. Compounds **2** and **4** were found to be more mildly toxic in the MTT assay as well. The *meta*-substituted **3** and **5** were similarly inactive, but slightly more toxic than the corresponding *para*-substituted analogues. Out of all the study compounds, compound **5** at 3 μM activated NKE-mediated luciferase activity the most. Compound **8** was devoid of any activity in all the assays, which hints total absence of binding to the site of action and lack of notable promiscuity. Finally, compound **10** shared characteristics with **9**, but was less toxic.

Five compounds were evaluated only in the toxicity assays. Considering that the activity on GATA4-NKX2-5 transcriptional synergy was not evaluated in this study, only some conclusions may be drawn. While the changes in structure between **12** and **13** are very slight, only the addition of a methyl group and the loss of an aromatic nitrogen, compound **13** is significantly more toxic on hiPSC than **12**. The nitrogen ring may have a stabilising effect on the binding site, which reduces toxicity. Off-target binding could be reduced as well. Compound **14** with inverted isoxazole ring and an additional isopropyl moiety in the northern amine had similar toxicity as **1**, while **16** with a larger substituted thiadiazole as the southern ring was by far the most toxic of all evaluated compounds. Compound **15** with an isothiazole ring instead of isoxazole, while lacking the other southern ring completely, was found to be very well tolerated on hiPSC.

Taken together, compounds with a small or no second southern ring were better tolerated than compounds with benzene-like large aromatic rings. Additionally, increasing the torsional angle between the two southern rings seems to rescue some stem cell toxicity, but not all; di-*ortho*-substituted phenyl ring derivative **7** was more toxic than mono-*ortho*-substituted alternative **6**. The di-*meta*-substituted **11** lacks the more evident torsional angle-altering characteristics of other active, but non-toxic compounds, which could signify another mechanism of toxicity avoidance.

Introducing hydrogen bond acceptors to a molecule may influence the permeability and solubility of a drug candidate. While none of the compounds in this study violate the famous Rule of Five (Lipinski et al. 1997), alterations of solubility may still be present. More precisely, the compound **11** was noted to have lower solubility to common solvents than other compounds during synthesis, but this characteristic was not experimentally evaluated. Two hydrogen bond acceptors in the form of methoxy groups were introduced to the molecule, which increase both polar surface area and number of hydrogen bond acceptors in the molecule. Should it be necessary to evaluate the cell wall permeation of this class of compounds, a basic permeability assay on Caco-2 cells would be warranted (Uchida et al. 2009).

While the dipolar cycloaddition reaction **b** was highly regioselective for our class of compounds, side products with similar elution times in flash purification were present in some crude products. This complicated the purification process somewhat and wasted solvents. A more thorough evaluation of a proper purification protocol and the use of SNAP Ultra cartridges could have improved the separation and saved solvents. Direct crystallisation protocol is an example of an environmentally-friendly purification protocol, where applicable. An ice bath was required for a good yield in reaction **b** and mishaps in temperature control resulted in lower yields. This was evident for compound **20a.** Additionally, the yield of final products **2-11** could have improved through delayed addition of *N,N*-diethyl-1,4-phenylenediamine to the reaction mixture to avoid unnecessary formation of guanidinium side products (Valeur & Bradley 2009).

Interestingly, the major product of oxime formation reaction for compound **19g** seemed to be the ethyl acetal derivative of 3,5-dimethoxybenzaldehyde (compound **17**; Figure 11). We were unable to analyse the mass of this unwanted product by MS, most likely due to degradation of this labile product in chemical ionisation conditions. Analysis of the compound by NMR revealed similar peaks as reported for 3,5-dimethoxybenzaldehyde diethyl acetal previously, which provides evidence for this plausible side reaction (Azzena et al. 1992). Mechanism of this reaction is unknown; acetal formation is usually an acid-catalysed reaction, while reaction **a** proceeds through basic catalysis.

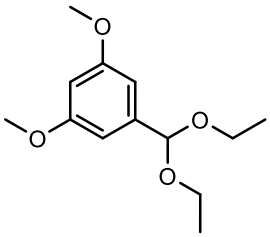

Figure 11. Structure of 3,5-dimethoxybenzaldehyde diethyl acetal (compound **17**).

GATA4 is expressed in several tissues throughout the body, which leaves GATA4-targeting HF therapies prone to causing adverse effects due to affecting non-cardiac tissues. Additionally, systemic exposure to therapeutic agents may cause general off-target toxicity, as is the case with chemotherapeutic agents (Poole et al. 2006). Nanoporous silica has been identified as a potential drug carrier, which may be functionalised to enable specific uptake to cardiac tissues (Tölli et al. 2014; Ferreira et al. 2016; Ferreira et al. 2017). These carriers are uptaken by cardiac tissue and are biocompatible *in vivo*. Some additional improvements in cellular uptake and cardiac targeting of these particles is required, but the particles hold great potential in targeted therapy nonetheless.

Preclinical toxicity and safety tests for drug candidates are done solely on cells and tissues of non-human origin (European Medicines Agency 2019a; European Medicines Agency 2019b). Consequently, no knowledge of toxicity on human tissues exists until first-in-man studies. Usage of hiPSC cells and hiPSC-derived tissues in

pre-clinical studies would allow for activity and toxicity trials on human tissues. Results obtained on these cells could translate more readily into clinical environments and human trials. Additionally, less laboratory animals would be required, providing a major ethical improvement to pre-clinical medical studies. Functionalised microchips and organs-on-a-chip are also promising approaches to reduce the amount of *in vivo* studies (Caplin et al. 2015; Zhang & Radisic 2017).

Despite GATA4-NKX2-5 transcriptional synergy being reduced in the luciferase assay by treatment with our test compounds, further tests need to be conducted to verify the effect of the compounds on GATA4-NKX2-5 interaction. Direct inhibition of GATA4 or NKX2-5 binding to DNA, enhancement of GATA4 transport from the nucleus and induction of GATA4 or NKX2-5 degradation by ubiquitination could explain current results. However, other compounds of this class have been confirmed to act specifically on GATA4-NKX2-5 synergy, which makes it improbable that the small structural changes made to **1** in this study would completely alter the mode of action (Karhu et al. 2018; Kinnunen et al. 2018). Validation of GATA4-NKX2-5 synergy inhibition mode of action remains a challenge as well.

The chemical space surrounding electron density-donating groups and compound **1** could be explored even further by preparing other combinations of mono-, di- and trisubstituted phenyl rings. Additionally, a 4-membered cyclobutyl derivative would be of interest as well. Unsaturated versions of cyclic hydrocarbons, such as mono- or dienes, could likewise be prepared to allow for different ring conformations and stages of planarity. Further evaluation of southern ring substituent effects on GATA4-NKX2-5 interaction could further help in refining the robustness of GATA4 homology model prior to successful crystallization of this TF. Additionally, activity tests on hiPSC-derived CMs and *in vivo* are warranted before any further conclusions of the activity of compounds **6**, **7** and **11** can be made. Other toxicity mechanisms should likewise be explored with extra toxicity assays, such as ones evaluating genotoxicity.

7 SUMMARY AND CONCLUSIONS

Heart failure remains as a major social and economic burden, despite advancements in classification, diagnosis and treatment in past decades. Traditional treatment strategies lack potential to restore lost cardiac function and instead only slow down pathological processes. Regeneration of lost cardiac cells has emerged as a promising therapy option to treat heart failure, but none of the investigated strategies have reached marketing approval. Targeting cardiac transcription factors, including GATA4-NKX2-5 transcriptional synergy, with small molecules remains as a compelling approach to treat heart failure. Toxicity of drug therapies remains a major concern, especially when targeting such fundamental processes as cell differentiation.

In the present study, active and less toxic derivatives of compound **1** with electron density-donating substituents were successfully synthesised. Favourable toxicity profile of compounds **6** and **7** supports the hypothesis that the torsion angle between the phenyl and isoxazole rings of **1** is a key factor in mediating stem cell toxicity of antagonists of GATA4-NKX2-5 transcriptional synergy. Furthermore, increasing the electron density of southern phenyl ring of compound **1** seems to diminish toxicity. In agreement with previous studies, none of the compounds induced significant necrosis on IMR90 hiPSCs. While additional experiments are necessary to confirm currently presented results, this study demonstrates the complexity of PPI-targeted drug discovery and promise of hiPSCs as a model of toxicity evaluation.

8 EXPERIMENTAL SECTION

General procedure I: Synthesis of aldoximes **19a-g**

Aldehydes **18a-g** and 1,1 equivalents (eq) of both hydroxylammonium chloride and pyridine were dissolved in anhydrous ethanol under normal atmosphere (Scheme

3). The reaction was stirred in room temperature for indicated time of 1-5 hours and the reaction was quenched with the addition of saturated aqueous NH_4Cl. The products were extracted with three portions of either dichloromethane (DCM) or ethyl acetate (EtOAc) and the organic phase was dried with anhydrous Na_2SO_4, followed by filtration and concentration under reduced pressure. The products were purified by flash chromatography on silica gel cartridges and increasing gradient of EtOAc in *n*-heptane as indicated.

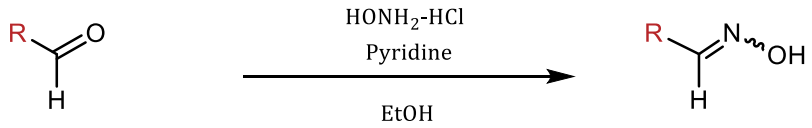

Scheme 3. Synthesis of aldoximes **19a-g**. Reagents and conditions: NH_2OH-HCl, pyridine, ethanol, rt, 1-5 h.

General procedure II: Synthesis of isoxazoles **20a-g** via dipolar cycloaddition

Aldoximes **19a-g** and ethyl-2-butynoate (1,5 eq) were dissolved in 2:1 mixture of acetonitrile (MeCN) and H_2O at 0 °C in normal atmosphere (Scheme 4). (Diacetoxyiodo)benzene (DIB; 1,2 eq) was dissolved into equal volume of 2:1 MeCN/H_2O and added dropwise to reaction mixture over 5 minutes' time. The reaction was stirred for a further 40–120 minutes, followed by evaporation of MeCN with a rotary evaporator. The water phase was washed with three portions of DCM and the resulting organic phase was concentrated under reduced pressure. The resulting crude oils were purified with flash chromatography on silica gel cartridges and increasing gradient of EtOAc in *n*-heptane as indicated.

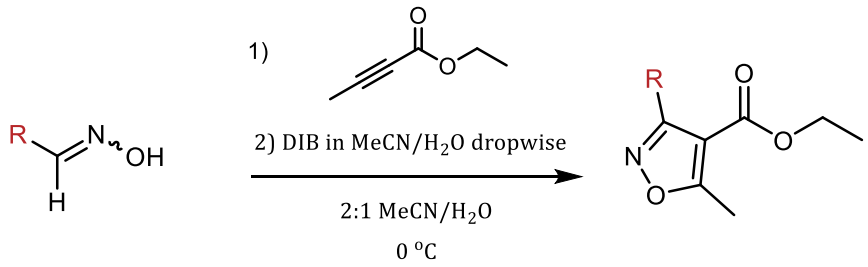

Scheme 4. Synthesis of isoxazoles **20a-g**. Reagents and conditions: ethyl-2-butynoate, dropwise DIB in 2:1 MeCN/H_2O, 2:1 MeCN/H_2O, 0 °C, 40–60 min.

General procedure III: Synthesis of carboxylic acids **21a-g** via ester hydrolysis

Carboxylic acid esters **20a-g** were dissolved into an equimixture of THF, MeOH and H_2O in rt (Scheme 5). Indicated amount of LiOH (1,5-2 eq) was added and the mixture was stirred for 1-3 days in rt. Purification was started by the addition of H_2O and 1 M NaOH. After shaking, the water phase was washed with EtOAc or DCM, followed by addition of EtOAc. The water phase was made acidic with 1 M HCl, followed by shaking. Water phase was removed, and organic phase was washed with two portions of water. Organic solvents were evaporated with a rotary evaporator and the product acids **21a-g** were used in reaction **d** without further purification or analysis.

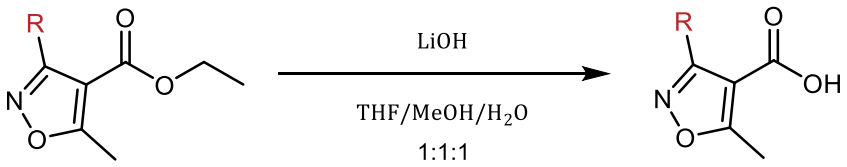

Scheme 5. Synthesis of carboxylic acids **21a-g**. Reagents and conditions: LiOH, 1:1:1 THF/MeOH/H_2O, rt, 1–3 d.

General procedure IV: Synthesis of **2-11** via HBTU-mediated amide coupling

Carboxylic acids **21a-j**, 1,3 eq of *N,N,N′,N′-t*etramethyl-O-(1H-benzotriazol-1-yl)uronium hexafluorophosphate (HBTU), 2 eq of *N,N*-diisopropylethylamine (DIPEA) and 1-1,3 eq of *N,N*-diethyl-1,4-phenylenediamine were dissolved in anhydrous *N,N*-dimethylformamide (DMF) under argon in rt (Scheme 6). The

solution was stirred overnight (16-20 hours) and diethyl ether or EtOAc was added as indicated. The organic phase was washed with three portions of water and concentrated under reduced pressure. The crude product was purified with flash chromatography on silica gel cartridges and increasing gradient of EtOAc in *n*-heptane as indicated.

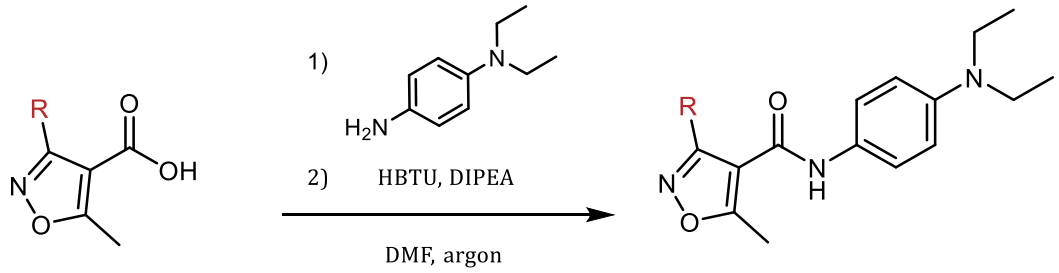

Scheme 6. Synthesis of amides **2-11**. Reagents and conditions: *N,N*-diethyl-1,4-phenylenediamine, HBTU, DIPEA, DMF, argon, rt, overnight.

Preparation of compounds **19a-g**

p-tolualdehyde oxime **19a**

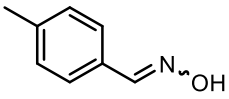

Synthesis according to general procedure I. *p*-tolualdehyde **18a** (500 mg, 4,161 mmol), hydroxylammonium chloride (318 mg, 4,577 mmol), pyridine (337 µL, 4,577 mmol), ethanol (10 mL), saturated aqueous NH_4Cl (12 mL). Reaction time 3h 40min, extraction solvent 3x15 mL EtOAc. Flash chromatography 8–58% EtOAc in *n*-heptane to yield **19a** as white crystals (76 mg, 13%). Some product lost due to flash chromatography leakage. ^{1}H NMR (400 MHz, $CDCl_3$) δ 8.13 (s, 1H), 7.50 – 7.44 (m, 2H), 7.22 – 7.16 (m, 2H), 2.37 (s, 3H). ^{13}C NMR (101 MHz, $CDCl_3$) δ 150.37, 140.30, 129.52, 129.21 (d, *J* = 3.8 Hz), 126.99, 21.47.

m-tolualdehyde oxime **19b**

Synthesis according to general procedure I. *m*-tolualdehyde **18b** 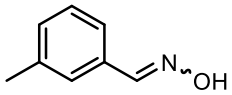 (500 mg, 4,161 mmol), hydroxylammonium chloride (318 mg, 4,577 mmol), pyridine (337 µL, 4,577 mmol), ethanol (10 mL), saturated aqueous NH_4Cl (12 mL). Reaction time 1h 50min, extraction solvent 3x15 mL EtOAc. Flash chromatography 8–54% EtOAc in *n*-heptane to yield **19b** as clear, colourless liquid (459 mg, 82%). ^1H NMR (400 MHz, $CDCl_3$) δ 8.15 (s, 0H), 7.43 – 7.40 (m, 1H), 7.38 (d, *J* = 7.7 Hz, 1H), 7.29 (dd, *J* = 7.6 Hz, 1H), 7.22 (d, *J* = 7.7 Hz, 1H), 2.38 (s, 1H). ^{13}C NMR (101 MHz, $CDCl_3$) δ 150.60, 138.66, 131.92, 131.07, 128.83, 127.71, 124.45, 21.44.

p-anisaldehyde oxime **19c**

Synthesis according to general procedure I. *p*-anisaldehyde 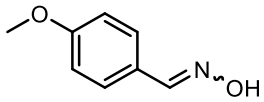 **18c** (500 mg, 3,672 mmol), hydroxylammonium chloride (281 mg, 4,040 mmol), pyridine (327 µL, 4,040 mmol), ethanol (10 mL), saturated aqueous NH_4Cl (12 mL). Reaction time 3h 10min, extraction solvent 3x15 mL DCM. Flash chromatography 5–40% EtOAc in *n*-heptane to yield **19c** as white crystals (538 mg, 97%). ^1H NMR (400 MHz, $CDCl_3$) δ 8.09 (s, 2H), 7.52 (dd, *J* = 8.9, 2.0 Hz, 4H), 6.91 (dd, *J* = 8.9, 2.1 Hz, 3H), 3.84 (s, 47H). ^{13}C NMR (101 MHz, $CDCl_3$) δ 161.08, 150.09, 128.52, 124.65, 114.24, 55.36.

m-anisaldehyde oxime **19d**

Synthesis according to general procedure I. *m*-anisaldehyde 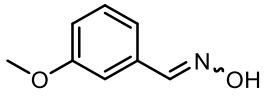 **18d** (500 mg, 3,672 mmol), hydroxylammonium chloride (281 mg, 4,040 mmol), pyridine (327 µL, 4,040 mmol), ethanol (10 mL), saturated aqueous NH_4Cl (12 mL). Reaction time 2h 10min, extraction solvent 3x15 mL EtOAc. Flash chromatography 0–30% EtOAc in *n*-heptane to yield **19d** as clear, colourless liquid (557 mg, 100%) with residual solvent remaining. ^1H NMR (400 MHz, $CDCl_3$) δ 8.40 (s, 1H), 8.13 (s, 1H), 7.30 (t, *J* = 7.9 Hz, 1H), 7.16 (dd, *J* = 2.7, 1.5 Hz, 1H), 7.13

(dt, *J* = 7.7, 1.4 Hz, 1H), 6.95 (ddd, *J* = 8.3, 2.6, 1.0 Hz, 1H), 3.83 (s, 3H). ^{13}C NMR (101 MHz, $CDCl_3$) δ 159.85, 150.36, 133.27, 129.83, 120.14, 116.43, 111.24, 55.34.

o-tolualdehyde **19e**

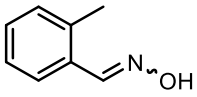

Synthesis according to general procedure I. *o*-tolualdehyde **18e** (500 mg, 4,161 mmol), hydroxylammonium chloride (318 mg, 4,577 mmol), pyridine (337 µL, 4,577 mmol), ethanol (10 mL), saturated aqueous NH_4Cl (12 mL). Reaction time 5h 35min, extraction solvent 3x15 mL DCM. Flash chromatography 2–20% EtOAc in *n*-heptane to yield **19e** as clear, light tan oil (427 mg, 76%). ^{1}H NMR (400 MHz, $CDCl_3$) δ 8.78 (s, 1H), 8.43 (s, 1H), 7.66 (dd, *J* = 7.7, 1.5 Hz, 1H), 7.28 (dd, *J* = 7.4, 1.4 Hz, 1H), 7.23 – 7.14 (m, 2H), 2.43 (s, 3H). ^{13}C NMR (101 MHz, $CDCl_3$) δ 149.29, 136.85, 130.88, 130.21, 129.91, 126.72, 126.29, 19.77.

2,6-dimethylbenzaldehyde oxime **19f**

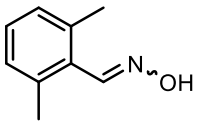

Synthesis according to general procedure I. 2,6-dimethoxybenzaldehyde **18f** (500 mg, 3,726 mmol), hydroxylammonium chloride (285 mg, 4,099 mmol), pyridine (332 µL, 4,099 mmol), ethanol (10 mL), saturated aqueous NH_4Cl (12 mL). Reaction time 5h 35min, extraction solvent 3x15 mL DCM. Flash chromatography 2–20% EtOAc in *n*-heptane to yield **19f** as white crystals (393 mg, 71%). ^{1}H NMR (400 MHz, $CDCl_3$) δ 8.44 (s, 1H), 8.36 (s, 1H), 7.17 (dd, *J* = 8.3, 6.8 Hz, 1H), 7.10 – 7.05 (m, 2H), 2.42 (s, 6H). ^{13}C NMR (101 MHz, $CDCl_3$) δ 149.82, 137.54, 129.32, 128.97, 128.47, 21.09.

3,5-dimethoxybenzaldehyde oxime **19g**

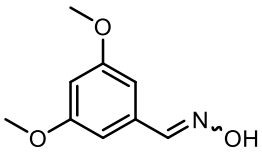

Synthesis according to general procedure I. *o*-tolualdehyde **18g** (500 mg, 3,009 mmol), hydroxylammonium chloride (230 mg, 3,310 mmol), pyridine (268 µL, 3,310 mmol), ethanol (10 mL), saturated aqueous NH_4Cl (12 mL). Reaction time 1h 45min, extraction solvent 3x15 mL EtOAc. Flash chromatography 10–30% EtOAc in *n*-heptane to yield **19g** as

white crystals (149 mg, 27%). ^{1}H NMR (400 MHz, $CDCl_3$) δ 8.07 (s, 1H), 7.86 (s, 1H), 6.74 (s, 2H), 6.50 (t, *J* = 2.3 Hz, 1H), 3.81 (s, 6H). ^{13}C NMR (101 MHz, $CDCl_3$) δ 160.98, 150.44, 133.79, 104.94, 102.59, 55.46.

Preparation of compounds **20a-g**

Ethyl 5-methyl-3-(*p*-tolyl)isoxazole-4-carboxylate **20a**

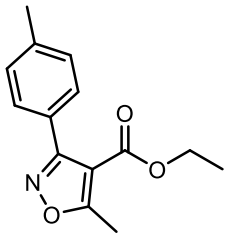

Synthesis according to general procedure II. **19a** (76 mg, 0,559 mmol), ethyl-2-butynoate (98 µL, 0,838 mmol), DIB (216 mg, 0,670 mmol), 2:1 MeCN/H_2O (12 ml). Reaction time 38min, extraction solvent 3x15 mL DCM. Flash chromatography 2–20% EtOAc in *n*-heptane to yield **20a** as clear, colourless syrup (35 mg, 26%). ^{1}H NMR (400 MHz, $CDCl_3$) δ 7.52 (d, *J* = 8.1 Hz, 2H), 7.26 – 7.21 (m, 2H), 4.24 (q, *J* = 7.1 Hz, 2H), 2.72 (s, 3H), 2.64 (s, 1H), 2.40 (d, *J* = 3.0 Hz, 4H), 2.16 (s, 5H), 1.24 (t, *J* = 7.1 Hz, 3H). ^{13}C NMR (101 MHz, $CDCl_3$) δ 175.76, 162.69, 162.19, 139.91, 129.38, 128.82, 125.61, 108.55, 60.80, 31.04, 21.54, 14.16.

Ethyl 5-methyl-3-(*m*-tolyl)isoxazole-4-carboxylate **20b**

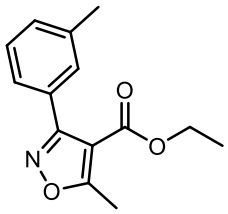

Synthesis according to general procedure II. **19b** (198 mg, 1,465 mmol), ethyl-2-butynoate (256 µL, 2,197 mmol), DIB (566 mg, 1,758 mmol), 2:1 MeCN/H_2O (20 ml). Reaction time 40min, extraction solvent 3x15 mL DCM. Flash chromatography 5–40% EtOAc in *n*-heptane to yield **20b** as clear, colourless syrup (70 mg, 19%). ^{1}H NMR (400 MHz, $CDCl_3$) δ 7.98 – 7.82 (m, 1H), 7.52 – 7.26 (m, 5H), 4.24 (q, *J* = 7.1 Hz, 2H), 2.73 (s, 3H), 2.40 (d, *J* = 0.7 Hz, 3H), 1.23 (t, *J* = 7.1 Hz, 3H). ^{13}C NMR (101 MHz, $CDCl_3$) δ 175.86, 162.76, 162.15, 137.72, 130.57, 130.04, 127.96, 126.66, 124.57, 108.59, 60.77, 21.47, 14.09, 13.67.

Ethyl 3-(*p*-methoxyphenyl)-5-methylisoxazole-4-carboxylate **20c**

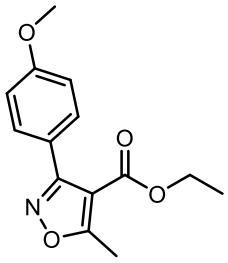

Synthesis according to general procedure II. **19c** (200 mg, 1,323 mmol), ethyl-2-butynoate (231 µL, 1,985 mmol), DIB (511 mg, 1,588 mmol), 2:1 MeCN/H_2O (20 ml). Reaction time 2h 5min, extraction solvent 3x15 mL DCM. Flash chromatography 0–20% EtOAc in *n*-heptane to yield **20c** as clear, colourless syrup (86 mg, 25%). ^{1}H NMR (400 MHz, $CDCl_3$) δ 7.60 (dd, *J* = 8.9, 2.2 Hz, 2H), 6.96 (dd, *J* = 8.9, 2.2 Hz, 2H), 4.26 (q, *J* = 7.1 Hz, 2H), 3.85 (s, 3H), 2.71 (s, 3H), 1.26 (t, *J* = 7.1 Hz, 3H). ^{13}C NMR (101 MHz, $CDCl_3$) δ 190.82, 175.72, 162.22, 162.15, 160.85, 130.83, 120.69, 114.33, 113.47, 108.33, 60.71, 55.32, 14.09, 13.70.

Ethyl 3-(*m*-methoxyphenyl)-5-methylisoxazole-4-carboxylate **20d**

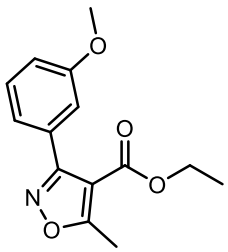

Synthesis according to general procedure II. **19d** (200 mg, 1,323 mmol), ethyl-2-butynoate (231 µL, 1,985 mmol), DIB (511 mg, 1,588 mmol), 2:1 MeCN/H_2O (20 ml). Reaction time 1h 35min, extraction solvent 3x15 mL DCM. Flash chromatography 0–10% EtOAc in *n*-heptane to yield **20d** as clear, colourless syrup (110 mg, 32%). ^{1}H NMR (400 MHz, $CDCl_3$) δ 7.41 – 7.30 (m, 1H), 7.23 – 7.16 (m, 2H), 7.12 – 6.97 (m, 1H), 4.24 (q, *J* = 7.1 Hz, 2H), 3.83 (s, 3H), 2.73 (s, 3H), 1.23 (t, *J* = 7.1 Hz, 3H). ^{13}C NMR (101 MHz, $CDCl_3$) δ 175.87, 162.53, 162.07, 159.28, 129.78, 129.13, 121.98, 115.76, 114.85, 108.66, 60.84, 55.45, 14.12, 13.69.

Ethyl 5-methyl-3-(*o*-tolyl)isoxazole-4-carboxylate **20e**

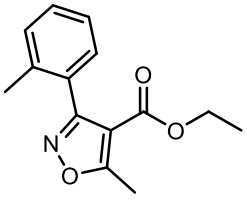

Synthesis according to general procedure II. **19e** (200 mg, 1,482 mmol), ethyl-2-butynoate (259 µL, 2,219 mmol), DIB (572 mg, 1,776 mmol), 2:1 MeCN/H_2O (20 ml). Reaction time 1h, extraction solvent 3x15 mL DCM. Flash chromatography 0–10% EtOAc in *n*-heptane to yield **20e** as clear, colourless syrup (184 mg, 51%). ^{1}H NMR (400 MHz, $CDCl_3$) δ 7.37 – 7.31 (m, 1H), 7.28 – 7.21 (m, 3H), 4.11 (q, *J* = 7.1 Hz, 2H), 2.76 (s, 3H), 2.20 (d, *J* = 0.7 Hz, 3H), 1.06 (t, *J* = 7.2 Hz, 3H). ^{13}C NMR (101 MHz, $CDCl_3$)

δ 175.43, 162.70, 161.93, 137.25, 129.89, 129.64, 129.48, 128.84, 125.40, 109.59, 60.57, 19.89, 13.83, 13.49.

Ethyl 3-(2,6-dimethylphenyl)-5-methylisoxazole-4-carboxylate **20f**

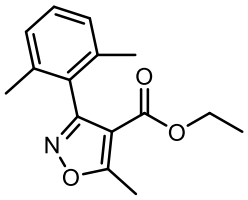

Synthesis according to general procedure II. **19f** (200 mg, 1,341 mmol), ethyl-2-butynoate (234 µL, 2,011 mmol), DIB (518 mg, 1,609 mmol), 2:1 MeCN/H_2O (20 ml). Reaction time 50min, extraction solvent 3x15 mL DCM. Flash chromatography 0–10% EtOAc in *n*-heptane to yield **20f** as clear, colourless syrup (255 mg, 73%). ^{1}H NMR (400 MHz, $CDCl_3$) δ 7.21 (dd, *J* = 8.1, 7.1 Hz, 1H), 7.07 (dq, *J* = 7.6, 0.7 Hz, 2H), 4.07 (q, *J* = 7.1 Hz, 2H), 2.78 (s, 3H), 2.09 (d, *J* = 0.8 Hz, 6H), 0.99 (t, *J* = 7.1 Hz, 3H). ^{13}C NMR (101 MHz, $CDCl_3$) δ 175.74, 161.87, 137.09, 129.02, 128.69, 127.13, 109.35, 60.43, 20.13, 13.74, 13.50.

Ethyl 3-(3,5-dimethoxyphenyl)-5-methylisoxazole-4-carboxylate **20g**

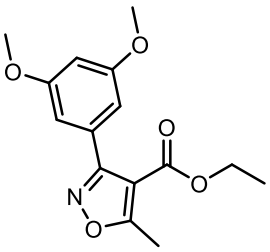

Synthesis according to general procedure II. **19g** (100 mg, 0,552 mmol), ethyl-2-butynoate (96 µL, 0,828 mmol), DIB (213 mg, 0,662 mmol), 2:1 MeCN/H_2O (10 ml). Reaction time 1h 20min, extraction solvent 3x15 mL DCM. Flash chromatography 5–15% EtOAc in *n*-heptane to yield **20g** as clear, colourless syrup (21mg, 13%). ^{1}H NMR (400 MHz, $CDCl_3$) δ 6.78 (d, *J* = 2.3 Hz, 2H), 6.56 (dd, *J* = 2.3 Hz, 1H), 4.25 (q, *J* = 7.1 Hz, 2H), 3.81 (s, 6H), 2.72 (s, 3H), 1.24 (t, *J* = 7.1 Hz, 3H). ^{13}C NMR (101 MHz, $CDCl_3$) δ 175.74, 162.39, 161.91, 160.34, 130.11, 108.59, 107.52, 104.97, 102.09, 60.73, 55.45, 14.02, 13.55.

Preparation of compounds **21a-g**

5-methyl-3-(*p*-tolyl)isoxazole-4-carboxylic acid **21a**

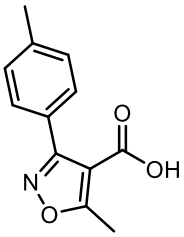

Synthesis according to general procedure III. **20a** (38 mg, 0,155 mmol), lithium hydroxide (5,6 mg, 0,232 mmol), 1:1:1 THF/MeOH/H_2O (2,4 ml). Reaction time 24 hours, extraction solvent EtOAc. Yield **21a** as white crystals (21mg, 67%).

5-methyl-3-(*m*-tolyl)isoxazole-4-carboxylic acid **21b**

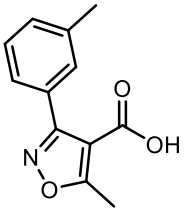

Synthesis according to general procedure III. **20b** (77 mg, 0,315 mmol), lithium hydroxide (11,3 mg, 0,472 mmol), 1:1:1 THF/MeOH/H_2O (4,6 ml). 4 mg LiOH was added after 46 hours to drive the reaction further towards products. Reaction time 50 hours, extraction solvent EtOAc. Yield **21b** as white crystals (56mg, 87%).

3-(*o*-methoxyphenyl)-5-methylisoxazole-4-carboxylic acid **21c**

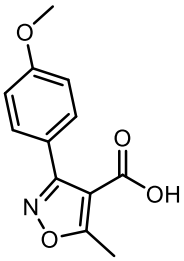

Synthesis according to general procedure III. **20c** (86 mg, 0,330 mmol), lithium hydroxide (15,8 mg, 0,659 mmol), 1:1:1 THF/MeOH/H_2O (5,4 ml). Reaction time 64 hours, extraction solvent EtOAc. Yield **21c** as white crystals (yield not measured).

3-(*m*-methoxyphenyl)-5-methylisoxazole-4-carboxylic acid **21d**

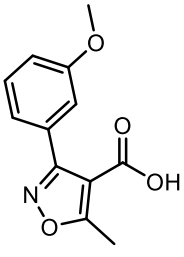

Synthesis according to general procedure III. **20d** (110 mg, 0,423 mmol), lithium hydroxide (15,2 mg, 0,634 mmol), 1:1:1 THF/MeOH/H_2O (6,6 ml). 5 mg LiOH was added after 23 hours to drive the reaction further towards products. Reaction time 71 hours, extraction solvent EtOAc. Yield **21d** as white crystals (yield not measured).

5-methyl-3-(*o*-tolyl)isoxazole-4-carboxylic acid **21e**

Synthesis according to general procedure III. **20e** (184 mg, 0,751 mmol), lithium hydroxide (36 mg, 1,501 mmol), 1:1:1 THF/MeOH/ H_2O (10,8 mL) Reaction time 93 hours, extraction solvent EtOAc. Yield **21e** as white crystals (149 mg, 91%).

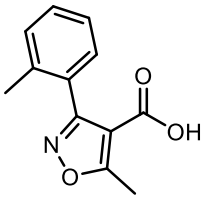

3-(2,6-dimethylphenyl)-5-methylisoxazole-4-carboxylic acid **21f**

Synthesis according to general procedure III. **20f** (237 mg, 0,912 mmol), lithium hydroxide (44 mg, 1,824 mmol), 1:1:1 THF/MeOH/ H_2O (14,4 mL) Reaction time 68 hours, extraction solvent EtOAc. Yield **21f** as white crystals (147 mg, 70%).

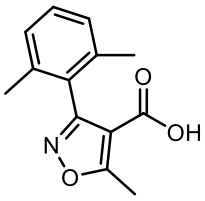

3-(3,5-dimethoxyphenyl)-5-methylisoxazole-4-carboxylic acid **21g**

Synthesis according to general procedure III. **20g** (64 mg, 0,219 mmol), lithium hydroxide (10,5 mg, 0,438 mmol), 1:1:1 THF/MeOH/ H_2O (3,9 mL) Reaction time 65 hours, extraction solvent EtOAc. Yield **21g** as white crystals (54 mg, 94%).

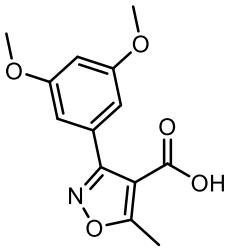

Preparation of compounds **2-11**

N-(4-(diethylamino)phenyl)-5-methyl-3-(*p*-tolyl)isoxazole-4-carboxamide **2**

Synthesis according to procedure IV. **21a** (21 mg, 0,103 mmol), HBTU (51 mg, 0,134 mmol), DIPEA (36 µL, 0,206 mmol), *N,N*-diethyl-1,4-phenylenediamine (17 µL, 0,103 mmol), DMF (3 mL). Reaction time 17 hours. Extraction solvent 20 mL diethyl ether. Flash chromatography 5–50% EtOAc in *n*-heptane to yield **2** as light-brown solid (31 mg,

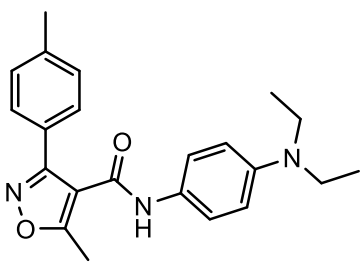

84%). ^{1}H NMR (400 MHz, $CDCl_3$) δ 7.55 (dd, *J* = 8.2, 1.8 Hz, 2H), 7.35 (dd, *J* = 7.7, 2.1 Hz, 2H), 7.08 (dd, *J* = 9.1, 2.0 Hz, 2H), 6.95 (s, 1H), 6.58 (dd, *J* = 9.0, 2.2 Hz, 2H), 3.30 (q, *J* = 7.0 Hz, 4H), 2.77 (s, 3H), 2.45 (s, 3H), 1.12 (t, *J* = 7.1 Hz, 6H). ^{13}C NMR (101 MHz, $CDCl_3$) δ 174.62, 159.91, 159.25, 145.42, 140.91, 130.00, 129.08, 125.68, 125.12, 122.11, 112.11, 111.33, 44.52, 21.50, 13.11, 12.49. HRMS calc. for $C_{22}H_{25}N_3O_2$ $[M+H]^+$: 364.2025, found 364.2029.

N-(4-(diethylamino)phenyl)-5-methyl-3-(*m*-tolyl)isoxazole-4-carboxamide **3**

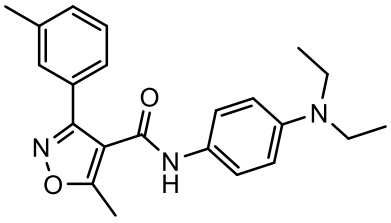

Synthesis according to procedure IV. **21b** (56 mg, 0,274 mmol), HBTU (135 mg, 0,356 mmol), DIPEA (95 µL, 0,548 mmol), *N,N*-diethyl-1,4-phenylenediamine (46 µL, 0,274 mmol), DMF (8 mL). Reaction time 16 hours. Extraction solvent 20 mL diethyl ether. Flash chromatography 5–30% EtOAc in *n*-heptane to yield **2** as light-brown solid (50 mg, 50%). ^{1}H NMR (400 MHz, $CDCl_3$) δ 7.47 (dq, *J* = 1.6, 0.9 Hz, 1H), 7.46 – 7.42 (m, 2H), 7.41 – 7.32 (m, 1H), 7.06 (dd, *J* = 9.0, 2.2 Hz, 2H), 6.97 (s, 1H), 6.57 (dd, *J* = 9.1, 2.4 Hz, 2H), 3.30 (q, *J* = 7.1 Hz, 4H), 2.78 (s, 3H), 2.43 (s, 3H), 1.12 (t, *J* = 7.1 Hz, 6H). ^{13}C NMR (101 MHz, $CDCl_3$) δ 174.75, 160.02, 159.12, 145.39, 139.35, 131.43, 129.85, 129.23, 128.07, 126.27, 125.75, 121.97, 112.44, 112.17, 111.35, 44.54, 21.43, 13.14, 12.49. HRMS calc. for $C_{22}H_{25}N_3O_2$ $[M+H]^+$: 364.2025, found 364.2029.

N-(4-(diethylamino)phenyl)-3-(*o*-methoxyphenyl)-5-methylisoxazole-4-carboxamide **4**

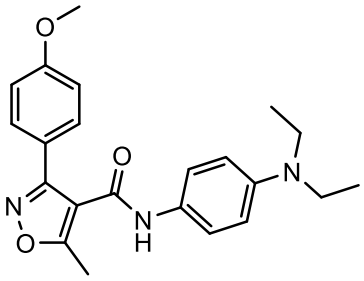

Synthesis according to procedure IV. **21c** (mass not known, used **20c** to calculate other reagents), HBTU (163 mg, 0,428 mmol), DIPEA (115 µL, 0,659 mmol), *N,N*-diethyl-1,4-phenylenediamine (60 µL, 0,362 mmol), DMF (10 mL). Reaction time 22 hours. Extraction solvent 20 mL diethyl ether. Flash chromatography 0–20% EtOAc in *n*-heptane to yield **4** as reddish solid (72 mg, 57%

in relation to **20c**). ^{1}H NMR (400 MHz, $CDCl_3$ δ 7.63 – 7.57 (m, 2H), 7.14 – 7.09 (m, 2H), 7.04 (dd, *J* = 9.7, 3.0 Hz, 3H), 6.60 – 6.56 (m, 2H), 3.88 (s, 3H), 3.31 (q, *J* = 7.0 Hz, 4H), 2.75 (s, 3H), 1.12 (t, *J* = 7.0 Hz, 6H). ^{13}C NMR (101 MHz, $CDCl_3$) δ 174.52, 161.52, 159.75, 159.43, 145.53, 130.74, 125.85, 122.16, 120.18, 114.86, 112.24, 111.48, 55.59, 44.64, 13.17, 12.62. HRMS calc. for $C_{22}H_{25}N_3O_3$ $[M+H]^+$: 380.1974, found 380.1972.

N-(4-(diethylamino)phenyl)-3-(*m*-methoxyphenyl)-5-methylisoxazole-4-carboxamide **5**

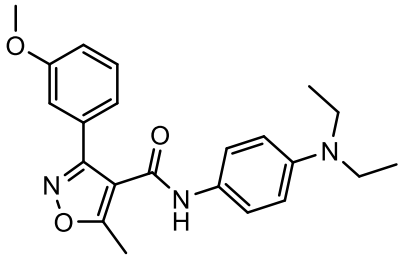

Synthesis according to procedure IV. **21d** (mass not known, used **20d** to calculate other reagents), HBTU (208 mg, 0,549 mmol), DIPEA (147 µL, 0,845 mmol), *N,N*-diethyl-1,4-phenylenediamine (78 µL, 0,465 mmol), DMF (13 mL). Reaction time 22 hours. Extraction solvent 20 mL diethyl ether. Flash chromatography 0–20% EtOAc in *n*-heptane to yield **5** as reddish solid (83 mg, 52% in relation to **20d**). ^{1}H NMR (400 MHz, $CDCl_3$) δ 7.45 (dd, *J* = 14.9, 7.9 Hz, 0H), 7.22 (ddd, *J* = 7.6, 1.6, 1.0 Hz, 0H), 7.18 (dd, *J* = 2.6, 1.5 Hz, 0H), 7.11 (ddd, *J* = 11.9, 2.7, 0.9 Hz, 0H), 7.08 (dd, *J* = 9.0, 2.1 Hz, 1H), 7.02 (s, 0H), 6.58 (dd, *J* = 9.2, 2.1 Hz, 1H), 3.83 (s, 1H), 3.30 (q, *J* = 7.1 Hz, 1H), 2.78 (s, 1H), 1.12 (t, *J* = 7.1 Hz, 2H). ^{13}C NMR (101 MHz, $CDCl_3$) δ 174.84, 160.28, 159.93, 159.17, 145.54, 130.58, 129.51, 125.82, 122.11, 121.44, 117.12, 114.14, 112.26, 111.54, 55.61, 44.64, 13.24, 12.62. HRMS calc. for $C_{22}H_{25}N_3O_3$ $[M+H]^+$: 380.1974, found 380.1974.

N-(4-(diethylamino)phenyl)-5-methyl-3-(*o*-tolyl)isoxazole-4-carboxamide **6**

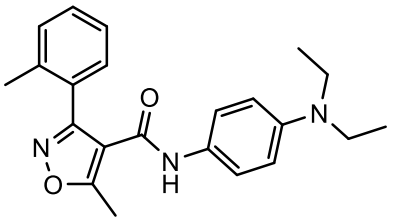

Synthesis according to procedure IV. **21e** (149 mg, 0,684 mmol), HBTU (337 mg, 0,889 mmol), DIPEA (238 µL, 1,368 mmol), *N,N*-diethyl-1,4-phenylenediamine (148 µL, 0,889 mmol), DMF (20 mL). Reaction time 17 hours. Extraction solvent 20 mL diethyl ether. Flash

chromatography 0–20% EtOAc in *n*-heptane to yield **6** as yellow syrup (222 mg, 89%). ^{1}H NMR (400 MHz, $CDCl_3$) δ 7.52 (ddd, *J* = 8.4, 6.4, 1.4 Hz, 1H), 7.46 – 7.37 (m, 3H), 6.91 (dd, *J* = 9.1, 2.2 Hz, 2H), 6.78 (s, 1H), 6.53 (dd, *J* = 9.0, 2.2 Hz, 2H), 3.28 (q, *J* = 7.1 Hz, 4H), 2.85 (s, 3H), 2.27 (s, 3H), 1.10 (t, *J* = 7.0 Hz, 6H). ^{13}C NMR (101 MHz, $CDCl_3$) δ 175.26, 159.47, 158.73, 145.22, 138.07, 131.17, 130.93, 130.08, 127.83, 126.84, 125.88, 121.58, 112.12, 111.41, 44.52, 19.69, 13.42, 12.48. HRMS calc. for $C_{22}H_{25}N_3O_2$ $[M+H]^+$: 364.2025, found 364.2022.

N-(4-(diethylamino)phenyl)-3-(2,6-dimethylphenyl)-5-methylisoxazole-4-carboxamide **7**

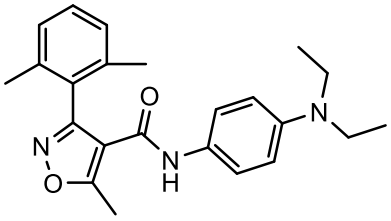

Synthesis according to procedure IV. **21f** (147 mg, 0,637 mmol), HBTU (314 mg, 0,826 mmol), DIPEA (222 µL, 1,273 mmol), *N,N*-diethyl-1,4-phenylenediamine (138 µL, 0,826 mmol), DMF (20 mL). Reaction time 23 hours. Extraction solvent 20 mL diethyl ether. Flash chromatography 0–20% EtOAc in *n*-heptane to yield **7** as yellow solid with yellow residual oil (212 mg, 88%). ^{1}H NMR (400 MHz, $CDCl_3$) δ 7.41 (dd, *J* = 8.1, 7.2 Hz, 1H), 7.26 (dq, *J* = 7.2, 1.1, 0.6 Hz, 2H), 6.88 (dd, *J* = 9.1, 2.3 Hz, 2H), 6.83 (s, 1H), 6.52 (dd, *J* = 9.1, 2.2 Hz, 2H), 3.27 (q, *J* = 7.1 Hz, 4H), 2.89 (s, 3H), 2.19 (s, 6H), 1.09 (t, *J* = 7.1 Hz, 6H). ^{13}C NMR (101 MHz, $CDCl_3$) δ 175.81, 158.59, 158.57, 145.09, 138.29, 130.70, 128.46, 127.38, 126.04, 121.36, 112.14, 110.69, 44.53, 20.02, 13.62, 12.46. HRMS calc. for $C_{23}H_{27}N_3O_2$ $[M+H]^+$: 378.2181, found 378.2180.

3-cyclopropyl-*N*-(4-(diethylamino)phenyl)-5-methylisoxazole-4-carboxamide **8**

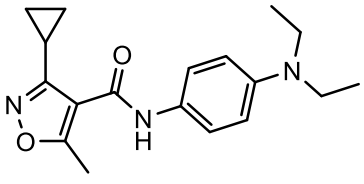

Synthesis according to procedure IV. 3-cyclopropyl-5-methyl-1,2-oxazole-4-carboxylic acid **21h** (50 mg, 0,299 mmol), HBTU (147 mg, 0,389 mmol), DIPEA (104 µL, 0,598 mmol), *N,N*-diethyl-1,4-phenylenediamine (65 µL, 0,389 mmol), DMF (9 mL). Reaction time 18 hours. Extraction solvent 20 mL diethyl ether. Flash chromatography 0–20% EtOAc in *n*-heptane to yield **8** as light-

brown solid (76 mg, 68%). ^{1}H NMR (400 MHz, $CDCl_3$) δ 7.90 (s, 1H), 7.38 (dd, *J* = 9.0, 2.2 Hz, 2H), 6.67 (dd, *J* = 9.0, 2.2 Hz, 2H), 3.34 (q, *J* = 7.1 Hz, 4H), 2.68 (s, 3H), 2.02 (tt, *J* = 8.0, 5.4 Hz, 1H), 1.18 – 1.11 (m, 10H). ^{13}C NMR (101 MHz, $CDCl_3$) δ 174.07, 160.86, 159.78, 145.55, 125.89, 122.32, 112.40, 112.35, 44.59, 12.96, 12.51, 7.14, 6.58. HRMS calc. for $C_{18}H_{24}N_3O_2$ $[M+H]^+$: 314.1869, found 314.1868.

3-cyclohexyl-*N*-(4-(diethylamino)phenyl)-5-methylisoxazole-4-carboxamide **9**

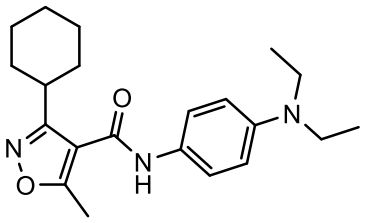

Synthesis according to procedure IV. 3-cyclohexyl-5-methyl-1,2-oxazole-4-carboxylic acid **21i** (50 mg, 0,239 mmol), HBTU (118 mg, 0,311 mmol), DIPEA (83 µL, 0,478 mmol), *N,N*-diethyl-1,4-phenylenediamine (52 µL, 0311 mmol), DMF (8 mL). Reaction time 21 hours. Extraction solvent 20 mL diethyl ether. Flash chromatography 0–20% EtOAc in *n*-heptane to yield **9** as light-brown solid (58 mg, 64%). ^{1}H NMR (400 MHz, $CDCl_3$) δ 7.34 (d, *J* = 8.4 Hz, 2H), 7.12 (s, 1H), 6.67 (d, *J* = 8.5 Hz, 2H), 3.35 (q, *J* = 7.1 Hz, 4H), 3.03 – 2.87 (m, 1H), 2.60 (s, 3H), 2.10 – 1.99 (m, 2H), 1.83 (dt, *J* = 12.6, 3.3 Hz, 2H), 1.76 – 1.67 (m, 1H), 1.59 (qd, *J* = 12.3, 3.2 Hz, 2H), 1.44 – 1.22 (m, 3H), 1.15 (t, *J* = 7.0 Hz, 6H). ^{13}C NMR (101 MHz, $CDCl_3$) δ 169.50, 166.02, 145.70, 125.56, 122.59, 112.23, 44.58, 36.19, 31.53, 26.29, 25.91, 12.59 (d, *J* = 15.3 Hz). HRMS calc. for $C_{21}H_{29}N_3O_2$ $[M+H]^+$: 356.2338, found 356.2338.

3-cyclopentyl-*N*-(4-(diethylamino)phenyl)-5-methylisoxazole-4-carboxamide **10**

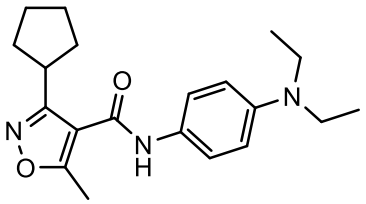

Synthesis according to procedure IV. 3-cyclopentyl-5-methyl-1,2-oxazole-4-carboxylic acid **21j** (50 mg, 0,256 mmol), HBTU (126 mg, 0,333 mmol), DIPEA (89 µL, 0,512 mmol), *N,N*-diethyl-1,4-phenylenediamine (55 µL, 0,333 mmol), DMF (8 mL). Reaction time 22 hours. Extraction solvent 20 mL EtOAc. Flash chromatography 0–30% EtOAc in *n*-heptane to yield **10** as light-brown solid (85 mg, 97%). ^{1}H NMR (400 MHz, $CDCl_3$) δ 7.37 – 7.29 (m, 2H), 7.16 (s, 1H), 6.66 (dd, *J* = 8.8, 2.2 Hz, 2H), 3.34 (q, *J* = 7.0 Hz, 5H), 2.60 (s, 3H), 2.16 – 2.03 (m, 2H),

1.97 – 1.85 (m, 2H), 1.85 – 1.72 (m, 2H), 1.73 – 1.57 (m, 2H), 1.15 (t, *J* = 7.1 Hz, 6H). ^{13}C NMR (101 MHz, $CDCl_3$) δ 170.54, 165.09, 160.41, 145.82, 125.70, 122.71, 112.90, 112.36, 44.70, 37.23, 31.61, 25.49, 12.81, 12.63. HRMS calc. for $C_{20}H_{27}N_3O_2$ $[M+H]^+$: 342.2182, found 342.2181.

N-(4-(diethylamino)phenyl)-3-(3,5-dimethoxyphenyl)-5-methylisoxazole-4-carboxamide **11**

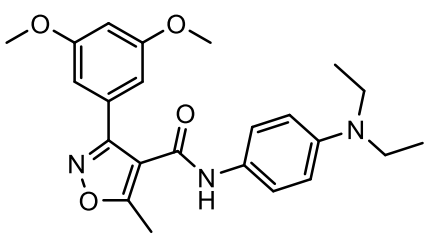

Synthesis according to procedure IV. **21g** (54 mg, 0,206 mmol), HBTU (101 mg, 0,267 mmol), DIPEA (72 µL, 0,512 mmol), *N,N*-diethyl-1,4-phenylenediamine (44 µL, 0,267 mmol), DMF (8 mL). Reaction time 20 hours. Extraction solvent 20 mL EtOAc. Flash chromatography 5–20% EtOAc in *n*-heptane to yield **11** as light-brown solid (56 mg, 66%). ^{1}H NMR (400 MHz, $CDCl_3$) δ 7.13 (s, 1H), 7.10 (dd, *J* = 9.1, 2.3 Hz, 2H), 6.77 (d, *J* = 2.3 Hz, 2H), 6.63 (t, *J* = 2.3 Hz, 1H), 6.59 (dd, *J* = 9.1, 2.3 Hz, 2H), 3.81 (s, 6H), 3.31 (d, *J* = 7.1 Hz, 4H), 2.78 (s, 3H), 1.12 (t, *J* = 7.0 Hz, 6H). ^{13}C NMR (101 MHz, $CDCl_3$) δ 174.85, 161.42, 159.82, 159.02, 145.44, 129.90, 125.68, 122.08, 112.16, 111.33, 106.86, 103.12, 55.64, 44.52, 13.17, 12.50. HRMS calc. for $C_{23}H_{27}N_3O_4$ $[M+H]^+$: 410.2080, found 410.2080.

9 REFERENCES

Aikawa R, Komuro I, Yamazaki T et al.: Rho family small G proteins play critical roles in mechanical stress–induced hypertrophic responses in cardiac myocytes. Circ Res 84: 458-466, 1999

Akazawa H, Komuro I: Roles of cardiac transcription factors in cardiac hypertrophy. Circ Res 92: 1079-1088, 2003

Ang Y, Rivas RN, Ribeiro AJ et al.: Disease model of GATA4 mutation reveals transcription factor cooperativity in human cardiogenesis. Cell 167: 1734-1749. e22, 2016

Azzena U, Melloni G, Piroddi AM, Azara E, Contini S, Fenude E: Regioselective reductive electrophilic substitution of derivatives of 3, 4, 5-trimethoxybenzaldehyde. J Org Chem 57: 3101-3106, 1992

Bardia A, Parton M, Kümmel S et al.: Paclitaxel with inhibitor of apoptosis antagonist, LCL161, for localized triple-negative breast cancer, prospectively stratified by gene signature in a biomarker-driven neoadjuvant trial. J Clin Oncol 36: 3126-3133, 2018

Beals CR, Sheridan CM, Turck CW, Gardner P, Crabtree GR: Nuclear export of NF-ATc enhanced by glycogen synthase kinase-3. Science 275: 1930-1934, 1997

Belaguli NS, Sepulveda JL, Nigam V, Charron F, Nemer M, Schwartz RJ: Cardiac tissue enriched factors serum response factor and GATA-4 are mutual coregulators. Mol Cell Biol 20: 7550-7558, 2000

Bergmann O, Bhardwaj RD, Bernard S et al.: Evidence for cardiomyocyte renewal in humans. Science 324: 98-102, 2009

Bernardo BC, Weeks KL, Pretorius L, McMullen JR: Molecular distinction between physiological and pathological cardiac hypertrophy: experimental findings and therapeutic strategies. Pharmacol Ther 128: 191-227, 2010

Bessems JG, Vermeulen NP: Paracetamol (acetaminophen)-induced toxicity: molecular and biochemical mechanisms, analogues and protective approaches. Crit Rev Toxicol 31: 55-138, 2001

Bisping E, Ikeda S, Kong SW et al.: Gata4 is required for maintenance of postnatal cardiac function and protection from pressure overload-induced heart failure. Proc Natl Acad Sci U S A 103: 14471-14476, 2006

Bonsu KO, Owusu IK, Buabeng KO, Reidpath DD, Kadirvelu A: Clinical characteristics and prognosis of patients admitted for heart failure: a 5-year retrospective study of African patients. Int J Cardiol 238: 128-135, 2017

Booz GW, Day JN, Baker KM: Interplay between the cardiac renin angiotensin system and JAK-STAT signaling: role in cardiac hypertrophy, ischemia/reperfusion dysfunction, and heart failure. J Mol Cell Cardiol 34: 1443-1453, 2002

Bowman JC, Steinberg SF, Jiang T, Geenen DL, Fishman GI, Buttrick PM: Expression of protein kinase C beta in the heart causes hypertrophy in adult mice and sudden death in neonates. J Clin Invest 100: 2189-2195, 1997

Bueno OF, Molkentin JD: Involvement of extracellular signal-regulated kinases 1/2 in cardiac hypertrophy and cell death. Circ Res 91: 776-781, 2002

Bui AL, Horwich TB, Fonarow GC: Epidemiology and risk profile of heart failure. Nat Rev Cardiol 8: 30-41, 2011

Bupha-Intr T, Haizlip KM, Janssen PM: Role of endothelin in the induction of cardiac hypertrophy in vitro. PLoS One 7: e43179, 2012

Bushdid PB, Osinska H, Waclaw RR, Molkentin JD, Yutzey KE: NFATc3 and NFATc4 are required for cardiac development and mitochondrial function. Circ Res 92: 1305-1313, 2003

Cao N, Huang Y, Zheng J et al.: Conversion of human fibroblasts into functional cardiomyocytes by small molecules. Science 352: 1216-1220, 2016

Caplin JD, Granados NG, James MR, Montazami R, Hashemi N: Microfluidic organ-on-a-chip technology for advancement of drug development and toxicology. Adv Healthc Mat 4: 1426-1450, 2015

Charron F, Paradis P, Bronchain O, Nemer G, Nemer M: Cooperative interaction between GATA-4 and GATA-6 regulates myocardial gene expression. Mol Cell Biol 19: 4355-4365, 1999

Charron F, Tsimiklis G, Arcand M et al.: Tissue-specific GATA factors are transcriptional effectors of the small GTPase RhoA. Genes Dev 15: 2702-2719, 2001

Chen J, Normand ST, Wang Y, Krumholz HM: National and regional trends in heart failure hospitalization and mortality rates for Medicare beneficiaries, 1998-2008. JAMA 306: 1669-1678, 2011

Cox D, Brennan M, Moran N: Integrins as therapeutic targets: lessons and opportunities. Nat Rev Drug Discov 9: 804-820, 2010

Davenport AP, Hyndman KA, Dhaun N et al.: Endothelin. Pharmacol Rev 68: 357-418, 2016

Davis FJ, Gupta M, Camoretti-Mercado B, Schwartz RJ, Gupta MP: Calcium/calmodulin-dependent protein kinase activates serum response factor transcription activity by its dissociation from histone deacetylase, HDAC4. Implications in cardiac muscle gene regulation during hypertrophy. J Biol Chem 278: 20047-20058, 2003

de Lemos JA, McGuire DK, Drazner MH: B-type natriuretic peptide in cardiovascular disease. Lancet 362: 316-322, 2003

Deeks ED: Venetoclax: first global approval. Drugs 76: 979-987, 2016

DeGorter M, Xia C, Yang J, Kim R: Drug transporters in drug efficacy and toxicity. Annu Rev Pharmacol Toxicol 52: 249-273, 2012

Dewenter M, von der Lieth A, Katus HA, Backs J: Calcium signaling and transcriptional regulation in cardiomyocytes. Circ Res 121: 1000-1020, 2017

Dong C, Yang X, Zhang C et al.: Myocyte enhancer factor 2C and its directly-interacting proteins: a review. Prog Biophys Mol Biol 126: 22-30, 2017

Durocher D, Charron F, Warren R, Schwartz RJ, Nemer M: The cardiac transcription factors Nkx2-5 and GATA-4 are mutual cofactors. EMBO J 16: 5687-5696, 1997

Ebashi S, KODAMA A, EBASHI F: Troponin: 1. Preparation and physiological function. J Biochem 64: 465-477, 1968

Efe JA, Hilcove S, Kim J et al.: Conversion of mouse fibroblasts into cardiomyocytes using a direct reprogramming strategy. Nat Cell Biol 13: 215, 2011

Engelhardt S, Hein L, Wiesmann F, Lohse MJ: Progressive hypertrophy and heart failure in beta1-adrenergic receptor transgenic mice. Proc Natl Acad Sci U S A 96: 7059-7064, 1999

European Medicines Agency: ICH S7A Safety pharmacology studies for human pharmaceuticals, CPMP/ICH/539/00, June 2001. Accessed 4.4.2019a. Available online: https://www.ema.europa.eu/en/ich-s7a-safety-pharmacology-studies-human-pharmaceuticals

European Medicines Agency: Repeated dose toxicity. CPMP/SWP/1042/99 Rev. 1 Corr., March 2010. Accessed 4.4.2019b. Available online: https://www.ema.europa.eu/en/repeated-dose-toxicity

Evans MJ, Kaufman MH: Establishment in culture of pluripotential cells from mouse embryos. Nature 292: 154, 1981

Fan Y, Xie P, Zhang T et al.: Regulation of the stability and transcriptional activity of NFATc4 by ubiquitination. FEBS Lett 582: 4008-4014, 2008

Ferreira MP, Ranjan S, Correia AM et al.: In vitro and in vivo assessment of heart-homing porous silicon nanoparticles. Biomaterials 94: 93-104, 2016

Ferreira MP, Ranjan S, Kinnunen S et al.: Drug-loaded multifunctional nanoparticles targeted to the endocardial layer of the injured heart modulate hypertrophic signaling. Small 13: 1701276, 2017

Fisher SA, Zhang H, Doree C, Mathur A, Martin-Rendon E: Stem cell treatment for acute myocardial infarction. Cochrane Database Syst Rev Issue 9, 2015

Fox AH, Liew C, Holmes M, Kowalski K, Mackay J, Crossley M: Transcriptional cofactors of the FOG family interact with GATA proteins by means of multiple zinc fingers. EMBO J 18: 2812-2822, 1999

Gai H, Leung EL, Costantino PD et al.: Generation and characterization of functional cardiomyocytes using induced pluripotent stem cells derived from human fibroblasts. Cell Biol Int 33: 1184-1193, 2009

Garbern JC, Lee RT: Cardiac stem cell therapy and the promise of heart regeneration. Cell Stem Cell 12: 689-698, 2013

Garg V, Kathiriya IS, Barnes R et al.: GATA4 mutations cause human congenital heart defects and reveal an interaction with TBX5. Nature 424: 443-447, 2003

Gasche Y, Daali Y, Fathi M et al.: Codeine intoxication associated with ultrarapid CYP2D6 metabolism. N Engl J Med 351: 2827-2831, 2004

Grubbs FE: Sample criteria for testing outlying observations. Ann Math Statist 21: 27-58, 1950

Grunstein M: Histone acetylation in chromatin structure and transcription. Nature 389: 349, 1997

Hajduk PJ, Greer J: A decade of fragment-based drug design: strategic advances and lessons learned. Nat Rev Drug Discov 6: 211-219, 2007

Hall LH, Kier LB: Structure-activity relationship studies on the toxicities of benzene derivatives: II. An analysis of benzene substituent effects on toxicity. Environ Toxicol Chem 5: 333-337, 1986

Hasegawa K, Lee SJ, Jobe SM, Markham BE, Kitsis RN: cis-Acting sequences that mediate induction of β-myosin heavy chain gene expression during left ventricular hypertrophy due to aortic constriction. Circulation 96: 3943-3953, 1997

Hautala N, Tenhunen O, Szokodi I, Ruskoaho H: Direct left ventricular wall stretch activates GATA4 binding in perfused rat heart: involvement of autocrine/paracrine pathways. Pflügers Arch 443: 362-369, 2002

Hautala N, Tokola H, Luodonpää M et al.: Pressure overload increases GATA4 binding activity via endothelin-1. Circulation 103: 730-735, 2001

He A, Kong SW, Ma Q, Pu WT: Co-occupancy by multiple cardiac transcription factors identifies transcriptional enhancers active in heart. Proc Natl Acad Sci U S A 108: 5632-5637, 2011

He A, Shen X, Ma Q et al.: PRC2 directly methylates GATA4 and represses its transcriptional activity. Genes Dev 26: 37-42, 2012

Heart failure: Current Care Guideline: Working group set up by the Finnish Medical Society Duodecim and the Finnish Cardiac Society. Helsinki: The Finnish Medical Society Duodecim. Available online at: www.kaypahoito.fi. Accessed 2.4.2019. Available online: www.kaypahoito.fi

Heikinheimo M, Scandrett JM, Wilson DB: Localization of transcription factor GATA-4 to regions of the mouse embryo involved in cardiac development. Dev Biol 164: 361-373, 1994

Heineke J, Molkentin JD: Regulation of cardiac hypertrophy by intracellular signalling pathways. Nat Rev Mol Cell Biol 7: 589-600, 2006

Herzig TC, Jobe SM, Aoki H et al.: Angiotensin II type1a receptor gene expression in the heart: AP-1 and GATA-4 participate in the response to pressure overload. Proc Natl Acad Sci U S A 94: 7543-7548, 1997

Hirai M, Ono K, Morimoto T et al.: FOG-2 competes with GATA-4 for transcriptional coactivator p300 and represses hypertrophic responses in cardiac myocytes. J Biol Chem 279: 37640-37650, 2004

Holland EJ, Luchs J, Karpecki PM et al.: Lifitegrast for the treatment of dry eye disease: results of a phase III, randomized, double-masked, placebo-controlled trial (OPUS-3). Ophthalmology 124: 53-60, 2017

Huisgen R: Kinetics and mechanism of 1,3-dipolar cycloadditions. Angew Chem Int Ed Engl 2: 633-645, 1963

Huttlin EL, Bruckner RJ, Paulo JA et al.: Architecture of the human interactome defines protein communities and disease networks. Nature 545: 505-509, 2017

Ieda M, Fu J, Delgado-Olguin P et al.: Direct reprogramming of fibroblasts into functional cardiomyocytes by defined factors. Cell 142: 375-386, 2010

Inagawa K, Miyamoto K, Yamakawa H et al.: Induction of cardiomyocyte-like cells in infarct hearts by gene transfer of Gata4, Mef2c, and Tbx5. Circ Res 111: 1147-1156, 2012

Ivanov AA, Khuri FR, Fu H: Targeting protein–protein interactions as an anticancer strategy. Trends Pharmacol Sci 34: 393-400, 2013

Jayawardena TM, Egemnazarov B, Finch EA et al.: MicroRNA-mediated in vitro and in vivo direct reprogramming of cardiac fibroblasts to cardiomyocytes. Circ Res 110: 1465-1473, 2012

Jhund PS, Fu M, Bayram E et al.: Efficacy and safety of LCZ696 (sacubitril-valsartan) according to age: insights from PARADIGM-HF. Eur Heart J 36: 2576-2584, 2015

Jones S, Thornton JM: Principles of protein-protein interactions. Proc Natl Acad Sci U S A 93: 13-20, 1996

Jun JH, Shim J, Ryoo H, Kwak Y: Erythropoietin-activated ERK/MAP kinase enhances GATA-4 acetylation via phosphorylation of serine 261 of GATA-4. J Cell Physiol 228: 190-197, 2013a

Jun JH, Shin EJ, Kim JH, Kim SO, Shim J, Kwak Y: Erythropoietin prevents hypoxia-induced GATA-4 ubiquitination via phosphorylation of serine 105 of GATA-4. Biol Pharm Bull 36: 1126-1133, 2013b

Kakita T, Hasegawa K, Iwai-Kanai E et al.: Calcineurin pathway is required for endothelin-1–mediated protection against oxidant stress–induced apoptosis in cardiac myocytes. Circ Res 88: 1239-1246, 2001

Karhu ST, Välimäki MJ, Jumppanen M et al.: Stem cells are the most sensitive screening tool to identify toxicity of GATA4-targeted novel small-molecule compounds. Arch Toxicol 92: 2897-2911, 2018

Katanasaka Y, Suzuki H, Sunagawa Y, Hasegawa K, Morimoto T: Regulation of cardiac transcription factor GATA4 by post-translational modification in cardiomyocyte hypertrophy and heart failure. Int Heart J 57: 672-675, 2016

Katrukha I: Human cardiac troponin complex. Structure and functions. Biokhimiya 78: 1447-1465, 2013

Keating GM: Lifitegrast ophthalmic solution 5%: A review in dry eye disease. Drugs 77: 201-208, 2017

Kerkelä R, Kockeritz L, Macaulay K et al.: Deletion of GSK-3beta in mice leads to hypertrophic cardiomyopathy secondary to cardiomyoblast hyperproliferation. J Clin Invest 118: 3609-3618, 2008

Kim J, Wende AR, Sena S et al.: Insulin-like growth factor I receptor signaling is required for exercise-induced cardiac hypertrophy. Mol Endocrinol 22: 2531-2543, 2008

Kim D, Kim CH, Moon JI et al.: Generation of human induced pluripotent stem cells by direct delivery of reprogramming proteins. Cell Stem Cell 4: 472-476, 2009

Kim Y, Ma AG, Kitta K et al.: Anthracycline-induced suppression of GATA-4 transcription factor: implication in the regulation of cardiac myocyte apoptosis. Mol Pharmacol 63: 368-377, 2003

King S, Short M, Harmon C: Glycoprotein IIb/IIIa inhibitors: the resurgence of tirofiban. Vasc Pharmacol 78: 10-16, 2016

Kinnunen S, Tölli M, Välimäki M et al.: Cardiac actions of a small molecule inhibitor targeting GATA4–NKX2-5 interaction. Sci Rep 8: 4611, 2018

Kinnunen S, Välimäki M, Tölli M et al.: Nuclear receptor-like structure and interaction of congenital heart disease-associated factors GATA4 and NKX2-5. PLoS One 10: e0144145, 2015

Kitta K, Clement SA, Remeika J, Blumberg JB, Suzuki YJ: Endothelin-1 induces phosphorylation of GATA-4 transcription factor in the HL-1 atrial-muscle cell line. Biochem J 359: 375-380, 2001

Kobayashi S, Volden P, Timm D, Mao K, Xu X, Liang Q: Transcription factor GATA4 inhibits doxorubicin-induced autophagy and cardiomyocyte death. J Biol Chem 285: 793-804, 2010

Kola I, Landis J: Can the pharmaceutical industry reduce attrition rates? Nat Rev Drug Discov 3: 711-715, 2004

Kuo CT, Morrisey EE, Anandappa R et al.: GATA4 transcription factor is required for ventral morphogenesis and heart tube formation. Genes Dev 11: 1048-1060, 1997

Laflamme MA, Murry CE: Heart regeneration. Nature 473: 326-335, 2011

Laflamme MA, Murry CE: Regenerating the heart. Nat Biotechnol 23: 845-856, 2005

Lambert SA, Jolma A, Campitelli LF et al.: The human transcription factors. Cell 172: 650-665, 2018

Leach JP, Martin JF: Cardiomyocyte proliferation for therapeutic regeneration. Curr Cardiol Rep 20: 63, 2018

Lee Y, Shioi T, Kasahara H et al.: The cardiac tissue-restricted homeobox protein Csx/Nkx2.5 physically associates with the zinc finger protein GATA4 and cooperatively activates atrial natriuretic factor gene expression. Mol Cell Biol 18: 3120-3129, 1998

Leeson PD, Springthorpe B: The influence of drug-like concepts on decision-making in medicinal chemistry. Nat Rev Drug Discov 6: 881-890, 2007

Lesizza P, Prosdocimo G, Martinelli V, Sinagra G, Zacchigna S, Giacca M: Single-dose intracardiac injection of pro-regenerative microRNAs improves cardiac function after myocardial infarction. Circ Res 120: 1298-1304, 2017

Levy D, Kenchaiah S, Larson MG et al.: Long-term trends in the incidence of and survival with heart failure. N Engl J Med 347: 1397-1402, 2002

Lew M: Good statistical practice in pharmacology Problem 2. Br J Pharmacol 152: 299-303, 2007

Li R, Li L, Qiu X et al.: GATA4 loss-of-function mutation underlies familial dilated cardiomyopathy. Biochem Biophys Res Commun 439: 591-596, 2013

Li T, He Z, Zhang X et al.: The status of MAPK cascades contributes to the induction and activation of Gata4 and Nkx2. 5 during the stepwise process of cardiac differentiation. Cell Signal 54: 17-26, 2019

Lian X, Hsiao C, Wilson G et al.: Robust cardiomyocyte differentiation from human pluripotent stem cells via temporal modulation of canonical Wnt signaling. Proc Natl Acad Sci U S A 109: E1848-E1857, 2012

Liang Q, De Windt LJ, Witt SA, Kimball TR, Markham BE, Molkentin JD: The transcription factors GATA4 and GATA6 regulate cardiomyocyte hypertrophy in vitro and in vivo. J Biol Chem 276: 30245-30253, 2001a

Liang Q, Wiese RJ, Bueno OF, Dai YS, Markham BE, Molkentin JD: The transcription factor GATA4 is activated by extracellular signal-regulated kinase 1- and 2-mediated phosphorylation of serine 105 in cardiomyocytes. Mol Cell Biol 21: 7460-7469, 2001b

Liebler DC, Guengerich FP: Elucidating mechanisms of drug-induced toxicity. Nat Rev Drug Discov 4: 410-420, 2005

Lin JH, Lu AY: Role of pharmacokinetics and metabolism in drug discovery and development. Pharmacol Rev 49: 403-449, 1997

Lipinski CA, Lombardo F, Dominy BW, Feeney PJ: Experimental and computational approaches to estimate solubility and permeability in drug discovery and development settings. Adv Drug Deliv Rev 23: 3-25, 1997

Lorenz K, Schmitt JP, Vidal M, Lohse MJ: Cardiac hypertrophy: targeting Raf/MEK/ERK1/2-signaling. Int J Biochem Cell Biol 41: 2351-2355, 2009

Lu J, McKinsey TA, Nicol RL, Olson EN: Signal-dependent activation of the MEF2 transcription factor by dissociation from histone deacetylases. Proc Natl Acad Sci U S A 97: 4070-4075, 2000

Luna-Zurita L, Stirnimann CU, Glatt S et al.: Complex interdependence regulates heterotypic transcription factor distribution and coordinates cardiogenesis. Cell 164: 999-1014, 2016

Maitra M, Schluterman MK, Nichols HA et al.: Interaction of Gata4 and Gata6 with Tbx5 is critical for normal cardiac development. Dev Biol 326: 368-377, 2009

Manning BD, Toker A: AKT/PKB Signaling: Navigating the Network. Cell 169: 381-405, 2017

Marin-Juez R, Marass M, Gauvrit S et al.: Fast revascularization of the injured area is essential to support zebrafish heart regeneration. Proc Natl Acad Sci U S A 113: 11237-11242, 2016

Martinez-Rumayor A, Richards AM, Burnett JC, Januzzi Jr JL: Biology of the natriuretic peptides. Am J Cardiol 101: S3-S8, 2008

Mascarenhas J, Lu M, Virtgaym E et al.: Open label Phase I study of single agent oral RG7388 (idasanutlin) in patients with polycythemia vera and essential thrombocythemia. Blood 130: 254, 2017

McClellan KJ, Goa KL: Tirofiban. Drugs 56: 1067-1080, 1998

McMullen JR: Role of insulin-like growth factor 1 and phosphoinositide 3-kinase in a setting of heart disease. Clin Exp Pharmacol Physiol 35: 349-354, 2008

Meyer UA: Pharmacogenetics and adverse drug reactions. Lancet 356: 1667-1671, 2000

Misra C, Chang S, Basu M, Huang N, Garg V: Disruption of myocardial Gata4 and Tbx5 results in defects in cardiomyocyte proliferation and atrioventricular septation. Hum Mol Genet 23: 5025-5035, 2014

Mohamed TM, Stone NR, Berry EC et al.: Chemical enhancement of in vitro and in vivo direct cardiac reprogramming. Circulation 135: 978-995, 2017

Molkentin JD, Antos C, Mercer B, Taigen T, Miano JM, Olson EN: Direct activation of a GATA6 cardiac enhancer by Nkx2.5: evidence for a reinforcing regulatory network of Nkx2. 5 and GATA transcription factors in the developing heart. Dev Biol 217: 301-309, 2000

Molkentin JD, Lu J, Antos CL et al.: A calcineurin-dependent transcriptional pathway for cardiac hypertrophy. Cell 93: 215-228, 1998

Molkentin JD: The zinc finger-containing transcription factors GATA-4, -5, and -6. Ubiquitously expressed regulators of tissue-specific gene expression. J Biol Chem 275: 38949-38952, 2000

Molkentin JD, Lin Q, Duncan SA, Olson EN: Requirement of the transcription factor GATA4 for heart tube formation and ventral morphogenesis. Genes Dev 11: 1061-1072, 1997

Mollova M, Bersell K, Walsh S et al.: Cardiomyocyte proliferation contributes to heart growth in young humans. Proc Natl Acad Sci U S A 110: 1446-1451, 2013

Morimoto T, Hasegawa K, Kaburagi S et al.: Phosphorylation of GATA-4 is involved in alpha 1-adrenergic agonist-responsive transcription of the endothelin-1 gene in cardiac myocytes. J Biol Chem 275: 13721-13726, 2000

Morin S, Charron F, Robitaille L, Nemer M: GATA-dependent recruitment of MEF2 proteins to target promoters. EMBO j 19: 2046-2055, 2000

Morin S, Paradis P, Aries A, Nemer M: Serum response factor-GATA ternary complex required for nuclear signaling by a G-protein-coupled receptor. Mol Cell Biol 21: 1036-1044, 2001

Morisco C, Seta K, Hardt SE, Lee Y, Vatner SF, Sadoshima J: Glycogen synthase kinase 3beta regulates GATA4 in cardiac myocytes. J Biol Chem 276: 28586-28597, 2001

Nam YJ, Song K, Luo X et al.: Reprogramming of human fibroblasts toward a cardiac fate. Proc Natl Acad Sci U S A 110: 5588-5593, 2013

Nevola L, Giralt E: Modulating protein–protein interactions: the potential of peptides. ChemComm 51: 3302-3315, 2015

Nguyen PK, Rhee J, Wu JC: Adult stem cell therapy and heart failure, 2000 to 2016: a systematic review. JAMA Cardiol 1: 831-841, 2016

Nishida W, Nakamura M, Mori S et al.: A triad of serum response factor and the GATA and NK families governs the transcription of smooth and cardiac muscle genes. J Biol Chem 277: 7308-7317, 2002

Nooren IM, Thornton JM: Diversity of protein-protein interactions. EMBO J 22: 3486-3492, 2003

Oberpriller JO, Oberpriller JC: Response of the adult newt ventricle to injury. J Exp Zool 187: 249-259, 1974

Oka T, Maillet M, Watt AJ et al.: Cardiac-specific deletion of Gata4 reveals its requirement for hypertrophy, compensation, and myocyte viability. Circ Res 98: 837-845, 2006

Palchaudhuri R, Hergenrother PJ: DNA as a target for anticancer compounds: methods to determine the mode of binding and the mechanism of action. Curr Opin Biotechnol 18: 497-503, 2007

Pathan H, Williams J: Basic opioid pharmacology: an update. Br J Pain 6: 11-16, 2012

Perimenis P, Galaris A, Voulgari A, Prassa M, Pintzas A: IAP antagonists Birinapant and AT-406 efficiently synergise with either TRAIL, BRAF, or BCL-2 inhibitors to

sensitise BRAFV600E colorectal tumour cells to apoptosis. BMC Cancer 16: 624, 2016

Peterkin T, Gibson A, Loose M, Patient R: The roles of GATA-4,-5 and-6 in vertebrate heart development. Semin Cell Dev Biol 16: 83-94, 2005

Phillips DR, Scarborough RM: Clinical pharmacology of eptifibatide. Am J Cardiol 80: 11B-20B, 1997

Picaud S, Wells C, Felletar I et al.: RVX-208, an inhibitor of BET transcriptional regulators with selectivity for the second bromodomain. Proc Natl Acad Sci U S A 110: 19754-19759, 2013

Pikkarainen S, Tokola H, Kerkelä R, Ruskoaho H: GATA transcription factors in the developing and adult heart. Cardiovasc Res 63: 196-207, 2004

Pikkarainen S, Tokola H, Majalahti-Palviainen T et al.: GATA-4 is a nuclear mediator of mechanical stretch-activated hypertrophic program. J Biol Chem 278: 23807-23816, 2003

Ponikowski P, Anker SD, AlHabib KF et al.: Heart failure: preventing disease and death worldwide. 1: 4-25, 2014

Ponikowski P, Voors AA, Anker SD et al.: 2016 ESC Guidelines for the diagnosis and treatment of acute and chronic heart failure: The Task Force for the diagnosis and treatment of acute and chronic heart failure of the European Society of Cardiology (ESC). Developed with the special contribution of the Heart Failure Association (HFA) of the ESC. Eur J Heart Fail 18: 891-975, 2016

Poole CJ, Earl HM, Hiller L et al.: Epirubicin and cyclophosphamide, methotrexate, and fluorouracil as adjuvant therapy for early breast cancer. N Engl J Med 355: 1851-1862, 2006

Porrello ER, Mahmoud AI, Simpson E et al.: Transient regenerative potential of the neonatal mouse heart. Science 331: 1078-1080, 2011

Poss KD, Wilson LG, Keating MT: Heart regeneration in zebrafish. Science 298: 2188-2190, 2002

Qian L, Huang Y, Spencer CI et al.: In vivo reprogramming of murine cardiac fibroblasts into induced cardiomyocytes. Nature 485: 593-598, 2012

Rathore R, McCallum JE, Varghese E, Florea A, Büsselberg D: Overcoming chemotherapy drug resistance by targeting inhibitors of apoptosis proteins (IAPs). Apoptosis 22: 898-919, 2017

Reis B, Jukofsky L, Chen G et al.: Acute myeloid leukemia patients' clinical response to idasanutlin (RG7388) is associated with pre-treatment MDM2 protein expression in leukemic blasts. Haematologica 101: e185-e188, 2016

Roberts AW, Davids MS, Pagel JM et al.: Targeting BCL2 with venetoclax in relapsed chronic lymphocytic leukemia. N Engl J Med 374: 311-322, 2016

Roberts RA, Kavanagh SL, Mellor HR, Pollard CE, Robinson S, Platz SJ: Reducing attrition in drug development: smart loading preclinical safety assessment. Drug Discov Today 19: 341-347, 2014

Roman BB, Geenen DL, Leitges M, Buttrick PM: PKC-β is not necessary for cardiac hypertrophy. Am J Physiol Heart Circ Physiol 280: H2264-H2270, 2001

Ruskoaho H: Atrial natriuretic peptide: synthesis, release, and metabolism. Pharmacol Rev 44: 479-602, 1992

Rysä J, Tenhunen O, Serpi R et al.: GATA-4 is an angiogenic survival factor of the infarcted heart. Circ Heart Fail 3: 440-450, 2010

Saadane N, Alpert L, Chalifour LE: Expression of immediate early genes, GATA-4, and Nkx-2.5 in adrenergic-induced cardiac hypertrophy and during regression in adult mice. Br J Pharmacol 127: 1165-1176, 1999

Sahara M, Santoro F, Chien KR: Programming and reprogramming a human heart cell. EMBO J 34: 710-738, 2015

Schlesinger J, Schueler M, Grunert M et al.: The cardiac transcription network modulated by Gata4, Mef2a, Nkx2. 5, Srf, histone modifications, and microRNAs. 7: e1001313, 2011

Scott CW, Peters MF, Dragan YP: Human induced pluripotent stem cells and their use in drug discovery for toxicity testing. Toxicol Lett 219: 49-58, 2013a

Scott DE, Bayly AR, Abell C, Skidmore J: Small molecules, big targets: drug discovery faces the protein–protein interaction challenge. Nat Rev Drug Discov 15: 533-550, 2016

Scott DE, Ehebauer MT, Pukala T et al.: Using a fragment-based approach to target protein–protein interactions. ChemBioChem 14: 332-342, 2013b

Senyo SE, Steinhauser ML, Pizzimenti CL et al.: Mammalian heart renewal by pre-existing cardiomyocytes. Nature 493: 433, 2013

Sepulveda JL, Belaguli N, Nigam V, Chen CY, Nemer M, Schwartz RJ: GATA-4 and Nkx-2.5 coactivate Nkx-2 DNA binding targets: role for regulating early cardiac gene expression. Mol Cell Biol 18: 3405-3415, 1998

Sepulveda JL, Vlahopoulos S, Iyer D, Belaguli N, Schwartz RJ: Combinatorial expression of GATA4, Nkx2-5, and serum response factor directs early cardiac gene activity. J Biol Chem 277: 25775-25782, 2002

Sergeeva IA, Christoffels VM: Regulation of expression of atrial and brain natriuretic peptide, biomarkers for heart development and disease. Biochim Biophys Acta 1832: 2403-2413, 2013

Seymour JF, Kipps TJ, Eichhorst B et al.: Venetoclax–rituximab in relapsed or refractory chronic lymphocytic leukemia. N Engl J Med 378: 1107-1120, 2018

Shah KS, Xu H, Matsouaka RA et al.: Heart failure with preserved, borderline, and reduced ejection fraction: 5-year outcomes. J Am Coll Cardiol 70: 2476-2486, 2017

Siebel AL, Trinh SK, Formosa MF et al.: Effects of the BET-inhibitor, RVX-208 on the HDL lipidome and glucose metabolism in individuals with prediabetes: A randomized controlled trial. Metab Clin Exp 65: 904-914, 2016

Singhal A, Parumala SKR, Sharma A, Peddinti RK: Hypervalent iodine mediated synthesis of di-and tri-substituted isoxazoles via [3+2] cycloaddition of nitrile oxides. Tetrahedron Lett 57: 719-722, 2016

Snyder M, Huang X, Zhang JJ: Stat3 directly controls the expression of Tbx5, Nkx2. 5, and GATA4 and is essential for cardiomyocyte differentiation of P19CL6 cells. J Biol Chem 285: 23639-23646, 2010

Song K, Nam Y, Luo X et al.: Heart repair by reprogramming non-myocytes with cardiac transcription factors. Nature 485: 599-604, 2012

Srivastava D, Yu P: Recent advances in direct cardiac reprogramming. Curr Opin Genet Dev 34: 77-81, 2015

Stilgenbauer S, Eichhorst B, Schetelig J et al.: Venetoclax in relapsed or refractory chronic lymphocytic leukaemia with 17p deletion: a multicentre, open-label, phase 2 study. Lancet Oncol 17: 768-778, 2016

Sultana N, Zhang L, Yan J et al.: Resident c-kit cells in the heart are not cardiac stem cells. Nat Commun 6: 8701, 2015

Sussman MA, Völkers M, Fischer K et al.: Myocardial AKT: the omnipresent nexus. Physiol Rev 91: 1023-1070, 2011

Sussman MA, Lim HW, Gude N et al.: Prevention of cardiac hypertrophy in mice by calcineurin inhibition. Science 281: 1690-1693, 1998

Sutton MG, Sharpe N: Left ventricular remodeling after myocardial infarction: pathophysiology and therapy. Circulation 101: 2981-2988, 2000

Suzuki YJ: Cell signaling pathways for the regulation of GATA4 transcription factor: Implications for cell growth and apoptosis. Cell Signal 23: 1094-1099, 2011

Suzuki YJ, Nagase H, Day RM, Das DK: GATA-4 regulation of myocardial survival in the preconditioned heart. J Mol Cell Cardiol 37: 1195-1203, 2004

Svensson EC, Huggins GS, Dardik FB, Polk CE, Leiden JM: A functionally conserved N-terminal domain of the friend of GATA-2 (FOG-2) protein represses GATA4-dependent transcription. J Biol Chem 275: 20762-20769, 2000

Takahashi K, Tanabe K, Ohnuki M et al.: Induction of pluripotent stem cells from adult human fibroblasts by defined factors. Cell 131: 861-872, 2007

Takahashi K, Yamanaka S: Induction of pluripotent stem cells from mouse embryonic and adult fibroblast cultures by defined factors. Cell 126: 663-676, 2006

Takaya T, Kawamura T, Morimoto T et al.: Identification of p300-targeted acetylated residues in GATA4 during hypertrophic responses in cardiac myocytes. J Biol Chem 283: 9828-9835, 2008

Talman V, Kivelä R: Cardiomyocyte–endothelial cell interactions in cardiac remodelling and regeneration. Front Cardiovasc Med 5: 101, 2018

Talman V, Ruskoaho H: Cardiac fibrosis in myocardial infarction—from repair and remodeling to regeneration. Cell Tissue Res 365: 563-581, 2016

Tani H, Sadahiro T, Ieda M: Direct cardiac reprogramming: a novel approach for heart regeneration. Int J Mol Sci 19: 2629, 2018

Tenhunen O, Sarman B, Kerkela R et al.: Mitogen-activated protein kinases p38 and ERK 1/2 mediate the wall stress-induced activation of GATA-4 binding in adult heart. J Biol Chem 279: 24852-24860, 2004

Tevosian SG, Deconinck AE, Cantor AB et al.: FOG-2: A novel GATA-family cofactor related to multitype zinc-finger proteins Friend of GATA-1 and U-shaped. Proc Natl Acad Sci U S A 96: 950-955, 1999

Tham YK, Bernardo BC, Ooi JY, Weeks KL, McMullen JR: Pathophysiology of cardiac hypertrophy and heart failure: signaling pathways and novel therapeutic targets. Arch Toxicol 89: 1401-1438, 2015

The UniProt Consortium: UniProtKB - P43694 (GATA4_HUMAN). Accessed 20.2.2019. Available online: https://www.uniprot.org/uniprot/P43694

Thibault B, Genre L, Le Naour A et al.: DEBIO 1143, an IAP inhibitor, reverses carboplatin resistance in ovarian cancer cells and triggers apoptotic or necroptotic cell death. Sci Rep 8: 17862, 2018

Thomson JA, Itskovitz-Eldor J, Shapiro SS et al.: Embryonic stem cell lines derived from human blastocysts. Science 282: 1145-1147, 1998

Tölli MA, Ferreira MP, Kinnunen SM et al.: In vivo biocompatibility of porous silicon biomaterials for drug delivery to the heart. Biomaterials 35: 8394-8405, 2014

Tomita-Mitchell A, Maslen C, Morris C, Garg V, Goldmuntz E: GATA4 sequence variants in patients with congenital heart disease. J Med Genet 44: 779-783, 2007

Trivedi CM, Zhu W, Wang Q et al.: Hopx and Hdac2 interact to modulate Gata4 acetylation and embryonic cardiac myocyte proliferation. Dev Cell 19: 450-459, 2010

Uchida M, Fukazawa T, Yamazaki Y, Hashimoto H, Miyamoto Y: A modified fast (4 day) 96-well plate Caco-2 permeability assay. J Pharmacol Toxicol Methods 59: 39-43, 2009

US National Institute of Health: ClinicalTrials.gov. Accessed 5.2.2019. Available online: https://clinicaltrials.gov

Valeur E, Bradley M: Amide bond formation: beyond the myth of coupling reagents. Chem Soc Rev 38: 606-631, 2009

Välimäki MJ, Tölli MA, Kinnunen SM et al.: Discovery of Small Molecules Targeting the Synergy of Cardiac Transcription Factors GATA4 and NKX2-5. J Med Chem 60: 7781-7798, 2017

van Berlo JH, Elrod JW, Aronow BJ, Pu WT, Molkentin JD: Serine 105 phosphorylation of transcription factor GATA4 is necessary for stress-induced cardiac hypertrophy in vivo. Proc Natl Acad Sci U S A 108: 12331-12336, 2011

van Berlo JH, Maillet M, Molkentin JD: Signaling effectors underlying pathologic growth and remodeling of the heart. J Clin Invest 123: 37-45, 2013

Vogler M, Dinsdale D, Dyer MJ, Cohen GM: Bcl-2 inhibitors: small molecules with a big impact on cancer therapy. Cell Death Differ 16: 360-367, 2009

Wada R, Muraoka N, Inagawa K et al.: Induction of human cardiomyocyte-like cells from fibroblasts by defined factors. Proc Natl Acad Sci U S A 110: 12667-12672, 2013

Walensky LD, Bird GH: Hydrocarbon-stapled peptides: principles, practice, and progress: miniperspective. J Med Chem 57: 6275-6288, 2014

Walker CA, Spinale FG: The structure and function of the cardiac myocyte: a review of fundamental concepts. J Thorac Cardiovasc Surg 118: 375-382, 1999

Wang H, Cao N, Spencer CI et al.: Small molecules enable cardiac reprogramming of mouse fibroblasts with a single factor, Oct4. Cell Rep 6: 951-960, 2014

Wang J, Schwartz RJ: Sumoylation and regulation of cardiac gene expression. Circ Res 107: 19-29, 2010

Wang J, Feng XH, Schwartz RJ: SUMO-1 modification activated GATA4-dependent cardiogenic gene activity. J Biol Chem 279: 49091-49098, 2004

Wang J, Paradis P, Aries A et al.: Convergence of protein kinase C and JAK-STAT signaling on transcription factor GATA-4. Mol Cell Biol 25: 9829-9844, 2005

Waring MJ, Arrowsmith J, Leach AR et al.: An analysis of the attrition of drug candidates from four major pharmaceutical companies. Nat Rev Drug Discov 14: 475-486, 2015

Witty AD, Mihic A, Tam RY et al.: Generation of the epicardial lineage from human pluripotent stem cells. Nat Biotechnol 32: 1026-1035, 2014

Wu P, Nielsen TE, Clausen MH: Small-molecule kinase inhibitors: an analysis of FDA-approved drugs. Drug Discov Today 21: 5-10, 2016

Yanazume T, Hasegawa K, Morimoto T et al.: Cardiac p300 is involved in myocyte growth with decompensated heart failure. Mol Cell Biol 23: 3593-3606, 2003

Yanazume T, Hasegawa K, Wada H et al.: Rho/ROCK pathway contributes to the activation of extracellular signal-regulated kinase/GATA-4 during myocardial cell hypertrophy. J Biol Chem 277: 8618-8625, 2002

Yoshimura N, Watanabe M, Motoya S et al.: Safety and efficacy of AJM300, an oral antagonist of α4 integrin, in induction therapy for patients with active ulcerative colitis. Gastroenterology 149: 1775-1783, 2015

Yu J, Vodyanik MA, Smuga-Otto K et al.: Induced pluripotent stem cell lines derived from human somatic cells. Science 318: 1917-1920, 2007

Zhang B, Radisic M: Organ-on-a-chip devices advance to market. Lab Chip 17: 2395-2420, 2017